GEORG-AUGUST-UNIVERSITÄT
GÖTTINGEN

# The role of the receptor tyrosine kinase-like orphan receptors (RORs) in human breast cancer

## Dissertation

for the award of the degree

**"Doctor rerum naturalium"**

of the Georg-August-Universitat Gottingen
within the doctoral program Molecular Medicine
of the Georg-August University School of Science (GAUSS)

submitted by

**Saskia Heinrichs**

from Frechen, Germany

Gottingen 2021

## *Thesis Committee*

***Prof. Dr. med. Annalen Bleckmann***
*Department of Hematology/Oncology, University Medical Center Göttingen*
*Department Internal Oncology Medical Clinic A, University Hospital Münster*

***Prof. Dr. Tim Beißbarth***
*Department Medical Bioinformatics*

***PD Dr. Laura Zelarayan-Behrend***
*Institute of Pharmacology and Toxicology*

## *Members of the Examination Board*

***Prof. Dr. med. Annalen Bleckmann***
*Department of Hematology/Oncology, University Medical Center Göttingen*

***Prof. Dr. Tim Beißbarth***
*Department Medical Bioinformatics*

***PD Dr. Laura Zelarayan-Behrend***
*Institute of Pharmacology and Toxicology*

## *Further members of the Examination Board*

***Prof. Dr. Stadelmann-Nessler***
*Department of neuropathology*

***Prof. Dr. Dieter Kube***
*Department of Hematology/Oncology, University Medical Center Göttingen*

***Prof. Dr. med. Michael Zeisberg***
*Department of Nephrology and Rheumatology, University Medical Center Göttingen*

# Table of contents

# List of publications

## Original articles:

Menck K, **Heinrichs S**, Baden C & Bleckmann A (2021) The WNT/ROR Pathway in Cancer: From Signaling to Therapeutic Intervention. *Cells* 10: 142

Menck K, **Heinrichs S**, Wlochowitz D, Sitte M, Noeding H, Janshoff A, Treiber H, Ruhwedel T, Schatlo B, von der Brelie C, et al. WNT11 Is a Novel Ligand for ROR2 in Human Breast Cancer. bioRxiv. 2020

## Abstracts:

**Heinrichs S**, Menck K, Sitte M, Wlochowitz D, Stefan Wiemann, Schatlo B, Pukrop T, Proescholdt M, Beißbarth T, Binder C, Bleckmann A (2020) WNT11 integrates PI3K and Rho/Rock signaling to mediate breast cancer invasion via Fzd6

**Heinrichs S,** Menck K, Sitte M, Wlochowitz D, Reinz E, Wiemann S, Schatlo B, Pukrop T, Proescholdt M, Beißbarth T, Binder C, Bleckmann A (2019) Wnt11 regulates breast cancer progression through integration of PI3K and Rho/Rock signaling via FZD4 and 6

Menck K, **Heinrichs S,** Sitte M**,** Beißbarth T, Noeding H, Janshoff A, Binder C, Bleckmann A (2019) The non-canonical Wnt ligand-receptor pair Wnt11/Ror2 mediates breast cancer invasion through Rho/Rock signaling

**Heinrichs S**, Menck K, Sitte M, Wachter A, Wlochowitz D, Reinz E, Wiemann S, Schatlo B, Pukrop T, Proescholdt M, Beißbarth T, Binder C, Bleckmann A (2019) Wnt11 verbindet PI3K und Rho/ROCK Signaling bei der Invasion des Mammakarzinoms

# Abstract

Breast and colorectal cancers are among the most common tumor types worldwide and the occurrence of metastases is often associated with a shortened lifespan. One of the signaling pathways that has been frequently associated with metastasis in these tumor entities is the Wnt signaling pathway. Wnt signaling can be either β-catenin dependent (canonical) or β-catenin independent (non-canonical). In breast and colorectal cancer, tumor-promoting properties could be attributed to members of the non-canonical Wnt signaling pathway. Preliminary results showed that overexpression of ROR2 as a non-canonical Wnt receptor, mediated an aggressive phenotype in breast cancer cells and could significantly increase invasion. Accordingly, the first aim of this work was to investigate which ligand binds ROR2 and thus triggers the invasive behavior of MCF-7 cells. RNA-seq analysis revealed increased expression levels of the non-canonical ligand Wnt11 in ROR2 overexpressing cells. Hence, Wnt11 was further investigated as a potential ROR2-ligand. Using co-immunoprecipitation experiments, this work demonstrated the interaction of ROR2 with Wnt11 in human breast cancer cells. To determine which domain facilitates the ROR2-mediated invasion, sequential deletions of the different ROR2 domains were induced. This demonstrated that the cysteine-rich and the tyrosine kinase domain mediate this effect. The next step was to determine whether Wnt11 binds other receptors that trigger the invasive behavior of MCF-7 cells since ROR2 is not expressed in these cells. Furthermore, a cell line screening of different breast and colorectal cancer cell lines identified *FZD4* and *FZD6* as highly expressed non-canonical Wnt receptors. An interaction between Wnt11 and FZD6 was validated by using Co-IP, in which PTK7 appears to act as a co-receptor. To investigate functional implications of Wnt11-mediated signaling in breast cancer, MCF-7 cells were stimulated with recombinant Wnt11, which caused increased invasion and migration rates, whereas loss of FZD6 resulted in a significant decrease of the elevated invasion rates. In line with the collected data, a signature with non-canonical Wnt pathway members including FZD receptors, ROR receptors, Wnt ligands and PI3K signaling members was defined and was analyzed for its DMFS prognostic values in breast and colorectal cancer patients. Therefore, the signature was applied to gene expression data of primary breast and colorectal cancer patients. For the primary breast cancer patients, the signature clustered the data set into two patient groups, among which the group with high *Wnt11* expression was associated with poor DMFS. Considering *FZD4* and *FZD6* individually, breast cancer patients with high *FZD6* gene expression showed worse DMFS, while high *FZD4* levels were associated with favorable DMFS. Interestingly, the defined

signature clustered the data set of the colorectal cancer patients into four groups and the cohort with a high *FZD6* expression exhibited a poor DMFS compared to the other groups.

Another important aspect of tumor progression is the reprogramming of the tumor microenvironment. It has been shown that tumor-derived extracellular vesicles can influence the tumor microenvironment in different ways. Preliminary data demonstrated that Wnt proteins can be transported via extracellular vesicles to target cells and induce Wnt signaling responses there. It was shown that RORs are transported on microvesicles and exosomes. Modulation of ROR1 and ROR2 expression resulted in altered protein compositions for both vesicle populations. However, no major impact on vesicle size or concentration was evident. Further analysis addressed functional consequences of ROR1 and ROR2 expression on extracellular vesicles. Tumor-derived EVs isolated from the aggressive breast cancer cell line MDA-MB231 induced invasiveness in MCF-7 cells, which was shown to be dependent on vesicular ROR1 expression. To determine whether ROR1/2 can function as a biomarker in breast cancer patients, plasma-derived microvesicles were analyzed for their ROR1 and ROR2 expression by flow cytometry, which is currently ongoing.

In conclusion, this work demonstrated the importance of non-canonical Wnt signaling in breast cancer progression. Wnt11 has been identified as a novel ligand for ROR2 and FZD6 by co-immunoprecipitation experiments, thereby mediating tumor-promoting properties in breast cancer. In particular, it has been shown that ROR proteins not only play an important role in breast cancer cells themselves, but also appear to be additionally involved in vesicle biogenesis and can furthermore be transferred to target cells. A clinical applicability of both ROR proteins regarding their usage as tumor biomarkers for breast cancer is still under investigation.

# List of abbreviations

| | |
|---|---|
| Alix | ALG-2 Interacting protein X |
| APC | Adenomatous polyposis coli |
| ARF6 | ADP-ribosylation factor 6 |
| BSA | Bovine serum albumin |
| CAMKII | Calmodulin-dependent kinase II |
| Car-T | Chimeric antigen receptor T cells |
| CD | Cluster of differentiation |
| cDNA | Complementary DNA |
| CKI | Casein kinase I |
| CK18 | Cytokeratin 18 |
| c-MYC | Myc proto-oncogene protein |
| Co-IP | Co-immunoprecipitation |
| CRC | Colorectal cancer |
| CRD | Cysteine-rich domain |
| DKK-1 | Dickkopf-1 |
| CRISPR | Clustered Regularly Interspaced Short Palindromic Repeats |
| DAPI | IUPAC-Bezeichnung: 4‘,6-Diamidino-2-phenylindol |
| DMSO | Dimethyl sulfoxide |
| DNA | Deoxyribonucleic acid |
| dNTPs | Deoxynucleoside Triphosphate |
| DTT | Dithiothreitol |
| DVL | Dishevelled |
| ECL | Enhanced chemiluminescence |
| ECM | Extracellular matrix |
| EDTA | Ethylenediaminetetraacetic acid |
| EGFR | Epidermal growth factor receptor |
| EMMPRIN | Extracellular matrix metalloproteinase inducer |
| EMT | Epithelial–mesenchymal transition |
| ER | Estrogen receptor |
| ESCRT | Endosomal Sorting Complexes Required for Transport |
| EV | Extracellular vesicles |
| EXOs | Exosomes |
| FACS | Fluorescence-activated cell sorting |
| FCS | Fetal calf serum |
| FZD | Frizzled |
| GPC6 | Glycoprotein glypican 6 |
| GSK3 | Glycogen synthase kinase-3 |
| HER2 | Human epidermal growth factor receptor 2 |
| HR | Hormone receptor |
| HRP | Horseradish peroxidase |
| ILVs | Intraluminal vesicles |
| JNK | Jun-N-terminal kinase |
| Kif4 | Kinesin family member 4a |
| KO | Knockout |
| KRD | Kringle domain |
| LB | Lysogeny both |
| LEF | Lymphoid enhancer-binding factor |
| LRP5/6 | Lipoprotein receptor-related protein 5 and 6 |

| | |
|---|---|
| LV | Large vesicles |
| MAPK | Mitogen-activated protein kinase |
| MSI | Microsatellite instability |
| MV | Microvesicles |
| MVB | Multivesicular body |
| nCas9 | Nicked Cas9 |
| NEB | New VouVand biolabs |
| NFAT | Nuclear factor of activated T-cells |
| NHS | N-hydroxysuccinimide |
| NTA | Nanoparticle Tracking Analysis |
| Pas | Phosphatidic acids |
| PBS | Phosphate buffered saline |
| PCP | Planar cell polarity |
| PCR | Polymerase chain reaction |
| PFA | Paraformaldehyde |
| PI3KCA | Phosphatidylinositol-3-kinase |
| PKC | Protein kinase C |
| PLC | Phospholipase C |
| PR | Progesterone receptor |
| PRD | Proline-rich domain |
| PTK7 | Protein tyrosine kinase 7 |
| qRT-PCR | Quantitative real-time polymerase chain reaction |
| Rgap1 | Rac GTPase-activating protein 1 |
| Rho | Ras homolog family member |
| RIPA | Radio-Immunoprecipitation Assay |
| ROCK1 | Rho-Associated Coiled-Coil Kinase 1 |
| ROR | Receptor Tyrosine kinase-like orphan receptor |
| RPMI-1640 | Roswell Park Memorial Institute – 1640 |
| RYK | Receptor Tyr kinase |
| SD | Standard deviation |
| SDS-PAGE | SDS polyacrylamide gel electrophoresis |
| siRNAs | Small interfering RNA |
| SRC | Proto-oncogene tyrosine-protein kinase Src |
| STAM1 | Signal Transducing Adaptor Molecule 1 |
| TAE | Tris-Acetat-EDTA |
| TBST | Tris-buffered saline with Tween20 |
| TCF | T cell factor |
| TKD | Tyrosine kinase domain |
| TME | Tumor microenvironment |
| TNBC | Triple-negative breast cancer |
| TRPM7 | Transient receptor potential cation channel subfamily member 7 |
| VAMP | Vesicle-associated membrane protein |
| Wnt | Proto-oncogene Wnt-1 |
| Wnt/STOP | Wnt-dependent stabilization of proteins |

# List of Figures

# List of Tables

# 1. Introduction

## 1.1 Breast cancer

Breast cancer is the most common invasive tumor entity worldwide and limits human life span through tumor progression and the emergence of metastasis (Sung *et al*, 2021; Siegel *et al*, 2020; Peart, 2017). In women, breast cancer is one of the leading causes of cancer-related deaths worldwide (Alkabban & Ferguson, 2021). Molecular biological investigations help to characterize the respective tumor entity and molecular subtypes to estimate the prognosis and choose therapy options. There are various therapeutic approaches for the respective stage ranging from surgery, over radiation, to systemic therapies (Moo *et al*, 2018; Toulouie *et al*, 2021). It has been shown that breast cancer cells frequently overexpress certain tumor markers or oncogenes that may promote increased cell growth and tumor progression (Zhou *et al*, 2020; Hasan *et al*, 2017; Bayerlová *et al*, 2017). Based on the expression of various markers, different subtypes of breast cancer can be distinguished, which also differ considerably in the prognosis of the patient. Breast cancer is thereby subdivided into four molecular subtypes: the two hormone-receptor-positive subtypes Luminal A and B, Her2-enriched and triple-negative breast cancer, as shown in Figure 1.

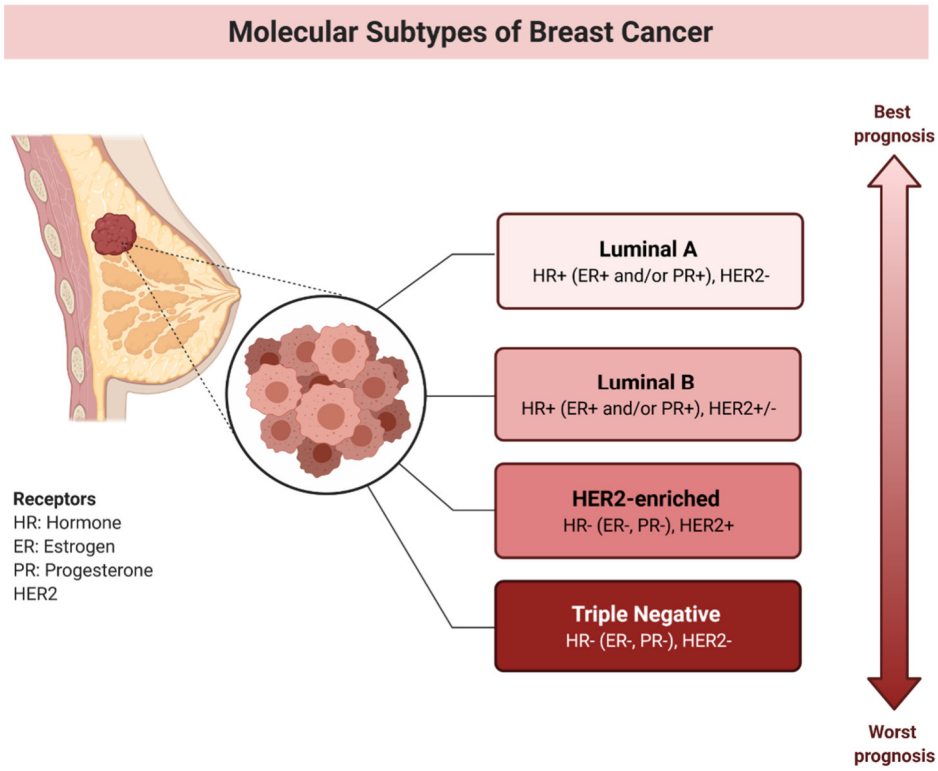


***Figure 1*: Schematic overview of the different breast cancer subtypes*:*** Classical characterization of the different breast cancer subtypes: Luminal A and B as hormone receptor-positive with the best

prognosis, Her2-enriched and triple-negative with the worst prognosis. (Adapted from a template from biorender, created by Anna Lazaratos)

The majority of patients are diagnosed with hormone receptor (HR) positive breast cancer (Lim *et al*, 2012). The HR-positive subtype is characterized by a better clinical prognosis in comparison to the other subtypes and affects especially older women. This subtype expresses either the progesterone receptor (PR), the estrogen receptor (ER) or both (Dunnwald *et al*, 2007) but exhibits a low expression of proliferation markers (Prat *et al*, 2013). The HR-positive subtype can be divided into the Luminal A and B subtypes. Patients diagnosed with Luminal A subtype have comparatively the best prognosis and respond better to hormonal therapy approaches than patients with Luminal B subtype. Luminal B is described as a very heterogeneous cancer type that shows a higher expression of proliferation markers compared to Luminal A subtype (Inic *et al*, 2014).

The molecular feature of the Her2-enriched subtype includes the overexpression of the human epidermal growth factor receptor 2 (Her2), which is encoded by *ERBB2* (Slamon *et al*, 1987). Her2 signaling is activated by binding of its ligand and has been associated with increased cell proliferation, survival and metastasis formation (Nikolai *et al*, 2016; Shen *et al*, 2020). Several therapy strategies target specifically Her2 and have shown to be effective in Her2-enriched breast cancer patients, for example monoclonal antibodies like Trastuzumab or Pertuzumab targeting Her2 (Burstein *et al*, 2007; Vogel *et al*, 2002; Gajria & Chandarlapaty, 2011; Ishii *et al*, 2019). The third group is characterized by its lack of expression of Her2, PR as well as ER and is therefore described as triple-negative breast cancer (TNBC). The TNBC subtype is often associated with a poor prognosis due to a high metastasis formation rate (Jitariu *et al*, 2017). The TBNC cells exhibit an aggressive cell phenotype, including increased proliferation, migration, invasion and cell survival. Interestingly, TNBC often occurs in young women (da Silva *et al*, 2020).

## 1.2 Colorectal cancer

Colorectal cancer (CRC) is the third most common cancer entity worldwide and is mostly diagnosed in western countries (Recio-Boiles & Cagir, 2021) and has therefore been classified as the second deadliest malignancy for both sexes. The emergence of CRC has been linked to strong environmental influences as well as mutations (Recio-Boiles & Cagir, 2021) resulting in disturbances of several highly regulated processes within the colon.

While a healthy colon reabsorbs water, minerals and nutrients, bacteria digest the proteins and reside within the crypts and villi of the colon. At the bottom of the crypts, colon stem cells with self-renewal properties are localized. To differentiate into the respective epithelial cells, the stem cells need to migrate up to the villus. Once they have reached the top of the villus, the epithelial cells participate in the digestive system. After several days, programmed cell death initiates apoptosis and the cells are excreted in the feces.

In CRC, on the other hand, there occur deviations from the above-mentioned process. CRC mostly arises from an aberrant crypt, changing into a neoplastic precursor lesion and later into a benign adenoma when the cells start to proliferate aberrantly and become resistant to cell death. The adenoma can develop into a carcinoma, as adenomas can degenerate through mutations and thus become carcinomas. They are then characterized by an increased proliferation rate and can then metastasize through migration and invasion (Hermsen *et al*, 2002; Roy & Bianchi, 2009; Mármol *et al*, 2017).

Different signaling pathways, including for example Mitogen-activated protein kinase (MAPK), Phosphatidylinositol-3-kinase (PI3KCA) and mutations in associated genes such as c-MYC, Kristen Rat Sarcoma Viral oncogene homolog (KRAS) and PI3KCA have been linked to CRC (Kramer *et al*, 2017; Koveitypour *et al*, 2019; Wang *et al*, 2004; Malinowsky *et al*, 2014). However, the association of colorectal cancer with Wnt signaling is particularly noteworthy. Adenomatosis polyposis coli (APC*)* mutations were found particularly frequently in CRC (~70%) (Schell *et al*, 2016; Rowan *et al*, 2000). APC is an important part of the destruction complex in association with GSK-3, AXIN1 and CK1, thereby degrading β-catenin (Li *et al*, 2012b; Gao *et al*, 2002; Ha *et al*, 2004; Liu *et al*, 2002). The respective mutation determines which therapy is the most promising. Current therapeutic strategies for the treatment of CRC range from surgical resection and chemotherapy to novel approaches like chimeric antigen receptor T cells (Car-T) (FLORESCU-ŢENEA *et al*, 2019; Sur *et al*, 2020).

## 1.3 Metastasis

Metastasis was defined as a secondary malignant cell collective that detached from the primary tumor through various steps and colonized then distant organs. Metastases frequently arise in the brain, lung, bones and liver (Lee, 1983). The occurrence of metastasis significantly shortens the patient's lifespan as there is still no curative treatment available for metastasized cancers and is therefore very often associated with the death of the patient

(Dillekås *et al*, 2019). During metastasis, cancer cells invade through the basement membrane and migrate through the circumjacent tissue. Then the cells then intravasate into the vascular system. Once there, the circulating cells have to survive the bloodstream in order to reach distant organs. To colonize the organs, the cells must first adhere to the blood vessels and then extravasation through the endothelial barrier. In the last step, colonization in the target organ can then take place (Elia *et al*, 2018). This process is shown schematically in Figure 2.

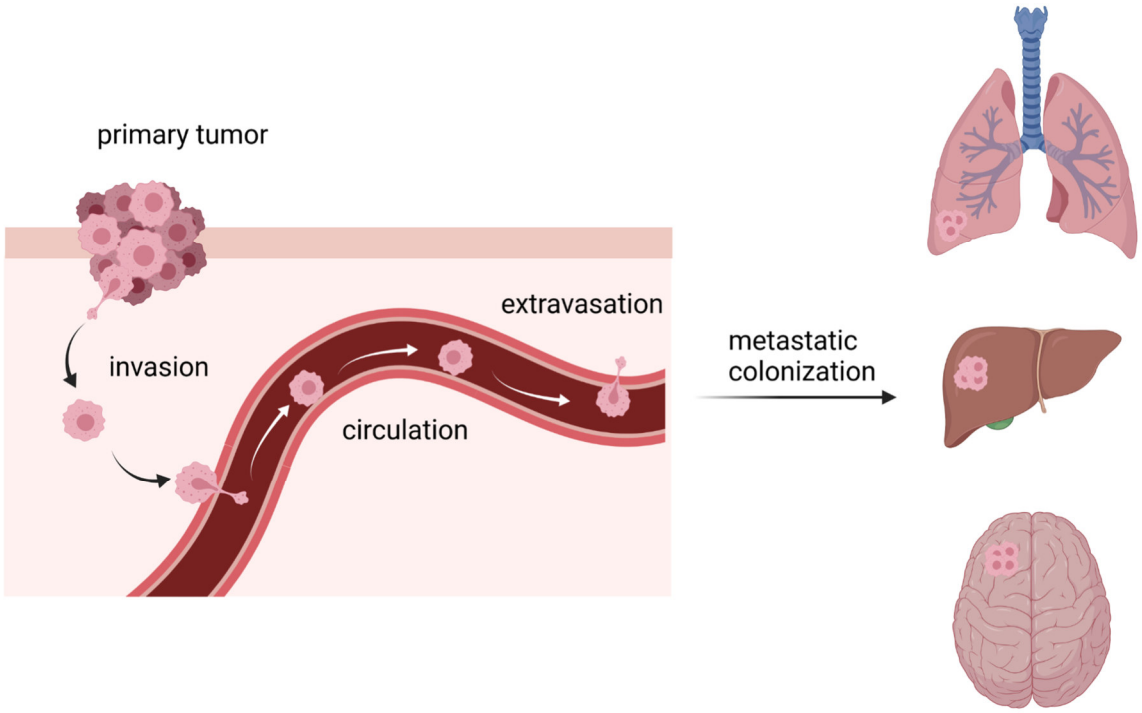


***Figure 2*: Simplified illustration of metastasis formation*:*** Several steps, including the invasion of malignant cells into the surrounding tissue at the site of primary tumor formation, their intravasation into the bloodstream and the subsequent extravasation followed by colonization of the distant tissue are required for successful metastasis formation in secondary organs. (Created with biorender.com)

An exciting aspect of metastasis formation is its organotropism, the preference of certain types of cancer for colonizing selected organs. In the case of breast cancer, for instance, most metastases are found in the lungs, brain, bones and liver (Minn *et al*, 2005), whereas CRC preferentially metastasizes to liver and lung (Penna & Nordlinger, 2002). The tumor microenvironment (TME) plays a decisive role in this process. It includes for instance endothelial cells, tumor-infiltrating immune cells, extracellular matrix (ECM) and a large number of others. It has been shown that cancer cells release a multitude of different signaling molecules such as growth factors and cytokines, as well as extracellular vesicles, which in turn reprogram the stroma, immune cells and fibroblasts and thus generate a tumor-promoting environment thereby enabling tumor progression (Neophytou *et al*, 2021; Menck *et al*, 2015;

Li *et al*, 2021). Research into the mechanisms that lead to metastasis is therefore essential and of central importance in today's science. Different signaling pathways, including PI3K and especially concise Wnt signaling have been linked to breast and colorectal cancer, their progression and metastasis formation (De *et al*, 2016; Lamb *et al*, 2013; Park *et al*, 2020; Kramer *et al*, 2017). Moreover, the activation of those signaling pathways have been shown to correlate with the clinical outcome (Khramtsov *et al*, 2010). In fact, it is still very difficult to use drugs to specifically interrupt these metastasis processes in order to prevent metastasis formation. This is one of the reasons why intensive research is still required in order to develop new therapeutic strategies. Interestingly, the non-canonical Wnt / PCP signaling is moving more and more into focus as a promising intervention target to prevent metastasis for example in breast cancer and chronic lymphocytic leukemia (Fultang *et al*, 2019; Choi *et al*, 2018; VanderVorst *et al*, 2019).

It is therefore important to further understand the respective signal pathways in order to be able to derive possible consequences from them, to find new biomarkers for breast cancer and, if necessary, to develop new therapeutic strategies.

## 1.4 Wnt signaling

The Wnt signaling pathway is named after its "Wnt" ligands. "Wnt" is a composition of Wg for "*wingless*" and "*Int-1*", whereby mutations in the *wingless* gene often lead to wingless mutants in drosophila (Nüsslein-Volhard & Wieschaus, 1980; Nüsslein-Volhard *et al*, 1984). The activation of the gene "*Int-1*", now known as Wnt1 promotes virus-driven breast cancer development in mice (Nusse & Varmus, 1982). The Wnt ligand family consists of about 19 Wnt ligands that can trigger different signaling cascades by their interaction with its receptor (Schubert & Holland, 2013). Wnt receptors comprise ten members of the Frizzled (Fzd) family and several co-receptors. The Wnt signaling pathway can be divided into the classical β-catenin-dependent (canonical) and the alternative β-catenin-independent (non-canonical) pathway (Fig.3). Non-canonical signaling was in the past and to some extent still today subdivided into the $Ca^{2+}$ and the planar cell polarity (PCP) signaling pathway.

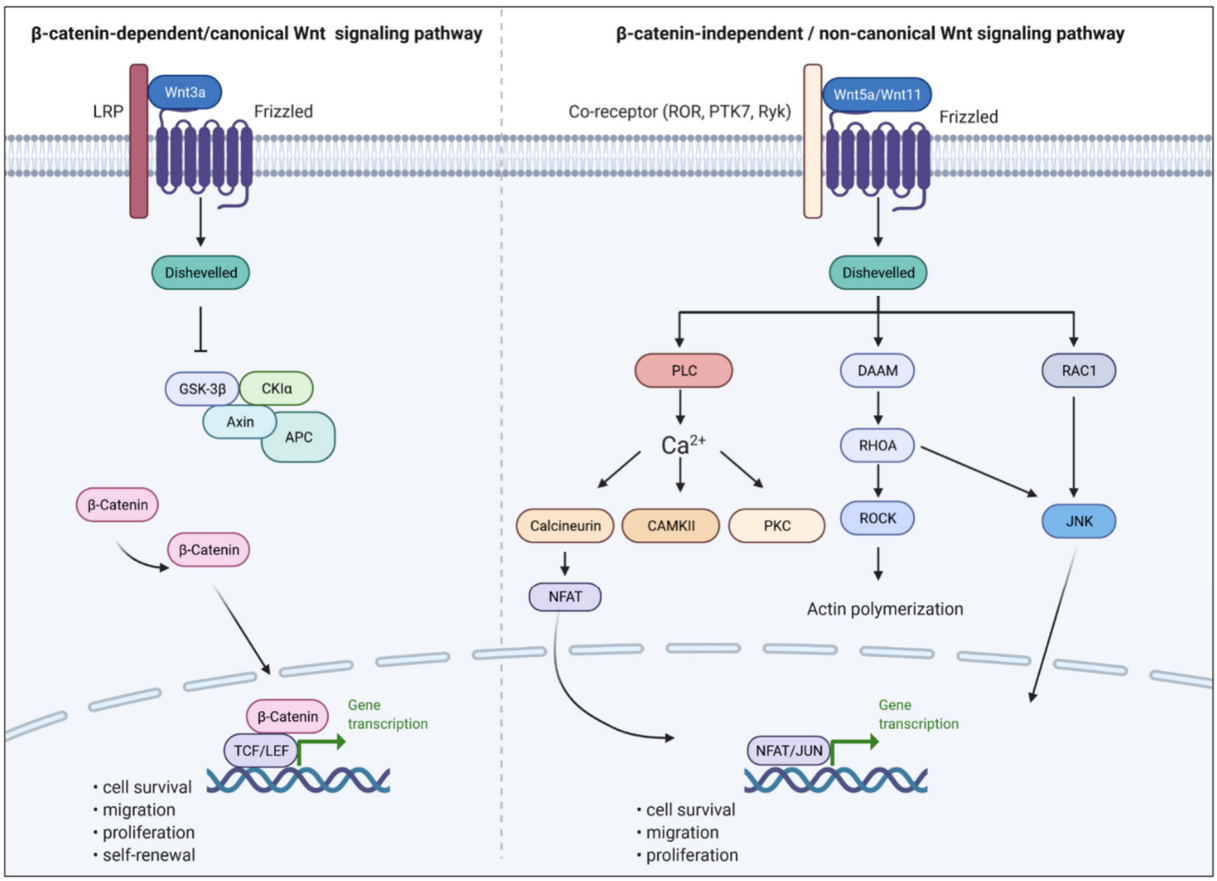


***Figure 3*: The Wnt signaling pathway at a glance:** The β-catenin dependent/canonical Wnt signaling pathway is activated when a Wnt ligand (e.g. Wnt3a) binds to a FZD and a co-receptor (e.g. lipoprotein receptor-related protein 5 and 6 [LRP5/6]) and thereby triggers the Dishevelled (DVL) protein to inhibit the destruction complex, consisting of glycogen synthase kinase-3 (GSK3), Axin, CKI and APC. Otherwise, the destruction complex targets cytoplasmic β-catenin for degradation. In the presence of Wnt ligands will β-catenin accumulate in the cytosol, because the destruction complex does not degrade β-catenin, resulting in its translocation into the nucleus where it binds to transcription factors of the LEF/TCF family and initiates the transcription of target genes associated with cell migration, proliferation and cell survival. The β-catenin independent/non-canonical Wnt signaling pathway is subdivided into the PCP and $Ca^{2+}$ signaling pathway. Both are activated by non-canonical Wnt ligands (e.g. Wnt5a, Wnt11) binding a FZD receptor and distinct co-receptor (e.g. ROR1/2, receptor tyrosine kinase [Ryk], protein tyrosine kinase 7 [PTK7]). In the $Ca^{2+}$ signaling pathway the interaction of Wnt ligands with its receptors thus triggers DVL to activate phospholipase C (PLC), resulting in increasing $Ca^{2+}$ levels in the cytoplasm. This on the other hand activates CAMKII, PKC and Calcineurin. Alternatively, Wnt ligands can recruit DVL that can activate the small GTPases RhoA (via Daam1) or Rac1, thereby inducing cytoskeletal rearrangements. (Created with biorender.com)

Wnt receptors comprise ten members of the Frizzled family (FZD) (Vinson *et al*, 1989) and the co-receptors encompass the low density lipoprotein receptor-related protein 5 and 6 (LRP5/6), protein tyrosine kinase 7 (PTK7) (Park *et al*, 1996), receptor tyrosine kinase (RYK) (Hovens *et al*, 1992), muscle skeletal receptor Tyr kinase (MUSK) (Fuhrer *et al*, 1997) and receptor Tyr kinase-like orphan receptor 1 and 2 (ROR1/2) (Masiakowski & Carroll, 1992). In total, 16 different Wnt ligands have been identified, whereby Wnt1 and Wnt3a are mostly characterized as canonical Wnt ligands, while Wnt5a and Wnt11 are traditionally rather associated with non-canonical Wnt signaling (Nygren *et al*, 2007; Young *et al*, 1998; Baarsma & Königshoff, 2013; Pandur *et al*, 2002). The combination of ligand, receptor and available co-receptor ultimately determines which Wnt sub pathway will be activated (Mikels & Nusse, 2006; Dijksterhuis *et al*, 2015).

### 1.4.1 Canonical Wnt signaling pathway

The best characterized Wnt signaling pathway is the β-catenin-dependent or canonical Wnt signaling pathway which was first described in 1982 by Nusse and Varmus (Nusse & Varmus, 1982). Here, the interaction of a canonical Wnt ligand (e.g. Wnt3a) with a FZD receptor and the LRP5/6 co-receptor recruits the intracellular scaffolding protein Dishevelled (DVL) (Corrigan *et al*, 2009; Dijksterhuis *et al*, 2015). The interaction of Wnt with its FZD receptor and LRP6 triggers a ternary complex formation (Tamai *et al*, 2000), thereby inducing an aggregation of ribosome-sized LRP6 signalosomes, required for LRP6 phosphorylation (Cong *et al*, 2004; Bilic *et al*, 2007). Furthermore, Axin was shown to interact with LRP5/6 through their intracellular domain at the phosphorylated PPPSP motif (Tamai *et al*, 2004; Mao *et al*, 2001), whereby GSK3 was shown to phosphorylate these PPPSP motifs. Interestingly, Casein kinase 1-γ (CK-1γ) phosphorylates on the other hand multiple sites within LRP5/6, thereby triggering the recruitment of Axin to LRP5/6 (Davidson *et al*, 2005). LRP6 not only initiates canonical Wnt signaling, but in addition, LRP6 was shown to inhibit non-canonical Wnt signaling (Bryja *et al*, 2009). In absence of Wnt, the destruction complex, consisting of GSK3, Axin, casein kinase I (CKI), and adenomatosis polyposis coli (APC) is formed. Casein kinase I (CKI) and GSK3 thereby phosphorylate β-catenin (Liu *et al*, 2002), which then initiates its ubiquitination and leads to its degradation in the 26S proteasome (Aberle *et al*, 1997). Under Wnt stimulation, GSK3-mediated phosphorylation is suppressed, thus leading to the accumulation of β catenin in the cytosol (Liu *et al*, 2002; van Noort *et al*, 2002). The β-catenin translocates into the nucleus, where it interacts with transcription factors of the T cell

factor (TCF) / lymphoid enhancer-binding factor (LEF) family which triggers the transcription of target genes associated with cell proliferation, survival and migration (Takemaru & Moon, 2000; Barker *et al*, 2001; Zhan *et al*, 2017).

### 1.4.2 Non-canonical Wnt signaling pathway

The non-canonical Wnt signaling pathway was mostly subdivided into the Wnt/planar cell polarity (PCP) and the Wnt/$Ca^{2+}$ pathway. Nowadays novel non-canonical Wnt signaling pathways were identified, including for instance the Wnt-dependent stabilization of proteins (Wnt/STOP) pathway (Acebron *et al*, 2014; Huang *et al*, 2015). The activation of the Wnt/Stop pathway was shown to inhibit GSK3β activity, resulting in the prevention of GSK3β-mediated degradation of proteins, including c-MYC (Acebron *et al*, 2014). In addition, the activation of this pathway was shown to increase the protein content required for cell division (Huang *et al*, 2015). However, this pathway is still largely unexplored. Furthermore, the Wnt/ROR signaling pathway was also described, with similarities to the Wnt/PCP signaling pathway and vice versa (Ho *et al*, 2012; Oishi *et al*, 2003; Menck *et al*, 2021). All these pathways are characterized by a β-catenin-independent Wnt signaling through the binding of a Wnt ligand to its FZD receptor and non-canonical Wnt co-receptors like ROR (Endo *et al*, 2012), PTK7 (Hayes *et al*, 2013) and Ryk (Andre *et al*, 2012). Interestingly, LRP6 predominantly categorized as canonical co-receptor, was shown to be also involved in β-catenin-independent Wnt/Stop signaling (Huang *et al*, 2015). In Wnt/PCP signaling a non-canonical Wnt ligand (e.g. Wnt5a) binds to a seven-pass transmembrane Frizzled (FZD) receptor and alternative co-receptor (e.g. PTK7) which recruits and activates DVL (Vinson *et al*, 1989; Wong *et al*, 2003). DVL, in turn, activates the small GTPases Rac1 and RhoA, the latter via Disheveled-associated activator of morphogenesis (Daam) (Liu *et al*, 2008; Endo *et al*, 2005). The small GTPases then activate RHO kinase (Rock) and Jun-N-terminal kinase (JNK), resulting in actin polymerization and microtubule (Marinissen *et al*, 2004). As a consequence, Wnt/PCP signaling thus regulates cell polarity in morphogenetic processes, as well as cell movement (VanderVorst *et al*, 2018). For example, in breast cancer cells it was shown that migration and metastasis was induced by PCP signaling in response to stromal cells (Luga *et al*, 2012). The second well-known non-canonical Wnt signaling pathway is the Wnt/$Ca^{2+}$ pathway, which can also be activated by stimulation of FZD receptors and its co-receptors with a non-canonical Wnt ligand, such as Wnt5a (McQuate *et al*, 2017). The translocation of PKC to the plasma membrane was shown to be induced by the

co-expression of FZD2 and Wnt5a in vitro, indicating an activation of PKC dependent on G proteins and β-catenin-independent for the first time (Sheldahl *et al*, 1999). This induction in turn initiates DVL to activate heterotrimeric G proteins, leading to an activation of the PLC which stimulates the production of diacyl-glycerol and inositol-1,4,5-trisphosphate (Ins(1,4,5) P3). As a result, intracellular $Ca^{2+}$ increases and activates effectors like $Ca^{2+}$- and calmodulin-dependent kinase II (CAMKII), calcineurin and protein kinase C (PKC) (Sheldahl *et al*, 2003). The activation of PKC results in actin polymerization, whereas Calcineurin activates the nuclear factor of activated T-cells (NFAT) that is associated with cell migration (9ou *et al*, 2011). In this study NFAT was shown to regulate the induction of the cell-surface glycoprotein glypican 6 (GPC6) that mediates migration and invasion. CAMKII and PKC were shown to inhibit the canonical Wnt pathway by impeding the interaction of β-catenin and TCF in the nucleus. Furthermore, it was demonstrated that the PCP and the β-catenin-dependent Wnt signaling pathway can antagonize each other. Wnt5a has been shown to preferentially initiate PCP signaling and can therefore inhibit the canonical Wnt signaling pathway (Bisson *et al*, 2015; Baarsma & Königshoff, 2013; Topol *et al*, 2003). Interestingly, however, Wnt5a has also been shown to induce not only non-canonical Wnt signaling but also canonical Wnt signaling (van Amerongen *et al*, 2012; Okamoto *et al*, 2014). As is now known, the classification of signaling pathways is therefore not entirely unambiguous but rather a rough classification.

#### 1.4.2.1 FZD receptors

There are various Wnt receptors in the Wnt signaling pathway, among them the receptors of the FZD family. They consist of an extracellular part with an N-terminal signal sequence, a highly conserved cysteine-rich domain (CRD), a seven-pass membrane domain and an intracellular part, which interacts with DVL after the binding of a Wnt ligand (Adler *et al*, 1990; Vinson *et al*, 1989; Wong *et al*, 2003). Ten different FZD receptors have been described so far (FZD1-FZD10). Every FZD receptor can interact with different Wnt ligands and therefore activate distinct subcellular Wnt signaling cascades (Dijksterhuis *et al*, 2015; Voloshanenko *et al*, 2017). Some FZD receptors, such as FZD1, are primarily associated with canonical Wnt signaling (Wang *et al*, 2005), while others tend to activate non-canonical Wnt signaling. There are also FZD receptors, like FZD2, that mediate both canonical and non-canonical Wnt responses (Gujral *et al*, 2014; Bazhin *et al*, 2010; Li *et al*, 2008). However, since most studies have focused primarily on Wnt3a and Wnt5a, it still remains unclear which

FZD receptors interact with which other Wnt ligands and which Wnt signaling response is activated by these interactions.

#### 1.4.2.2 Wnt co-receptors

For some receptors, it is unclear whether they can bind Wnts themselves, although they are more likely to interact with Wnts via FZDs and to induce signal transduction through this interaction. However, there are also co-receptors such as ROR1/2 and PTK7 that gain a Wnt-binding domain. This group of receptors was shown to interact directly with Wnts and partly also with each other (Bai *et al*, 2014; Martinez *et al*, 2015; Yu *et al*, 2017). Whether this group then still needs Fzds as interaction partners at all has not yet been conclusively clarified.

As mentioned before, Wnt co-receptors include LRP5/6, Ryk, PTK7 and ROR receptors. LRP5/6 primarily belong to canonical Wnt signaling, while ROR receptors, for example, are primarily assigned to non-canonical Wnt signaling (Sebastian *et al*, 2017; Bryja *et al*, 2009). LRP5/6 directly bind to FZD receptors and function as co-receptors for Wnt ligands. A 2015 study showed that the interaction of LRP5/6 with FZD8 prevents the FZD-regulated non-canonical Wnt signaling activation and therefore suppresses migration and metastasis of tumor cells (Ren *et al*, 2015). This in turn underlines the importance of the non-canonical Wnt signaling pathway with regard to metastasis and tumor progression (Binda *et al*, 2017; Liu *et al*, 2020). Receptor-like tyrosine kinases (Ryks) are highly conserved receptors and play a crucial role in embryogenesis (Lin *et al*, 2010). Ryk was shown to interact with the non-canonical Wnt ligand Wnt5a and FZD5 in prostate cancer and promotes non-canonical Wnt signaling (Thiele *et al*, 2018). It has been demonstrated that the knockdown of Ryk leads to inhibited cell migration, invasion and EMT in gastric cancer cells and suppresses tumorigenesis and liver metastasis in vivo (Fu *et al*, 2020). Protein tyrosine kinase 7 (PTK7) is another evolutionarily conserved non-canonical Wnt receptor that was previously found in colon cancer cells (Mossie *et al*, 1995). In several studies the importance of PTK7 in tumor progression was demonstrated by describing the effects of PTK7 on cell-cell communication, migration, tissue regeneration and cell polarity (Hayes *et al*, 2013, 7; Lhoumeau *et al*, 2015; Lander & Petersen, 2016; Lu *et al*, 2004). It was shown that high PTK7 expression is associated with carcinogenesis, tumor progression and metastasis in several cancer cell contexts (Shin *et al*, 2018; Tian *et al*, 2016; Lhoumeau *et al*, 2015; Ataseven *et al*, 2013). A further important family of non-canonical Wnt receptors are receptor tyrosine kinase-like

orphan receptors (ROR1/2), which play a crucial role in embryogenesis and are often associated with cancer progression and metastasis (Menck et al, 2021).

#### 1.4.2.3 ROR receptors – a family of its own

ROR receptors consist of an extracellular domain, containing the Ig-like domain, the cysteine-rich domain (CRD) and the kringle domain. The intracellular domain possesses a tyrosine kinase domain (TKD), two serine-threonine rich domains and frequently an interposed proline-rich domain (PRD) (Masiakowski & Carroll, 1992). It has been shown, that Wnt5a interacts with the ROR receptors via the cysteine-rich domain and triggers non-canonical Wnt signaling (Oishi *et al*, 2003; Mikels & Nusse, 2006; Enomoto *et al*, 2009; Fukuda *et al*, 2008). Both ROR receptors induce non-canonical Wnt signaling, but predominantly ROR2 seems to inhibit β-catenin-dependent WNT signaling (Yuan *et al*, 2011). Nevertheless, some studies demonstrated an Wnt3a-induced canonical Wnt signaling with ROR2, suggesting that ROR receptors cannot exclusively induce one signaling, but can induce different signaling by interacting with the corresponding Wnt ligand. (Li *et al*, 2008; Rasmussen *et al*, 2013; Flores-Hernández *et al*, 2020). Again, it is hypothesized that the output of Wnt/ROR signaling depends on the cellular context and the combination of available ligands and receptors. ROR receptors have been found to be overexpressed in several cancer entities and trigger tumorigenic processes such as cancer cell survival, migration, proliferation and invasion (Zhou *et al*, 2020; Hasan *et al*, 2017; Bayerlová *et al*, 2017). In fact, some studies have been able to show the association between high ROR1/2 expression and poorer survival in breast cancer (Henry *et al*, 2015b; Chien *et al*, 2016) Although most studies have acknowledged ROR1 as an oncogene, the role of ROR2 in cancer has been controversially discussed. For instance, in prostate cancer ROR2 was shown to suppress cell invasion, migration and epithelial–mesenchymal transition (EMT) (Tseng *et al*, 2020) and moreover inhibited the proliferation of gastric cancer cells through non-canonical Wnt signaling (Yan *et al*, 2016b). Other studies indicated the opposite, with ROR2 showing tumor-promoting properties. In contrast, preliminary results from our group demonstrated that ROR1/2 with its Wnt ligands Wnt5a/b mediates a highly motile and invasive phenotype in breast cancer cells via non-canonical Wnt signaling (Bleckmann *et al*, 2016; Bayerlová *et al*, 2017; Klemm *et al*, 2011). In 2017, RNA-seq analysis of MCF-7 cells overexpressing ROR2 revealed upregulation of Wnt11 (Bayerlová *et al*, 2017). This suggests a possible interaction of ROR2 with the non-canonical Wnt ligand Wnt11, although such an interaction has so far only been shown in

zebrafish (Bai *et al*, 2014). The question of whether Wnt11 also functions as a ligand for ROR2 in the human context remains unresolved.

#### 1.4.2.4 Wnt11 – a non-canonical Wnt ligand

The large Wnt family comprises at least 19 different Wnt proteins that are involved in different cellular processes, in particular during development. In one study WNT11 was found to play an important role in various steps in embryogenesis through non-canonical or canonical Wnt signaling (Tao *et al*, 2005; Lako *et al*, 1998). The misregulation of Wnts, in contrast, has been linked to cancer (Parsons *et al*, 2021; Enomoto *et al*, 2009; Gorroño-Etxebarria *et al*, 2019). Wnt11 was described as a ligand that can activate non-canonical Wnt signaling and can inhibit the canonical Wnt signaling pathway (Bisson *et al*, 2015). Wnt11 was thereby shown to trigger PCP signaling (Luga *et al*, 2012) and in its function as non-canonical Wnt ligand, it was demonstrated to activate PKC and JNK thereby increasing ATF2-dependent gene expression (Flaherty *et al*, 2008; Geetha-Loganathan *et al*, 2014; Zhou *et al*, 2007).

Not only non-canonical Wnt signaling itself, but specifically Wnt11 as non-canonical Wnt ligand itself, seems to hold importance in this regard. For instance, it has been shown that the overexpression of Wnt11 *in vitro* was associated with proliferation and migration of various tumor cells, including prostate, breast and colon cancer cells (Dwyer *et al*, 2010; Wei *et al*, 2016). In addition, Wnt11 could further be associated with proliferation and transformation of intestinal epithelial cells (Ouko *et al*, 2004). Consistent with these findings, it is suggested that Wnt11 occupies a critical role in metastasis and tumor progression.

Moreover it has been shown that Wnt11 is upregulated in different cancer entities and might function as prognostic biomarker or therapeutic target, for example in colorectal cancer (Gorroño-Etxebarria *et al*, 2019; Bond *et al*, 2003; Rodriguez-Hernandez *et al*, 2020). As a non-canonical Wnt ligand, Wnt11 can bind diverse receptors and thereby induce Wnt signaling. Which receptors Wnt11 can bind has not yet been conclusively determined. However, several receptors have already been linked to Wnt11, although not all studies have demonstrated a direct interaction. For example, one study investigated which FZD receptors can integrate Wnt11 and thereby induce transforming growth factor-β signaling in prostate cancer. Silencing of FZD8 had the largest effect reducing Wnt11 activation of ATF2-dependent transcription the most. A slight effect could also be induced by FZD2 silencing, whereas silencing of FZD3, FZD4, and FZD5 had no effect. Interestingly, FZD8 silencing

also led to a reduction in FZD5 expression. Co-localization and co-immunoprecipitation experiments confirmed the interaction of FZD8 and Wnt11 *in vitro* (Murillo-Garzón *et al*, 2018). However, Wnt11 has been shown to interact with FZD4 and FZD8 in mice (Ye *et al*, 2011), with FZD7 in Xenopus (Djiane *et al*, 2000; Yamanaka & Nishida, 2007), and moreover with FZD5 in zebrafish (Cavodeassi *et al*, 2005). An association between Wnt11 and FZD6 has been suggested in colorectal cancer, although a direct interaction of the proteins has not been demonstrated (Gorroño-Etxebarria *et al*, 2019). In addition, Wnt11 was shown to interact with ROR2 in zebrafish (Bai *et al*, 2014) and also with Ryk in Xenopus (Kim *et al*, 2008). Consistent with these findings, these results suggest that Wnt11 acts in a highly context-dependent manner and requires further investigation. Preliminary results have shown that Wnt11 is upregulated in ROR2 overexpressing MCF-7 cells, suggesting an interaction of the proteins (Bayerlová *et al*, 2017). However, which receptor of Wnt11 triggers the non-canonical Wnt signaling and thereby the aggressive behavior in breast cancer is still unclear and will be further investigated in this work.

## 1.5 Extracellular vesicles

The progression of cancer is based on the crosstalk of cancer cells and their microenvironment to generate a tumor-supporting setting which allows metastasis formation. To ensure this, extracellular vesicles (EV) can be secreted from tumor cells (Menck *et al*, 2013, 2015). EVs are small submicron particles that are surrounded by a lipid bilayer and released by all living cells. They were found in almost all body fluids like urine (Viñuela-Berni *et al*, 2015), blood (Wolf, 1967), breast milk (Zonneveld *et al*, 2014), ejaculate (Höög & Lötvall, 2015), bronchoalveolar lavages (Lyberg *et al*, 1990), and synovial fluid (György *et al*, 2011) and used for biomarker identification (Cheng *et al*, 2019). Their composition and size can vary, depending on the cell of origin and type of vesicle (Yáñez-Mó *et al*, 2015; Antonyak & Cerione, 2014) and they carry various cellular components such as DNA, RNA and proteins. There are different EV populations, which are divided into different categories: exosomes, microvesicles and large vesicles, as shown in Figure 4.

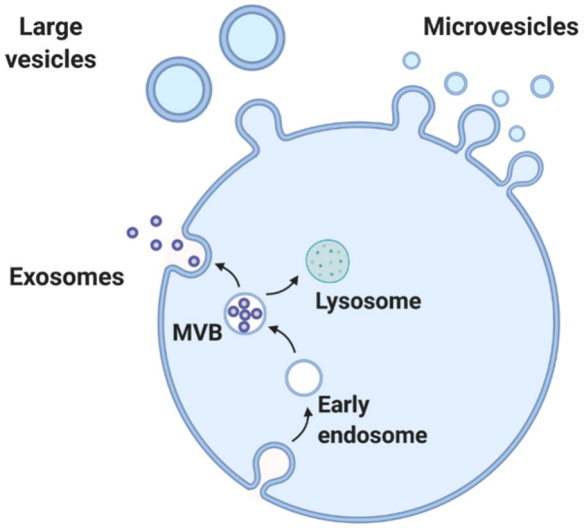


***Figure 4:*** **An overview of the various EV subtypes*:*** Every living cell can secrete different populations of EVs which differ in size and biogenesis. EXOS are small Evs and derive from intraluminal budding processes at late endosomal membranes thus creating the multivesicular body (MVB). EXOs are further released from fusion with the plasma membrane. In comparison, microvesicles (MV) and large vesicles (LV) originate by outward shedding from the cell membrane. (created with biorender.com)

EVs can release their cargo into target cells to perform various functions. For example, it was demonstrated that tumor-derived vesicles can generate a tumor-promoting microenvironment in target cells and thus drive cancer progression and metastasis (Abels *et al*, 2019; Hoshino *et al*, 2015). It has been shown that HeLa cells take up a variety of EVs, which are originally produced by different cells (Costa Verdera *et al*, 2017; Svensson *et al*, 2013). This argues for generic targeting, as EV uptake can also occur between different species such as human and mouse (Valadi *et al*, 2007). Most studies suggest internalization of EVs by target cells, although it is not yet clear how the uptake occurs. However, several surface proteins on EVs and target cells have been identified that appear to be involved in EV uptake and therefore could also be causative for specificity. For example, proteoglycans (Christianson *et al*, 2013) or integrins (Antonyak *et al*, 2011; Hoshino *et al*, 2015) have been identified as such. Currently, it is mostly assumed that EV uptake by endocytosis functions either in a clathrin-dependent or -independent manner (Tian *et al*, 2014; Costa Verdera *et al*, 2017), suggesting that the kind of uptake might be more acceptor cell type dependent than EV-dependent. So far, it has not been possible to elucidate what exactly happens during EV uptake. However, most studies suggest that EVs enter target cells through internalization and then deliver their cargo, presumably to the endosome. Lipids such as cholesterol and phosphatidylserine are

also thought to be involved in membrane fusion, as annexin V, predominantly present on many EV surfaces, has been shown to bind to phosphatidylserine and mediate the fusion of monocyte-derived EVs and activated platelets (Del Conde *et al*, 2005). Due to the fact that not all EVs contain phosphatidylserines (Arraud *et al*, 2014), it is most likely that other proteins are involved in this process. Interestingly, a direct transmission of EV components to the endoplasmic reticulum (Heusermann *et al*, 2016) or nucleus (Santos *et al*, 2018) was shown, although this should be investigated further.

### 1.5.1 Exosomes

The endosomal-derived small exosomes (EXOs) have a size of 50-150 nm and can be isolated by differential ultracentrifugation from cell culture supernatants or body fluids at 100.000xg (Théry *et al*, 2006). EXOs originate from intraluminal vesicles (ILVs) that are formed through inward budding of the membrane of late endosomes which thus become multivesicular bodies (MVB). These MVBs can then either fuse with the lysosome which leads to the degradation of their cargo, or they can fuse with the plasma membrane and release the ILVs as EXOs. They can be characterized by specific marker proteins like the CD63, CD9, CD81, syntenin and ALG-2 Interacting protein X (Alix) (Deng & Miller, 2019).

Syndecans belong to the proteoglycans, which are multiply localized on the cell membrane (Brauker *et al*, 1991). When a ligand such as EGFR binds to syndecans by their heparan-sulfate chains (Wang *et al*, 2015), initiating a chain reaction that can ultimately emerge exosomes. Interestingly, EGFR is frequently mutated in several cancer types and can also be found on EXOs from cancer-derived tumor cells or patient blood samples (Ortega *et al*, 2019; Li *et al*, 2020; Nanou *et al*, 2020). The exosome biogenesis is initiated by this interaction of syndecan with its ligands. Through endocytosis receptor-bound and soluble cargo proteins are transported into the cell within and at the membrane of so-called “early endosomes”, on which many syndecans are now localized (Baietti *et al*, 2012). The small GTPase ADP-ribosylation factor 6 (ARF6) and the tyrosine kinase SRC phosphorylate PLD2, which in turn catalyzes Phosphatidic acids (Pas) on the membrane (Imjeti *et al*, 2017; Roucourt *et al*, 2015). This results in enriched amounts of tetraspanins like CD63 and CD9 at the endosomal membrane (Abels & Breakefield, 2016), which is why these proteins are used as marker proteins for EXOs. The adapter scaffold protein syntenin binds then to the C-terminus of syndecans (Baietti *et al*, 2012), initiating Alix to bind syntenin and therefore the syndecan-syntenin-ALIX complex is formed, which in turn can interact with the ”Endosomal Sorting

Complexes Required for Transport'' (ESCRT) machinery. This leads to reconstruction in the late endosome, resulting in intraluminal vesicles (ILVs) in the now designated multivesicular body (MVB) (Baietti *et al*, 2012). These MVBs can then either be degraded in the endolysosome or fuse with the membrane with the help of Rab proteins and can then release their ILVs as EXOs (Baietti *et al*, 2012). The ESCRT-independent pathway is associated with a sphingolipid ceramide and raft-based microdiams that cause a membrane constriction (Trajkovic *et al*, 2008). Although the entire process is not yet fully understood, it has been shown that ceramides seem to be important for reprogramming the tumor microenvironment and that they can be found on lipid rafts in EXO membranes (Elsherbini & Bieberich, 2018).

### 1.5.2 Microvesicles

Microvesicles (MVs) are characterized by a size range of 100 – 1000 nm and they can be isolated by differential ultracentrifugation at 10.000-20.000xg from cell culture supernatants or patient blood samples. The biogenesis of MVs differs significantly from that of EXOs, as the MVs are generated by outward budding of the cell membrane (Raposo & Stoorvogel, 2013) and their release can be triggered by proliferation, inflammation, shearing stresses and increased cytosolic calcium levels (George *et al*, 1982; Holme *et al*, 1997; Yu *et al*, 2006; Ginestra *et al*, 1999; Crawford *et al*, 2010). Through intracellular $Ca^{2+}$ increase the cysteine protease calpain is activated, which leads to Talin degradation (Miyoshi *et al*, 1996) and therefore destabilizes the membrane (Piccin *et al*, 2007; Kunzelmann-Marche *et al*, 2001). Interestingly, calpain translocates to the membrane cytoskeleton interface and co-localizes with the $Ca^{2+}$ channel TRPM7. Moreover, its activation was shown to be associated with increased vesicle shedding (Taylor & Bebawy, 2019). TRPM7 was shown to be overexpressed in several human cancers and regulates cell migration through calcium influx (Rybarczyk *et al*, 2012; Chen *et al*, 2017a; Gao *et al*, 2017). This might be the explanation of increased vesicle shedding of cancer cells compared to benign cells.

Furthermore, the formation and shedding of MVs were shown to be associated with cholesterol and ceramide (Del Conde *et al*, 2005). Inhibition of the neutral sphingomyelinase activity, and therefore the reduced hydrolysis of lipid sphingomyelin into phosphorylcholine and ceramide, led to a reduction of EXO concentrations, but at the same time increased MV release (Menck *et al*, 2017), indicating that reduced ceramide lead to increased MV release. This indicates that ceramide triggers the budding of MVs. Moreover, it has been demonstrated that the small GTPase protein ARF6 activates a signaling cascade, resulting in a contraction

of actomyosin, which stimulates MV release at the cell membrane (Muralidharan-Chari *et al*, 2009). Furthermore, Ras homolog family member A (RhoA) and further downstream proteins regulate actin cytoskeletal movement and are therefore important for MV release (Li *et al*, 2012a). In conclusion, this leads to the suggestion that cytoskeletal movements and dynamics are important for MV budding and their release.

Based on the fact that ARF6 is associated with MV and EXO biogenesis, although it was higher expressed on MVs and LVs (Di Vizio *et al*, 2012), the question of suitable markers arose. Preliminary results of this working group indicated Kif4 as a promising marker protein for the characterization of MVs. Rgap1 and α-Actinin4 have already been described as MV marker (Kowal *et al*, 2016; Dozio & Sanchez, 2017) Both LVs and MVs are shed off by the plasma membrane, so it is not surprising that these two EV populations show similarities regarding their protein composition (Minciacchi *et al*, 2015).

### 1.5.3 Large vesicles

Comparable to MVs, large vesicles (LVs) shed off directly from the plasma membrane (Di Vizio *et al*, 2009). They exhibit a size of 1 – 10 µm and can be isolated by centrifugation at 1.500-2.000xg. They have been found in a variety of different tumor entities, including glioma (Yekula *et al*, 2020), melanoma (Surman *et al*, 2018) as well as breast (Wright *et al*, 2014), colorectal (Kang *et al*, 2019) and prostate cancer (Ciardiello *et al*, 2019). It appears that all cancer cells and benign cells, as well as cells from the tumor microenvironment are able to secrete LVs (Ciardiello *et al*, 2016).

Since LVs, like MVs, are directly shed from the plasma membrane, it is not entirely clear to what extent the biogenesis of both EV populations differs. Again, the intracellular calcium increase is thought to enable the shedding of LVs by activating divergent proteins involved in plasma membrane remodulation (Surman *et al*, 2018; Ender *et al*, 2019). In line with this, it is reasonable to assume that calcium-dependent activation of calpain also enables remodulation of the plasma membrane. Alterations of the cytoskeleton and increased cholesterol in the plasma membrane (Ciardiello *et al*, 2020) was demonstrated to lead to an increased release of LVs (Ciardiello *et al*, 2019). Cytokeratin 18 (CK18) was detected as a marker for LVs from tumor cells or plasma (Minciacchi *et al*, 2015). Although Rgap1 and α-Actinin4 have been used as MV markers, they seem to be expressed on LVs as well (own unpublished observation). Therefore, Rgap1, α-Actinin4 and CK18 were used as LV markers in this study.

### 1.5.4 Extracellular vesicles in cancer

The communication between cells is very important and EVs are one of the communication tools of cells. EVs are released not only from benign cells but also from tumor cells, which use EVs to modulate the surrounding stroma cells and thus create a permissive microenvironment for cancer progression and metastasis. Interestingly, it could be shown that the concentration of several cancer cell-derived EVs is considerably higher than that of benign cells (Baran *et al*, 2010; Tesselaar *et al*, 2007; Galindo-Hernandez *et al*, 2013; König *et al*, 2017). In tumor progression, the tumor microenvironment (TME) plays a crucial role. In early stages, the microenvironment assumes antitumor features by controlling tumor growth. As this progression develops, the characteristics of the TME shift to tumor-promoting features, with various regulators coming into play (Sullivan *et al*, 2017). It has been shown that signaling exchange occurs not only through direct contact between tumor cells and benign cells of the TME, but also through secreted EVs that act as intercellular communication mediators (Menck *et al*, 2015; Sullivan *et al*, 2017). In this process, they contain various cargoes such as proteins, lipids and nucleic acids, which are protected from enzymatic degradation by the lipid bilayer (Raposo & Stoorvogel, 2013). Cancer-derived EVs mediate tumor-promoting effects in target cells, such as increased proliferation, invasion and angiogenesis (Corcoran *et al*, 2012; Al-Nedawi *et al*, 2008; Maji *et al*, 2017). Wnt signaling was found to trigger cell proliferation and was therefore linked to a higher EV release (Sándor *et al*, 2021). Tumor-derived EVs (MVs and EXOs) have been shown to induce Wnt5a in tumor-associated macrophages. Also the macrophage-derived EVs transferred Wnt5a to target cells and induced non-canonical Wnt signaling, resulting in increased cell invasiveness (Menck *et al*, 2013). This indicates a bidirectional communication between the tumor microenvironment and tumor cells via EVs.

Since EVs can be secreted by all cells and induce tumor-supporting effects in target cells, EVs have become the focus of attention in the search for suitable biomarkers. EVs can be isolated from various body fluids and subsequently analyzed. One example displays the extracellular matrix metalloproteinase inducer (EMMPRIN) as it was found to be enriched on tumor MVs and was also associated with poorer overall survival in breast cancer (Zhao *et al*, 2013).

In addition, cancer cell-derived MVs have been shown to induce breast cancer cell invasion via EMMPRIN (Menck *et al*, 2015), suggesting that EMMPRIN might function as an interesting biomarker for breast cancer. This raises the question of what other proteins are transferred via EVs and whether they can be used as biomarkers and possibly as potential targets for cancer therapies.

### 1.5.5 Interaction of Wnt proteins and EVs

Aberrant activation of Wnt signaling has been associated with tumor development and progression in several cancer entities, including breast and colorectal cancer. Wnt ligands belong to the lipid-modified glycoproteins, which bind the cell surface receptor protein FZD. Lipid modifications are required for the binding to its FZD receptors, which involves covalent binding of palmitic acid to the first cysteine residue and, in addition, binding of palmitoleic acid to the highly conserved serine residue. In addition, glycosylation of Wnts was shown to be necessary for their secretion (Kurayoshi *et al*, 2007). These lipid modifications render the proteins hydrophobic; and moreover they are chaperoned in vivo by heparan sulfate proteoglycans to prevent clumping (Fuerer *et al*, 2010). Accordingly, the question arose as to how Wnt proteins, despite their hydrophobic properties, can be transported from cell to cell and continue to functionally induce Wnt signaling at their target cells. It has been demonstrated that Wnt ligands, such as Wnt3a and Wnt5a can be transferred to distant cells on EVs (Gross *et al*, 2012; Menck *et al*, 2013). EVs carrying Wnt proteins were shown to mediate Wnt signaling in different cancer subtypes, including breast cancer (Luga *et al*, 2012; Chen *et al*, 2017b), colorectal cancer (Harada *et al*, 2017), B-cell lymphoma (Koch *et al*, 2014) and further subtypes. Interestingly, EXOs secreted by fibroblasts enhanced the motility and metastasis in breast cancer cells by the activation of PCP/Wnt signaling. Therefore, the association of these EXOs with Wnt11 was indispensable, indicating a crosstalk between stroma and tumor cells (Luga *et al*, 2012). Moreover, it was shown that Wnt5a is not only transferred to target cells on EXOs and MVs, but furthermore that EV-transferred Wnt5a was shown to be signal active in SKBR3 breast cancer cells (Menck *et al*, 2013). Not only Wnt ligands themselves, but also Wnt receptors were recently detected on EVs. Scavo and colleagues identified FZD10 on EVs and observed it to trigger cell proliferation in gastric, hepatic, colorectal and bile duct cancer cells (Scavo *et al*, 2019). This finding raised the question of whether EVs carrying FZD10 can function as biomarkers in intestinal cancer patients. Indeed, FZD10-positive EVs were found to be increased in plasma of colorectal and gastric cancer patients and were associated with tumor progression (Scavo *et al*, 2019a). Considering the fact that Wnt proteins are transferred to target cells by EVs and can trigger there non-canonical Wnt signaling, the question arises to what extent the transport of Wnt proteins and the associated activation of Wnt signaling influences the MV biogenesis itself. Several studies have demonstrated that ROR/Wnt signaling affects the activation of RhoA and Rho-Associated Coiled-Coil Kinase 1 (ROCK1) in breast cancer (Roarty *et al*, 2017). This point seems particularly interesting because it has also been demonstrated that RhoA itself

plays a central role in MV biogenesis. RhoA was shown to trigger a specific signaling pathway that is crucial for MV biogenesis. Inhibiting the activation of different proteins in this pathway blocks the MV biogenesis and consequently tumor progression in mice through RhoA activation (Li *et al*, 2012a). Therefore, it would be interesting to investigate whether Wnt receptors can also be transferred via EVs and induce Wnt signaling in target cells.

## 1.6 Aims of this work

Breast and colorectal cancer are linked to Wnt signaling expression (Koveitypour *et al*, 2019; Bleckmann *et al*, 2016; Bayerlová *et al*, 2017, Bienz & Clevers, 2000). Several members of the Wnt signaling pathway like ROR1/2 or FZD receptors have been linked to an aggressive cancer cell phenotype and poor clinical outcome (Zhang *et al*, 2012; Chien *et al*, 2016; Bayerlová *et al*, 2017; Yang *et al*, 2011; Yin *et al*, 2013). Non-canonical signaling appears to play an important role in metastasis in breast cancer (Bleckmann *et al*, 2016; Klemm *et al*, 2011; Bayerlová *et al*, 2017) whereas its relevance in CRC has not yet been clearly elucidated, as predominantly canonical Wnt signaling has been identified as a main driver. Preliminary data have shown that in breast cancer, ROR1+2 in particular may play an important role in metastasis, as they are highly expressed here. ROR1/2 was shown to be associated with poorer patient survival in breast cancer (Chien *et al*, 2016; Zhang *et al*, 2012a; Henry *et al*, 2015b). In search of the underlying molecular mechanisms of ROR signaling, RNA-Seq analysis has shown that high expression of ROR2 leads to upregulation of Wnt11 (Bayerlová *et al*, 2017). This finding was very surprising, since this interaction had not been identified yet in humans. Studies in zebrafish have shown that Wnt11 may be a novel ligand for ROR2 (Bai *et al*, 2014). Whether other receptors for WNT11 exist in breast cancer is not yet known. In addition, the question arises whether WNT receptors (Menck *et al*, 2013), similar to WNT ligands, can also be transferred to surrounding cells via EVs and may be functionally involved in the establishment of a promoting microenvironment here.

These objectives are to be achieved by answering the following questions:

*E) Which ligand binds the non-canonical receptor ROR2?*

In order to answer this question, a gene expression analysis of several breast and colorectal cancer cell lines will first provide information about available Wnt receptors and co-receptors. Based on previous data, Wnt11 might act as a promising ligand for ROR2 and further FZD

receptors. Subsequently, a co-immunoprecipitation (Co-IP) protocol will be established to detect a possible interaction of the potential ligand for ROR2 and further receptors.

*2) What impact do these interactions have on tumor progression of breast cancer cells?*

The functional impact of the identified interactions on breast cancer cell proliferation, migration and invasion will be clarified by performing different cell line modifications (i.e. overexpression, knockdown, stimulation) followed by analysis of their effect in functional assays. Sequential deletions of the individual receptor domains can then be used in structure-function-analyses to further pin down the exact domains implicated in receptor function. In addition, various gene expression analyses of microarray data from primary breast cancer patients will be performed in cooperation with bioinformatics to determine whether there is a correlation between the expression of those non-canonical Wnt receptors investigated here and the clinical outcome regarding overall and metastasis-free survival of breast cancer patients.

*3) Are ROR receptors expressed on extracellular vesicles and are they involved in EV biogenesis?*

The next step is to clarify whether ROR receptors can also be transferred via EVs and, if so, on which EV subpopulation they are expressed. Cell line modifications will then help to determine whether ROR1/2 have an influence on the respective vesicle composition, size or concentration.

*4) Does ROR1 have a functional impact on EVs in regards to cancer cell invasiveness?*

In line with the preliminary results, showing that tumor cell-derived EVs are able to increase the cell invasiveness of surrounding cells, the question is if ROR1/2 plays a role in this effect. Therefore, the last step will then elucidate whether and to what extent EVs of ROR1-modified cells affect the invasiveness of MCF-7 cells.

# 2. Material and Methods

## 2.1 Material

### 2.1.1 Cell lines

***Table 1: Cell lines***

| Cell line | Cell type | characteristics | Obtained from | Reference |
|---|---|---|---|---|
| MCF-7 | Human breast cancer cell line | ER+, PR+, Her2- | ATCC | (Soule *et al*, 1973; Brooks *et al*, 1973) |
| MDA-MB231 | Human breast cancer cell line | ER-, PR-, Her2- | ATCC | (Cailleau *et al*, 1974) |
| SKBR3 | Human breast cancer cell line | ER-, PR-, Her2+ | ATCC | (Trempe, 1976) |
| T47d | Human breast cancer cell line | ER+, PR+, Her2- | AG Götte | (Freake *et al*, 1981, 47) |
| SW48 | Human colorectal cancer cell line | CSAp negative | AG Prof. Felix Brembeck | (Leibovitz *et al*, 1976) |
| MCF-7 pROR2 | Human breast cancer cell line | overexpression of hROR2 | Alexandra Schambony | (Bleckmann *et al*, 2016; Bayerlová *et al*, 2017) |
| MCF-7 pcDNA3.1 | Human breast cancer cell line | overexpression of empty vector | AG Prof. Claudia Binder | (Bleckmann *et al*, 2016; Bayerlová *et al*, 2017) |
| MCF-7 pROR2 Δig | Human breast cancer cell line | overexpression of hROR2 with deletion of Ig-like domain | Obtained from this work | (Menck *et al*, 2020) |
| MCF-7 pROR2 Δig ΔCRD | Human breast cancer cell line | overexpression of hROR2 with deletion of Ig-like and cysteine-rich domain | Obtained from this work | (Menck *et al*, 2020) |
| MCF-7 pROR2 Δig ΔCRD ΔKr | Human breast cancer cell line | overexpression of hROR2 with deletion of the extracellular domain | Obtained from this work | (Menck *et al*, 2020) |
| MCF-7 pROR2, pROR2_ΔPRDΔTKD | Human breast cancer cell line | overexpression of hROR2 with deletion of the proline-rich and tyrosine kinase domain | Obtained from this work | (Menck *et al*, 2020) |

| | | | | |
|---|---|---|---|---|
| MCF-7 pROR2, pROR2_ΔPRD | Human breast cancer cell line | overexpression of hROR2 with deletion of the proline-rich domain | Obtained from this work | (Menck *et al*, 2020) |
| MCF-7 pWnt11 | Human breast cancer cell line | overexpression of hWnt11 | AG Prof. Claudia Binder | (Kim *et al*, 2020) |
| MCF-7 pcDNA3.2 | Human breast cancer cell line | overexpression of empty vector | AG Prof. Claudia Binder | |
| MCF-7 V5-Wnt11 | Human breast cancer cell line | overexpression of V5-tagged Wnt11 | AG Prof. Claudia Binder | (Menck *et al*, 2020) |
| MCF-7 pCMV | Human breast cancer cell line | overexpression of empty vector | Obtained from this work | |
| MCF-7 pROR1 | Human breast cancer cell line | overexpression of hROR1 | Obtained from this work | |
| MCF-7 pFZD6-Flag | Human breast cancer cell line | overexpression of FLAG-tagged hFzd6 | Obtained from this work | |
| MCF-7 CRISPR FZD6 | Human breast cancer cell line | Knockout of FZD6 | Obtained from this work | |
| MCF-7 CRISPR ctl | Human breast cancer cell line | transfection of empty vectors without sgRNA | Obtained from this work | |
| MDA-MB231 CRISPR ROR1 | Human breast cancer cell line | Knockout of ROR1 | Obtained from this work | |
| MDA-MB231 CRISPR ctl | Human breast cancer cell line | transfection of empty vector without sgRNA | Obtained from this work | |

### 2.1.2 Cell culture media and additives

***Table 2: Media and additives for cell culture***

| **Name** | **Company** |
|---|---|
| DMEM/F12 | PAN $^{TM}$ Biotech |
| FCS | Anprotec |
| FugeneHD | Promega (#E231A) |

| | |
|---|---|
| K4® Transfection System | Biontex (#T080-1.0) |
| OptiMEM | Gibco |
| PBS w/o $Ca^{2+}$, w/o $Mg^{2+}$ | PAN $^{TM}$ Biotech |
| Recombinant Wnt11 (rWnt11) | R&D (#6179-WN/CF) |
| RPMI-1640 | PAN $^{TM}$ Biotech |
| RNAimax Lipofectamine | Thermo Fisher (#2067506) |
| Trypan blue | Sigma |
| Trypsin 10x | Biochrom |

### 2.1.3 Bacteria

***Table 3: Bacteria***

| Name | Company |
|---|---|
| *E. coli* 5-alpha F'$I^q$ | NEB |
| *E. coli* 10-beta | NEB |
| *E. coli* DH5α | Thermo Fisher |
| *E. coli* Stable3 | Thermo Fisher |
| *E. coli* Top10 | Thermo Fisher |

### 2.1.4 Plasmids

***Table 4: Plasmids***

| Name | Backbone | Insert | Reference |
|---|---|---|---|
| active Wnt11-V5 | pcDNA3.2/V5-DEST | active form of hWnt11 | Active Wnt11-V5 was a gift from Xi He (Addgene plasmid #43824; http://n2t.net/addgene:43824; RRID: Addgene_43824) |
| pCMV3 | pCMV3-hSMPD3 | hSMPD3 sequence cut out by KpnI+XbaI | Kerstin Menck |
| pcDNA3.1 | pcDNA3.1/Zeo (+) | none | Invitrogen |

| | | | |
|---|---|---|---|
| pcDNA3.2 | pcDNA3.2 | sequence of hWnt11 removed by SacII from Addgene #35922 | Florian Klemm |
| pFZD6-FLAG | pCMV3 | hFZD6 full length with C-terminal FLAG-tag | Sinobiological #HG16004-CF |
| pROR1 | pCMV3 | hROR1 full length | Sinobiological #HG13968-UT |
| pROR2 | pcDNA3.1 neo | hRor2 full length | kindly provided by A. Schambony |
| pROR2_Δlg | pcDNA3.1 neo | hRor2 with deletion of bp 1-435 | Obtained from this work |
| pROR2_ΔIgΔCRD | pcDNA3.1 neo | hRor2 with deletion of bp 1-909 | Obtained from this work |
| pROR2_ΔIgΔCRDΔKr | pcDNA3.1 neo | hRor2 with deletion of bp 1-1182 | Obtained from this work |
| pROR2_ΔPRDΔTKD | pcDNA3.1/Zeo (+) | hRor2 with stop codon at amino acid position 467 | hRor2 mit Stop codon bei AS 783, non-tagged |
| pROR2_ΔPRD | pcDNA3.1/Zeo (+) | hRor2 with stop codon amino acid position 783 | hRor2 mit Stop codon bei AS 783, non-tagged |
| pWnt11 | pcDNA3.2 | hWnt11 full length | pcDNA-Wnt11 was a gift from Marian Waterman (Addgene plasmid #35922; http://n2t.net/addgene:35922; RRID: Addgene_35922) |
| PX461-GFP_hFzd4_#1 | pSpCas9n(BB)-2A-GFP | sgRNA for hFzd4 (targeting Exon 1) | Obtained from this work |
| PX461-mCh_hFzd4_#2 | PX461-mCh | sgRNA for hFzd4 (targeting Exon 1) | Obtained from this work |
| PX461-GFP_hFzd4_#3 | pSpCas9n(BB)-2A-GFP | sgRNA for hFzd4 (targeting Exon 1) | Obtained from this work |
| PX461-mCh_hFzd4_#4 | PX461-mCh | sgRNA for hFzd4 (targeting Exon 1) | Obtained from this work |

| | | | |
|---|---|---|---|
| PX461-GFP_hFzd6_#1 | pSpCas9n(BB)-2A-GFP | sgRNA for hFzd6 (targeting Exon 2) | Obtained from this work |
| PX461-mCh_hFzd6_#2 | PX461-mCh | sgRNA for hFzd6 (targeting Exon 2) | Obtained from this work |
| PX461-GFP_hFzd6_#3 | pSpCas9n(BB)-2A-GFP | sgRNA for hFzd6 (targeting Exon 2) | Obtained from this work |
| PX461-mCh_hFzd6_#4 | PX461-mCh | sgRNA for hFzd6 (targeting Exon 2) | Obtained from this work |
| PX461-GFP | pSpCas9n(BB)-2A-GFP | Cas9n (D10A nickase mutant) from S. pyogenes with 2A-EGFP, cloning backbone for sgRNA | pSpCas9n(BB)-2A-GFP (PX461) was a gift from Feng Zhang (Addgene plasmid #48140; http://n2t.net/addgene:48140 ; RRID:Addgene_48140) |
| PX461-GFP_hROR1_#1 | pSpCas9n(BB)-2A-GFP | sgRNA for hRor1 (targeting Exon 1) | Obtained from this work |
| PX461-mCh_hROR1_#2 | PX461-mCh | sgRNA for hRor1 (targeting Exon 1) | Obtained from this work |
| PX461-GFP_hROR1_#3 | pSpCas9n(BB)-2A-GFP | sgRNA for hRor1 (targeting Exon 2) | Obtained from this work |
| PX461-mCh_hROR1_#4 | PX461-mCh | sgRNA for hRor1 (targeting Exon 2) | Obtained from this work |
| PX461-mCherry | pSpCas9n(BB)-2A-GFP | GFP substituted for mCherry | kindly provided by P. Zimmermann |

### 2.1.5 Antibodies

**Table 5: Antibodies**

| Target | Conjugat | Dilution | Host species | Company |
|---|---|---|---|---|
| a-Actinin 4 | | 1:1000 | mouse | #sc-390205, Santa cruz |
| Alix | | 1:1000 | mouse | #sc-53540, Santa cruz |
| Calregulin | | 1:1000 | mouse | #sc-166837, Santa cruz |
| CD9 | | 1:1000 | mouse | #sc-13118, Santa cruz |
| CD63 | | 1:1000 | mouse | #sc-5275, Santa cruz |
| CD81 | | 1:1000 | mouse | #sc-166028, Santa cruz |
| FLAG | | 1:1000 | mouse | #9A3, cell signaling |

| | | | | |
|---|---|---|---|---|
| FZD6 | | 1:1000 | rabbit | #5158S, cell signaling |
| GAPDH | | 1:1000 | mouse | #sc-3233, Santa cruz |
| GM130 | | 1:1000 | rabbit | #12480, cell signaling |
| IgG | | 1 µg Co-IP | rabbit | #2729, cell signaling |
| IgG | | 1,5 µg Co-IP | mouse | # M 5284, Sigma |
| rabbit IgG (Conformation-specific) | | 1:2000 | mouse | #3678, cell signaling |
| RGap1 | | 1:1000 | mouse | #sc-76335, Santa cruz |
| ROR1 | | 1:2000 | rabbit | #4102, cell signaling |
| ROR2 | | 1:1000 | rabbit | #sc-98486, Santa cruz |
| ROR2 | | 1:1000 | mouse | #sc-374174, Santa cruz |
| ROR2 | | 1:2000 | mouse | #FAB20641G, R&D |
| Syntenin | | 1:2000 | rabbit | #133267, abcam |
| Tubulin | | 1:1000 | mouse | #sc-8035, Santa cruz |
| V5 | | 1:2000<br>1 µg (Co-IP) | rabbit | #13202, cell signaling |
| V5 | | 1,5 µg (Co-IP) | mouse | #SAB2702199, Sigma |
| rabbit | HRP | 1:10.000 | goat | #7074, cell signaling |
| mouse | HRP | 1:10.000 | horse | #7076, cell signaling |
| mouse IgG | FITC | 1:500 | goat | #sc-2010, Santa cruz |
| CD326/EpCAM- | APC | | mouse | #324208, BioLegend |
| CD340/Her2- | APC | | mouse | #324407, BioLegend |
| IgG1κ - | APC | | mouse | #324407, BioLegend |
| IgG1κ | PE | | mouse | #400113, BioLegend |
| IgG2a | AlexaFluor488 | | mouse | #IC003G, R&D systems |
| Ror1 | PE | | mouse | #357803, BioLegend |
| Ror2 | AlexaFluor488 | | mouse | #FAB20641G, R&D systems |

### 2.1.6 Equipment

***Table 6: Equipment***

| Type | Name | Company |
|---|---|---|
| Agarose Gel Imager | Epichemi 3 Darkroom | Intas |
| Autoclave | Systec VX-95 | Systec |
| cell counting chamber | Neubauer cell counting chamber | Brand |
| Centrifuge | Labofuge M | Heraeus |
| Centrifuge | Universal 320R | SEPATECH<br>Hettich Zentrifugen |
| Centrifuge | BIOFUGE fresco | Heraeus |
| Chemiluminescence imager | Amersham Imager 600 | GE Healthcare |
| Chemiluminescence imager | ChemoStar | Intas |

| | | |
|---|---|---|
| Confocal microscope | FV 1200 | Olympus |
| Ultracentrifuge | Optima XPN-60 | Beckman Coulter |
| Flow cytometer | Attune Nxt | Thermo Scientific |
| Incubator | BBD 6220 | Heraeus |
| Incubator | BB 6620 | Heraeus |
| Incubator | Function line | Function line |
| Laminar flow | HS12 | Heraeus |
| Laminar flow | CleanAir | PMV |
| Microscope | Axio Cam Mrm | Zeiss |
| Microplate photometer | Victor X3 | PerkinElmer |
| NanoDrop | NanoDrop 1000 | Thermo Scientific |
| Nanoparticle tracking device | ZetaView videomicroscope PMX-120 | ParticleMetrix |
| PCR cycler | Mastercycler personal | Eppendorf |
| Pipetting aid | Pipetboy 2 | Integra |
| pH meter | FiveEasy | Mettler Toledo |
| Photometer | bio Photometer | Eppendorf |
| Photometer | Photometer infinite F50 | Tecan |
| qRT-PCR cycler | 7500 Fast Real-Timer PCR system | Applied Biosystems |
| Rotor | TLA-55 | Beckman Coulter |
| Rotor | SW 32/32.1 Ti | Beckman Coulter |
| Shaking plate | BenchRocker | Benchmark |
| Thermomixer | Thermomixer compact | Eppendorf |
| Ultracentrifuge | Optima MAX-XP | Beckman Coulter |
| Water bath | Water bath | Köttermann Jürgens |

### 2.1.7 Kits

***Table 7: Kits***

| Kits | Company |
|---|---|
| CellTrace™ Violet Cell Proliferation Kit | Thermo Scientific |
| DC Protein Assay (Lowry assay) | BioRad |
| High Pure RNA isolation Kit | Roche |
| innuPREP Plasmid Mini Kit 2.0 | Analytik Jena |
| Monarch® PCR & DNA Cleanup Kit | New England Biolabs |
| Monarch® Plasmid Miniprep Kit | New England Biolabs |
| NucleoSpin™ Gel and PCR Clean-up Kit | Macherey-Nagel |

### 2.1.8 Chemicals, Materials and Reagents

***Table 8: Chemicals, Material and Reagents***

| Chemicals | Company |
|---|---|
| 2-ß-Mercaptoethanol | PanReac AppliChem |
| Acrylamide | PanReac AppliChem |
| Agarose | Biozym |
| Albumin Fraktion V (BSA) | Roth |
| Calcium Chloride | PanReac AppliChem |
| Mounting medium with DAPI | Abcam |
| DMSO | PanReac AppliChem |
| Ethanol | PanReac AppliChem |
| Formic acid | Chemsolute |
| 1 kb plus DNA Ladder | New England Biolabs |
| Gel loading dye, purple (6x) | New England Biolabs |
| Glycine | PanReac AppliChem |
| Glycerol | PanReac AppliChem |
| HEPES | Sigma |
| IGEPAL® CA-630 (NP-40) | Sigma |
| Isopropanol | Merck |
| Laemmli Buffer 4x | BioRad |
| LB-Agar/Medium | Roth |
| Midori Green Advance DNA Stain | Nippon Genetics |
| MTT | Sigma |
| Natriumchlorid | Sigma |
| Nitrocellulose membrane | Amersham |
| PFA | Santa cruz |
| Phalloidin | Sigma |

| | |
|---|---|
| PhosStop Phosphatase Inhibitor | Roche |
| Pierce ™ DSS | Thermo Scientific |
| Ponceau S Solution | PanReac AppliChem |
| Precision Plus Protein™ Dual Color Standards | Bio-Rad |
| Protease Inhibitor Cocktail | Sigma |
| SDS Solution 20% | PanReac AppliChem |
| Skimmed milk powder | Sucofin |
| Sodium azide | Merck |
| TEMED | PanReac AppliChem |
| Triton X-100 | PanReac AppliChem |
| TRIS Base | Fisher BioReagents ™ |
| Trypan blue | Sigma |
| Tween 20 | Merck |

### 2.1.9 Enzymes

***Table 9: Enzymes***

| **Enzymes** | **Company** |
|---|---|
| AgeI-HF | NEB |
| BamHI-HF | NEB |
| DpnI | NEB |
| EcoNI | NEB |
| EcoRI-HF | NEB |
| HindIII-HF | NEB |
| Hot FIREPol DNA-polymerase | Solis BioDyne |
| KpnI-HF | NEB |
| NheI-HF | NEB |
| Phusion polymerase | NEB |
| Primestar polymerase | TaKaRa |
| Q5 polymerase | NEB |
| T4 ligase | NEB |
| XbaI | NEB |
| XhoI | NEB |

### 2.1.10 Antibiotics

***Table 10: Antibiotics***

| Antibiotics | Working Concentration | Company |
|---|---|---|
| Ampicillin | 100 µg/ml | Roth |
| Geneticin Disulfate (G418) | 750 µg/ml | Roth |
| Hygromycin | 300 µg/ml | Roth |
| Kanamycin | 50 µg/ml | Roth |
| Penicillin-Streptomycin | 100 µg/ml | Anprotec |
| Zeocin | 130 µg/ml | Invitrogen |

### 2.1.11 Primer pairs for qRT-PCR

***Table 11: Primer pairs for qRT-PCR***

| Name | Forward primer | Reverse primer |
|---|---|---|
| hsFZD1_52 | CACACCACCAATAATAACCTG | TATTCCACCTTCTTTACCTCC |
| hsFZD2_70 | TTCCCTACTCATTTGTCCTG | TTTCCACGTCTTCATCTCTG |
| hsFZD3_72 | TATGACCAACAGACAGCAG | AATCCCGAGAACAATCCAG |
| hsFZD4_78 | AGCTGACAACTTTCACACC | GGCACATAAACAGAACAAAGG |
| hsFZD5_75 | ACAACCACATCCACTACGA | ATGCCGAAGAAGTAGACCA |
| hsFZD6_128 | ACCTTGTCGTAAACTTTGTGAG | GTTACAGGAACAGTCTCATCAC |
| hsFZD7_122 | GCCTCTGTTCGTCTACCTC | ATGAGCTTCTCCAGCTTCTC |
| hsFZD8_121 | TACAACTACACCTACATGCC | AGGAAGAACTTGAGATCGG |
| hsFZD9_56 | GTCTTCTCCATCCTCTACAC | GTAGACATAGCAAACGATGAC |
| hsFZD10_117 | TAGTTGATTCAGCCCTCAG | GCAAAGCAGTTATCTGTCC |
| hsGN2BL1_84 | AAC CCTATCATCGTCTCCT | CAATGTGGTTGGTCTTCAG |
| hsHPRT1_89 | TATGCTGAGGATTTGGAAAGG | CATCTCCTTCATCACATCTCG |
| hsPTK7_63 | CATGGTGCTGGAATATGTG | CTTGCTCTTGGAAATCCTC |
| hsROR2_143 | TTCTTCTTGGTTTGCATGTG | CTGATCTCTTTGAGTTTGGC |
| hsROR1_115 | CGTCTATATGGAGTCTTTGCAC | GAATGGCGAACTGAGAACAC |
| hsRyk_103 | ACCTTATTAGTCACTACGCTC | CAGCTTATATTCAACCTTGGAC |
| hsWNT4_150 | CTGAAGGAGAAGTTTGATGGTG | TGTCCTGCTCACAGAAGTC |
| hs Wnt5a_109 | AGGGCTCCTACGAGAGTGCT | GACACCCCATGGCACTTG |
| hs Wnt5b_102 | AGAAGAACTTTGCCAAAGGA | CTACGTCTGCCATCTTATACAC |
| hsWNT6_150 | GGAGCGTTTAAAGGACACTG | GATACTAACCTCACCCACCA |
| hsWNT7a_113 | CTTCGCCAAGGTCTTTGTG | TCCAGCTTCATGTTCTCCTC |
| hsWNT7b_94 | CGCAGATCTTTCTCCTCCT | GCCAGGAATCTTGTTGCAG |
| hsWnt11_102 | CTCGGAACTCGTCTATCTG | GTTGGATGTCTTGTTGCAC |

### 2.1.12 Primer pairs for PCR-based cloning

**Table 12: Primer pairs for PCR-based cloning**

| Name | Sequence |
|---|---|
| hsRor2-dIG_fw | TACTCAGCTAGCACCATGGCCACTGGCGTCCTG |
| hsRor2-dIG_rev | TGCTTACTCGAGTCAAGCTTCCAGCTGGACTTGGG |
| hsRor2-dIG-dCRD_fw | TACTCAGCTAGCACCATGGGCATCCCAGCCGAGA |
| hsRor2-dIG-dCRD_rev | TGCTTACTCGAGTCAAGCTTCCAGCTGGACTTGGG |
| hsRor2-dIG-dCRD-dKr_fw | TACTCAGCTAGCACCATGAGTCCCCGAGACAGCAGC |
| hsRor2-dIG-dCRD-dKr_rev | TGCTTACTCGAGTCAAGCTTCCAGCTGGACTTGGG |
| hsRor2_467Stop_fw | GGCCAAACTCAAATAGATCAGCCTGTCTGCGGTGAGG |
| hsRor2_467Stop_rev | CCTCACCGCAGACAGGCTGATCTATTTGAGTTTGGCC |
| hsRor2_783Stop_1x_fw | CCAGTGAGCAATGTGAGCTACGCCCGCTACGTGG |
| hsRor2_783Stop_1x_rev | CCACGTAGCGGGCGTAGCTCACATTGCTCACTGG |
| hsRor2_783Stop_fw | CCAGTGAGCAATGTGAGCTAGGCCCGCTACGTGG |
| hsRor2_783Stop_rev | CCACGTAGCGGGCCTAGCTCACATTGCTCACTGG |

### 2.1.13 Oligonucleotides with sgRNA sequences

***Table 13: Oligonucleotides with sgRNA sequences***

| Name | Sequence |
|---|---|
| sgRNA_ hsFZD6_1_fw | CACCGTGAGTAAAATAGTGAAATG |
| sgRNA_ hsFZD6_1_rev | AAACCATTTCACTATTTTACTCA |
| sgRNA_hsFZD6_2_fw | CACCGCTTTCCTGAAAATGAGTCC |
| sgRNA_hsFZD6_2_rev | AAACGGACTCATTTTCAGGAAAG |
| sgRNA_hsFZD6_3_fw | CACCGAGTATTGCCGCGGTGGAAA |
| sgRNA_hsFZD6_3_rev | AAACTTTCCACCGCGGCAATACT |
| sgRNA_hsFZD6_4_fw | CACCGCATAATGACCCATCAGATT |
| sgRNA_hsFZD6_4_rev | AAACAATCTGATGGGTCATTATG |
| sgRNA_hsROR1_1_fw | CACCGCGCTGCTGCTGGCCGCACG |
| sgRNA_hsROR1_1_rev | AAACCGTGCGGCCAGCAGCAGCGC |
| sgRNA_hsROR1_2_fw | CACCGGAGCGGCGGGCGCGTCCCG |
| sgRNA_hsROR1_2_rev | AAACCGGGACGCGCCCGCCGCTCC |
| sgRNA_hsROR1_3_fw | CACCGAAGAGCCCGGCTGAGCCTG |
| sgRNA_hsROR1_3_rev | AAACCAGGCTCAGCCGGGCTCTTC |
| sgRNA_hsROR1_4_fw | CACCGTACCGGCTCAGACGCAGCA |
| sgRNA_hsROR1_4_rev | AAACTGCTGCGTCTGAGCCGGTAC |

## 2.2 Methods

### 2.2.1 Cultivation of *E. coli*

*E. coli* (see 2.1.3) was cultivated in autoclaved LB medium under aerobic conditions or plated on LB agar plates and incubated at 37 °C. If necessary, 100 µg / ml ampicillin or 50 µg/ml kanamycin were added to the medium for selection. For long-term storage a glycerol (100 %) solution was diluted in 60 % dd$H_2O$. 500 µl bacteria suspension and 500 µl glycerol (60 %) solution were then mixed in 2 ml safety tubes and frozen at -80 °C.

### 2.2.2 Generation of chemocompetent bacteria

In order to generate chemocompetent *E. coli* bacteria, the bacteria were treated with 100 mM $CaCl_2$ solution, according to the method established by (Hanahan *et al*, 1991). An excess of calcium ions changes the permeability of the membrane and increases the ability of the cells to uptake foreign DNA under heat-shock at 42 °C. The *E. coli* were first grown in LB medium without magnesium up to an $OD_{600}$ of 0.3. Then the bacteria were incubated on ice for 10 min and centrifuged at 4 °C for 10 min (6080 g). To dissolve the cell pellet 100 mM $CaCl_2$ were used and the mixture was then incubated again for 20 min on ice. The cells were then aliquoted in 50 µl per sample and frozen in liquid nitrogen. Afterwards the cells were stored at -80 °C. The ability of the bacteria to uptake foreign DNA was tested before first use.

### 2.2.3 Cloning

Cloning describes a method to integrate a specific DNA fragment into a vector. In order to study the impact of ROR2 in breast cancer cells, different vectors with serial deletions of extracellular and intracellular domains of the ROR2 vector were generated by classical cloning as shown in Figure 5.

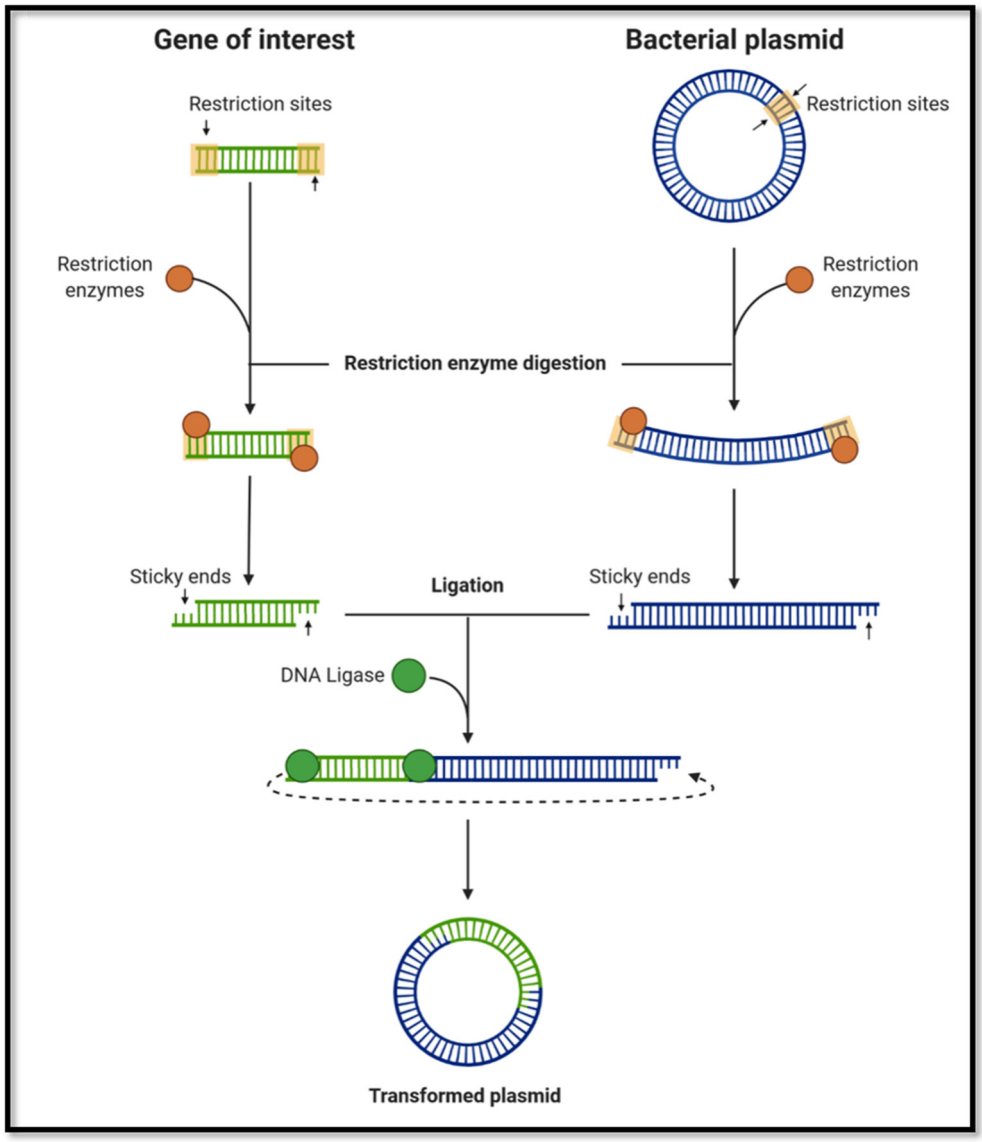


***Figure 5:*** **Schematic view of classical cloning*:*** This requires a gene of interest (insert) and a vector or plasmid, in which the insert will be integrated. Classical cloning includes the cutting of the vector and insert with two restriction enzymes, ideally resulting in two non-compatible, sticky ends. This approach lowers the chance of re-ligation of the vector and thus the transformation background. After ligating the vector and insert with T4 DNA ligase, the new plasmid is transformed into chemically competent E. coli bacteria. The illustration was taken from biorender.com.

### 2.2.3.1 PCR

The polymerase chain reaction (PCR) method is used to amplify specific, double-stranded DNA fragments (Mullis *et al*, 1986; Bell, 1989; White *et al*, 1989) with the help of primers and dNTPs. The reaction takes place in a two-step PCR: First, double-stranded DNA is heated to 98 °C and is thereby denatured and converted into single-stranded DNA. Second, the binding of the PCR primers to the DNA single strands (annealing) and the elongation of the

DNA takes place at a temperature of 71°C. In this step starting from the primers, the thermostable polymerase synthesizes a complementary DNA strand, followed by restarting the cycle all over again. The PCRs were carried out in a final volume of 20 µl and run according to protocol indicated below:

Reaction mix:
10 µl 5x PCR-Puffer
1 µl dNTPs (10 mM)
1 µl 5'Primer (10 µM)
1 µl 3'Primer (10 µM)
50 ng template DNA
0,2 µl (2U/µl) Phusion DNA polymerase
$H_2O$ ad 20 µl

Protocol:
1. 99°C preheating
2. 98°C 30 s
3. 98°C 10 s
4. 71°C 3 min
5. 71°C 10 min
6. Hold at 4°C

The steps 2-4 were repeated 34 times.

### 2.2.3.2 Agarose gel electrophoresis

The agarose gel electrophoresis method (Sharp *et al*, 1973) was used to separate DNA fragments according to their size. For this purpose, gels with 1% agarose in Tris-Acetate-EDTA (TAE) buffer were prepared. The suspension was boiled until the agarose was dissolved completely. The suspension was then cooled down to 60 °C. Afterwards the agarose suspension was mixed with midori green (0.05 µl/ml) as a DNA staining dye and poured into a chamber with a gel comb. After the gel had hardened, the comb was removed and the gel was placed in an electrophoresis chamber filled with TAE buffer. The DNA samples were mixed with loading dye (6x) and loaded into the pockets of the gel. As a reference, the commercially available size standard Quick-load purple 1 kb Plus DNA ladder (NEB) was also loaded into a gel pouch. The DNA strands were separated based on their length by applying a constant voltage of 120 V. In such a process, smaller fragments of DNA run faster than larger ones. After separation, the gel was placed on an UV transilluminator (Intas) and

imaged for documentation purposes. UV light visualizes the midori green intercalated in the DNA.

For 50x TAE stock:

| | |
|---|---|
| Tris-Base: | 242 g |
| Acetate (100% Acetic acid): | 57.1 ml |
| EDTA: | 100 ml 0.5 M Natrium EDTA |
| | Ad 1 l MilliQ $H_2O$ |

**2.2.3.3 Restriction**

During plasmid cloning, a restriction digest with restriction enzymes (NEB) is necessary to generate sticky ends of the plasmid and insert match each other. Thereby 1 µg of the respective DNA was mixed with 1 µl (50 U) restriction enzyme and 5 µl CutSmart restriction buffer in 50 µl total volume. The samples were then incubated for 16 h at 37 °C. Afterwards, the first enzyme was heat-inactivated for 20 minutes at 65 °C. Then the second enzyme was added and the mixture again incubated for 16 h at 37°C. The cut DNA fragments or plasmids were then purified according to the manufacturer's instructions using the "Monarch® PCR & DNA Cleanup Kit" (NEB) or from an agarose gel. A NanoDrop was used to measure the DNA concentrations.

**2.2.3.4 Ligation**

Ligation describes the enzyme-catalyzed process of linking two DNA sections at their ends. By forming a phosphodiester bond the enzyme "ligase" connects the 3'-hydroxy end to the 5'-phosphate end of the nucleic acid segments. Ligation reactions were performed with the T4 ligase (NEB) using the indicated concentrations of the insert and plasmids.

150 ng digested insert
180 ng digested vector
2 µl T4 ligation buffer (10x)
1 µl T4 ligase
Ad 20 µl $H_2O$

The ligation mix was incubated at room temperature overnight and then transformed into 50 µl competent bacteria.

#### 2.2.3.5 Transformation of competent *E. coli* with plasmid DNA

To transform the chemocompetent bacteria, 100 ng DNA was mixed with 50 µl of competent bacteria and incubated on ice for 20 min. The plasmid-bacteria solution was then heat-shocked at 42 °C for 45 seconds. For subsequent cooling, the mixture was incubated on ice for 2 min and then 150 µl of LB medium was added. The cells were then incubated for 45 min under aerobic conditions at 37 °C. Afterwards the bacteria were then plated on LB selection plates. To cultivate and select for transformed bacteria, the plates were incubated at 37 °C overnight.

#### 2.2.3.6 Miniprep

After successful transformation of the plasmid, the selection plates usually exhibited several colonies, of which 3 were picked with a yellow, sterile pipette tip and then cultivated overnight at 37 °C in 4 ml of liquid LB with an appropriate selection antibiotic. The next morning, plasmid DNA from this culture was obtained with an innuPREP Plasmid Mini kit or Monarch® Plasmid Miniprep Kit and purified according to the manufacturer's protocol. DNA concentration was measured using a NanoDrop spectrophotometer and sequence identity was confirmed by sequencing.

#### 2.2.3.7 Sequencing

The sequencing of DNA fragments was carried out by eurofins genomics, Ebersberg, LGC genomics or MicroSynth Seqlab, using the chain termination method (Sanger *et al*, 1977). For sequencing, the sample preparation was prepared following the manufacturer's instructions containing plasmid DNA with primers in a total volume of 17 µl. The results were analyzed with the Snapgene or ApE software.

#### 2.2.3.8 Midiprep

The midiprep "DNA NucleoBond Xtra Midi EF kit" (Macherey-Nagel) was used for a large-scale isolation of plasmid DNA from bacteria. First, a colony was picked with a sterile,

yellow pipet tip and transferred into a 4 ml liquid LB culture with antibiotics. After 3-4 hours of incubation at 37 °C and 220 rpm shaking, the starter culture was transferred to a 1000 ml Erlenmeyer flask containing 300 ml fresh LB liquid medium with selection antibiotics, either ampicillin 100 µg/ml, or kanamycin 50 µg/ml, depending on the plasmid and its selection marker. The culture was then incubated overnight at 37 °C and 220 rpm. The next day, the plasmid DNA was isolated and purified according to the manufacturer's protocol. The DNA concentration was measured using a NanoDrop spectrophotometer.

#### 2.2.3.9 Mutagenesis PCR

A site-directed mutagenesis PCR can be used to introduce short point mutations, insertions or deletions in a certain gene at a specific location. For this purpose, primers were designed to create a stop codon at the respective position to generate ROR2-ΔPRD or ROR2-ΔTKDΔPRD constructs. To generate the ROR2-ΔPRD construct, two stop codons were necessary, which is why the point mutations were carried out in two steps with an additional primer. The samples were prepared with Primestar polymerase to generate the mutations in a PCR in a final volume of 50 µl:

| | |
|---|---|
| 5x Primestar PCR buffer | 10 µl |
| dNTPs (10mM) | 4 µl |
| primer (fw+rev at 10µM) | 2 µl |
| Template DNA | 50 ng |
| Primestar polymerase | 0.5µl |
| RNase-free Water | ad 50µl |

The mutagenesis PCR was executed following the thermal protocol:

98 °C 10 sec
55 °C 15 sec
72 °C 8 min
Hold at 4°C

The steps were repeated 20 times.

To digest the original, methylated and non-mutated vector, the DpnI enzyme (NEB) was used. Therefore, 1 µl of the enzyme was added to the PCR samples and incubated for 4 h at 37 °C. After digestion, 2 µl of the PCR product was used for the transformation of 50 µl competent

bacteria (*Top10* or *DH5α*). The bacteria were grown overnight at 37 °C on a LB plate containing antibiotics for selection. The next day, colonies were picked and grown overnight in 4 ml LB medium with antibiotics. The culture was subjected to DNA isolation and DNA prepared for sequencing as described in 2.2.3.7.

## 2.2.4 Cell culture methods

The cells were cultivated at 37 °C and 5% $CO_2$ in either RPMI-1640 or DMEM/F12 medium, supplemented with 10 % heat-inactivated (56 °C, 30 min) fetal calf serum (FCS) and, if required, with selection antibiotics. To detach adherent cells from the bottom of the cell culture flask, the cells were first washed with PBS and afterwards incubated with 1-2 ml trypsin at 37°C for 5-15 minutes. After detaching the cells, they were either split 1:2-1:20 or they were seeded into flasks, wells or petri dishes for further experiments. All cells were routinely tested for mycoplasma contamination. To freeze and store cells, cell pellets were resuspended in 95% FCS with 5% DMSO, transferred to cryovials and stored in liquid nitrogen tanks.

### 2.2.4.1 Gene overexpression

In order to generate cell lines overexpressing selected genes of interest, MCF-7 cells were transfected with the respective overexpression plasmids, encoding for i.e. Wnt11, ROR1, ROR2 and FZD6.

For transfection, $1 \cdot 10^6$ or $6 \cdot 10^6$ cells were seeded in 6-well plates or 10 cm Petri dishes, respectively, and allowed to adhere for 24 h. For transfections in 6-well plates 200 µl OptiMEM, 1 µg DNA and 5 µl FugeneHD transfection reagent or for transfections in 10 cm Petri dishes 500 µl OptiMEM, 6 µg DNA and 15 µl FugeneHD transfection reagent were mixed, incubated at room temperature for 5 min and then added dropwise to the cells. The cells were incubated at 37 °C for 24 up to 72 h after transfection. After incubation, the cells were washed with PBS and then either directly destructed with a cell scraper to isolate DNA and RNA or trypsinized or and used for flow cytometry staining. In order to generate stable cell lines, transfected cells were continuously treated with the respective selection antibiotics determined by the selection cassette on the overexpression plasmid.

#### 2.2.4.2 Gene knockdown

To further investigate the effects of ROR2 on EV biogenesis, composition, size or concentration in comparison to empty vector cells, a knockdown was performed by using small interfering RNAs (siRNAs) targeted against FZD6 and ROR2. siRNAs are short double-stranded oligonucleotides with a size of 20-25 bp, that bind to specific mRNA sequences and thus prevent their translation. Typically, siRNAs are transfected in presence of a transfection agent, containing liposomes which internalize the siRNAs to permit it to cross cell membranes. For transfection two mastermixes were prepared. The first master mix contains 100 µl OptiMEM and 6 µl Lipofectamine RNAimax for 6-well plate transfections or 300 µl OptiMEM and 13 µl Lipofectamine RNAimax in a petri dish. The second mastermix consists of 100 µl OptiMEM (6-well plate) or 300 µl OptiMEM (petri dish) and 10 nM siRNA. After preparation of both mastermixes, the solutions were blended and incubated for 5 minutes. Then $1 \cdot 10^6$ or $6 \cdot 10^6$ cells were seeded in 6-well plates, or Petri dishes, respectively, and filled up with RPMI+10% FCS to a total volume of 2, or 8 ml. 72h post transfection, the cells were used for further experiments.

#### 2.2.4.3 Generation of CRISPR/Cas9 knockout cells

Stable knockout (KO) cell lines were generated with the CRISPR/Cas9 method in order to understand the effects of FZD6 on breast cancer cell migration, proliferation and invasion, as well as ROR1 and its impacts on EV biogenesis, composition, size and concentration in breast cancer. Therefore, the GFP-tagged pSpCas9n(BB)-2A-GFP plasmid (PX461) and the mCherry-tagged PX461 comprise single guide RNA (sgRNA) sequences, targeting FZD6 or ROR1 in the first exons of the genes and a gene encoding for the nicked Cas9 (nCas9). The nCas9 differs from the wildtype Cas9 and is characterized by one inactive nuclease domain. Therefore, it induces a single-strand break in the genomic region, targeted specifically by the previously designed sgRNAs. The induced two single strand breaks with overhangs significantly reduces off-target effects compared to WT Cas9 (Mali *et al*, 2013; Ran *et al*, 2013). To generate the knockout of FZD6 and ROR1, MCF-7 or MDA-MB231 cells were seeded into 6-well plates and incubated for at least four hours at 37 °C, to allow the cells to attach to the bottom of the plate. A mixture of 1 µg of each plasmid in 200 µl OptiMEM was prepared and 5-15 µl of the transfection reagent (FugeneHD/K4® transfection system) were added. The solution was vortexed, spun down and incubated for 5 min at room temperature, then added dropwise to the cells. The total volume in the 6-well plate was adjusted to 2 ml

with RPMI + 10% FCS per well. 48 h post transfection, the cells were trypsinized and filtered with a cell strainer to separate the cells from each other for FACS sorting into the tubes, containing 4 ml of PBS + 1% EV-free FCS. The $GFP^+/mCh^+$ double positive cells were sorted by FACS into two 96-well plates at a concentration of 1 cell per well in 1 ml RPMI +10%FCS + 1% Pen/Strep. After two to six weeks, depending on the cell line, the resulting cell colonies were tested for a successful and complete knockout of ROR1 and FZD6 by using Western blots.

## 2.2.5 Functional assays

### 2.2.5.1 MTT assay

The MTT assay is a test to determine the metabolic activity of cells and can be used to measure the toxicity of certain substances on cells. In order to descry a suitable concentration of the proliferation inhibitor mitomycin C, that is non-toxic to the cells, $7.5 \cdot 10^4$ MCF-7 and MDA-MB231 cells were seeded in duplicates in a 24-well plate and incubated with the indicated concentrations of mitomycin C in RPMI+10% FCS for 20 h. Subsequently, the cells were incubated with 500 µl culture medium + 10% MTT (stock solution 6 mg/ml) for 4 h at 37 °C. After the incubation, the cells were lysed in 500 µl lysis buffer (5 % formic acid + 63 % isopropanol + 32 % DMSO) for 5-10 minutes at room temperature under constant shaking. The absorption of the samples at 540 nm was measured with a photometer (Victor X3/Photometer infinite F50) in 96-well plates and the values were correlated to the untreated control.

### 2.2.5.2 Invasion assay

Modified Boyden chambers (Hagemann *et al*, 2004) were used to determine the invasiveness of cancer cells as demonstrated in Figure 6. The Boyden chamber system consists of a chamber sealed with a porous membrane (10 µl pore diameter, Pieper) and a second chamber underneath, both filled with cell culture medium. $1 \cdot 10^5$ cells were seeded on the membrane previously coated with ECM (#3432-001-01, R&D) to mimic a preferably *in vivo* setting for tumor invasion through the tissue. Then the cells were incubated at 37 °C for 72-96 h under or without stimulation (1 µg EVs or 100 ng/ml rhWnt11). Successfully invaded cells, which had migrated through the pores, were then counted in the lower wells. Cell invasion was calculated by relating the number of invasive cells to the unstimulated control.

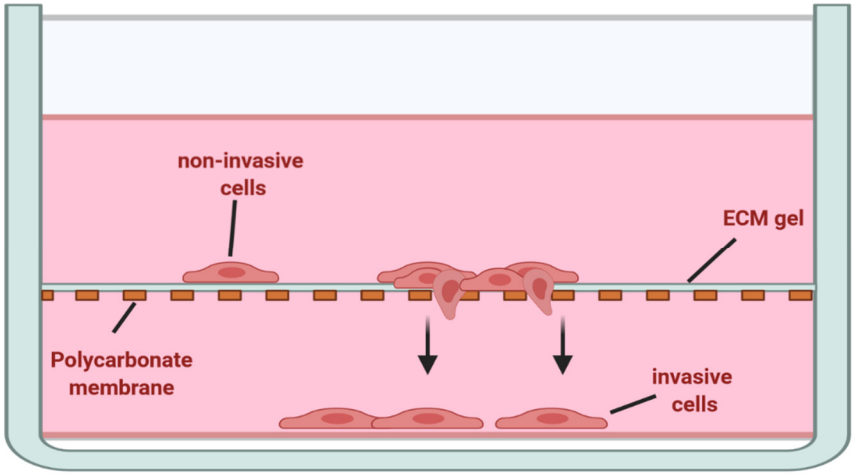


***Figure 6*: Schematic representation of a modified Boyden chamber*:*** The Boyden chamber system was used to measure the invasion rates of cancer cells under stimulation with tumor EVs or tumor-derived soluble factors such as Wnt11. Therefore, cells were seeded on the upper well of the chambers, containing medium and stimulated with the indicated factors. The cells were allowed to invade through the ECM and the pores of the polycarbonate membrane to the second chamber underneath for 96 h. Afterwards, the number of invasive cells in the lower wells was counted and compared to the unstimulated control (*C*reated with biorender.com).

### 2.2.5.3 Proliferation assay

In order to analyze if the knockdown of FZD6 has an impact on cell proliferation, MCF-7 FZD6 knockout and control cells were counted and stained with CellTrace Violet (Thermo Fisher Scientific) according to the manufacturer's protocol (Fig. 7). The unstained and stained controls at time point 0h were either directly measured or fixed in PBS with 3% PFA and stored at 4°C. $3.5 \cdot 10^5$ or $2.5 \cdot 10^5$ cells were incubated for 24 or 72 h, respectively, and the V450 fluorescence intensity of single cells was measured by flow cytometry using the Attune Nxt acoustic focusing cytometer and finally analyzed by FlowJo (FlowJo 10.6.1). The representative gating strategy for cells is described in 2.2.10.

For calculating the number of cell divisions, the following formula was used:

$$n = LOG2(MFI[0\ h] \div MFI[\text{incubation time in } h])$$

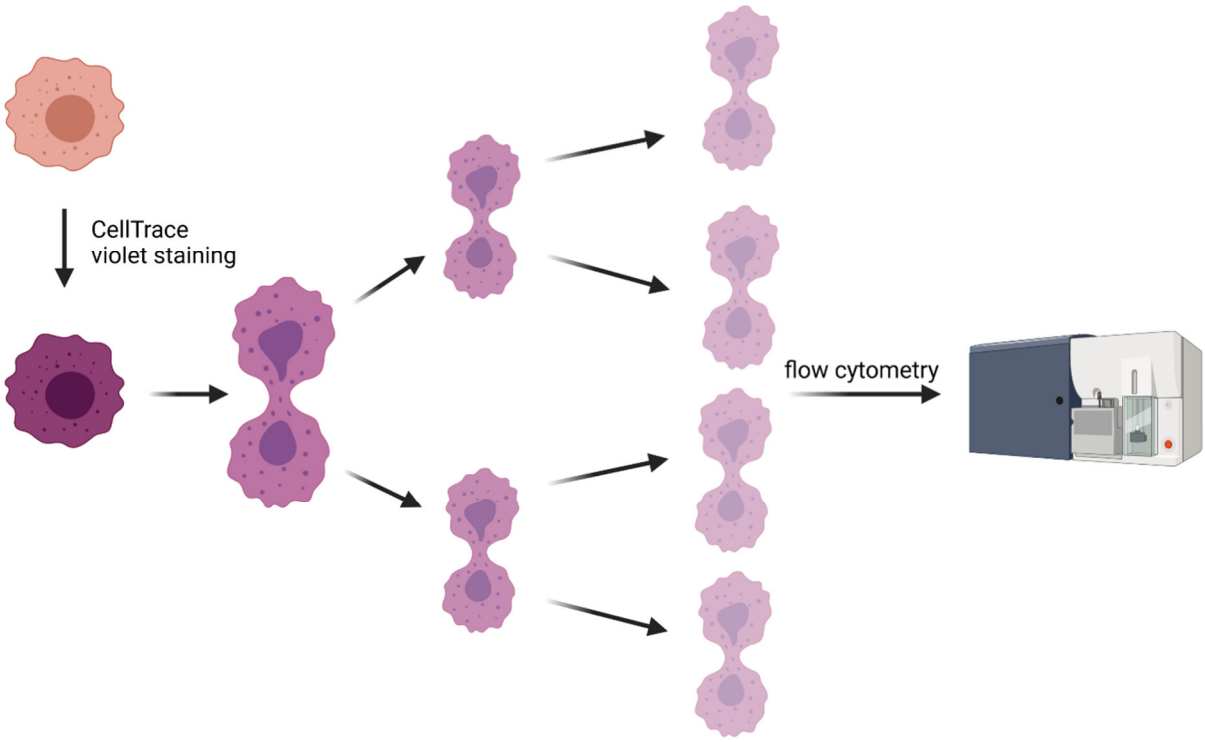


***Figure 7:*** **Proliferation assay*:*** CellTrace violet is a fluorescent dye that labels all living cells. With each cell division, it is equally distributed among the dividing cells leading to a reduction of the fluorescence by half. Thus, by measuring the fluorescence prior to the start of the experiment (at 0 h) as well as after a given time (24 or 72 h), cell proliferation can be quantified by flow cytometry (Created with biorender.com).

### 2.2.5.4 Wound-healing assay

To investigate cell migration, a new assay was developed which is depicted in Figure 8. First, the bottom of a 6-well plate was coated with 30 µl ECM (#3432-001-01, R&D) of a 1:16 dilution with RPMI without FCS. $4.5 \cdot 10^4$ MCF-7 cells were seeded in each half of the Ibidi insert chambers and let adhere overnight. To exclude that the effects were caused by cell proliferation instead of migration, RPMI+10% FCS plus the proliferation inhibitor mitomycin C (#sc-3514, Santa Cruz) was added. The following day, the inserts were carefully removed without damaging the cell monolayer. Fresh medium including mitomycin C was carefully added to the wells and a microscopic image was taken with a 2.5 lens (t= 0 h). The 6-well plates were then incubated for 20 h at 37 °Cand the plates were imaged again. The migration rate was determined by measuring and calculating the area between the cell monolayers after 20 h in relation to the area after 0 h using FIJI software (Schindelin *et al*, 2012) with the "trainable weka segmentation" plugin.

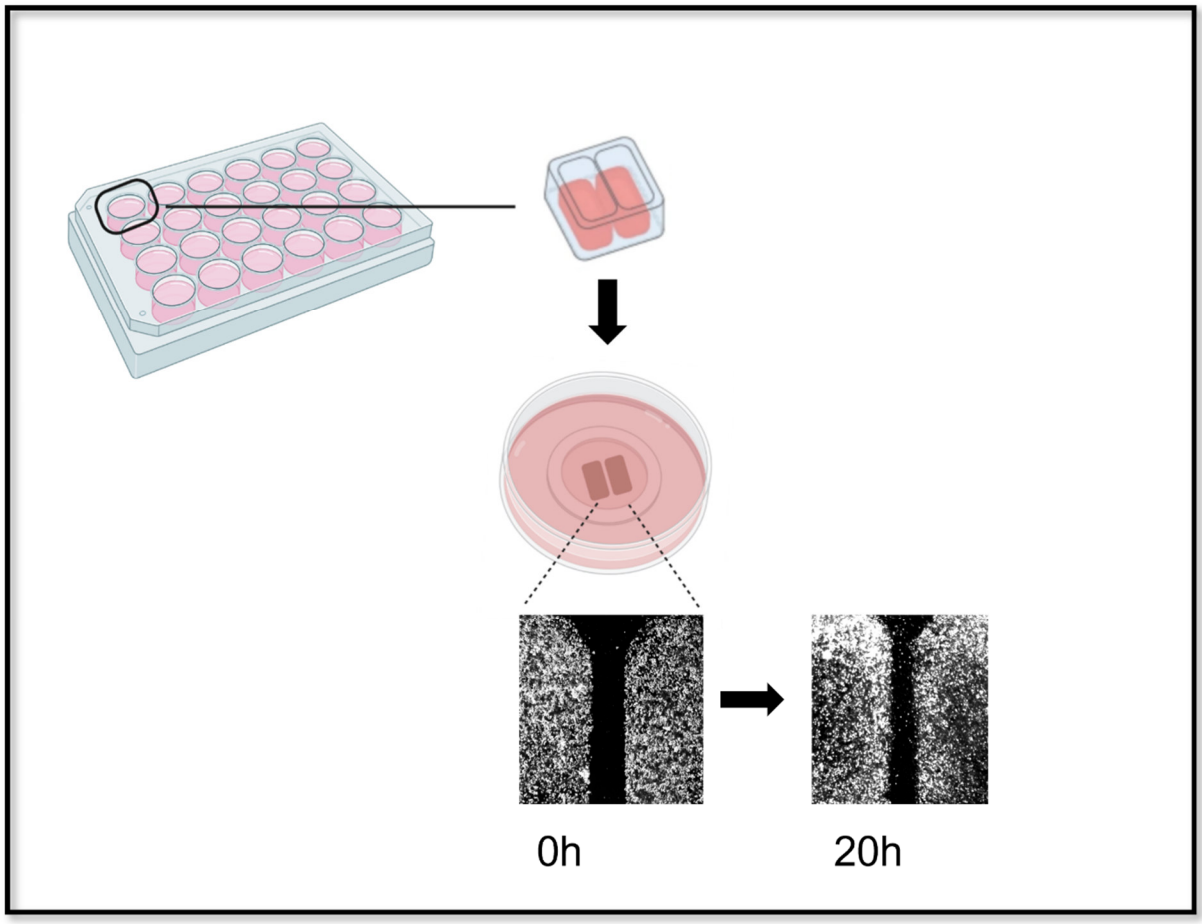


***Figure 8:*** **Wound healing assay*:*** In a wound healing assay, an equal number of cells was seeded into the opposing chambers of the Ibidi inserts and allowed to adhere overnight. The next day, the inserts were removed and the migration rate was measured by quantifying the migration into the slot between the cell monolayers. The Fiji software with the plugin "trainable weka segmentation" can be used to mark cells and background and quantify the area differences between the cells of time point 0h and time point 20h. This determined difference was analyzed in relation to the comparative conditions (Created with biorender.com).

## 2.2.6 RNA isolation, cDNA synthesis and qRT-PCR

### 2.2.6.1 RNA isolation

To isolate RNA for gene expression analysis, the cells were seeded into 6-well plates or Petri dishes and incubated overnight at 37 °C. After washing the cells with PBS, the RNA was isolated with the High Pure RNA Isolation Kit (Roche) according to the manufacturer's protocol. To determine the isolated RNA concentration and purity, 1 µl of the RNA isolation was used for Nanodrop measurements.

### 2.2.6.2 cDNA synthesis

Since qRT-PCR is a PCR method in which DNA is amplified, the RNA must first be transcribed into complementary DNA (cDNA) in order to be able to amplify it first and accordingly to be able to quantify and analyze the expression of various genes. Therefore, 1 µg of total RNA was transcribed using the iScript reverse transcriptase kit (Bio-Rad) following the manufacturer's instructions. The reverse transcriptase binds to random hexamer oligonucleotides and oligo (dT) primers complementary to the poly-A tail of mRNAs to transcribe as much RNA into cDNA as possible and is included in the kit. The required steps for a successful reaction are listed below:

| | |
|---|---|
| 5x iScript reaction mix | 4 µl |
| iScript reverse transcriptase | 1 µl |
| RNA template (1 µg) | x µl |
| Nuclease-free water | y µl |
| Total volume | 20 µl |

The solution was then incubated in a thermal cycler with a pre-programmed protocol:

5 minutes at 25 °C
30 minutes at 42 °C
5 minutes at 85 °C
Hold at 4°C

Depending on the respective subsequent experiment, the cDNA samples were then diluted in nuclease-free water at a concentration of 10 ng/µl or 50 ng/µl for primer testing.

### 2.2.6.3 Establishment of primers for qRT-PCR

In order to analyze and compare relative gene expression in different samples in a comparable and quantitative manner, the quality and efficiency of the designed primers must be validated prior to analysis. The primer pairs for qRT-PCR were designed with PerlPrimer (version V1.1.21). Primer efficiency was tested by preparing a serial dilution of cDNA of a cell line with high expression of the gene of interest. The qRT-PCR was run as described in 2.2.6.4. and the measured $C_t$ values were plotted against the amount of input cDNA. Based on the slope of the resulting curve, primer efficiency can be calculated using the following formula:

Efficiency = $(10^{(-1 / \text{slope value})}) - 1$

Only primer pairs with an efficiency of 90-110 % were chosen for subsequent qRT-PCR analysis. With exception of FZD9 and FZD10, since several primers were tried for these genes and these genes are not expressed in the tested cell lines.

#### 2.2.6.4 qRT-PCR

Quantitative real-time PCR was used to determine the gene expression level of a gene of interest in comparison to two housekeeping genes in order to investigate how strongly a gene is expressed in a certain cell line. The qRT-PCR method is based on the principle of PCR with the additional aspect of real-time quantification. First, the hot-start polymerase is activated, the DNA denatures, the gene-specific primers anneal to the cDNA and is then amplified in repetitive cycles. After each cycle, the fluorescent dye SYBR green intercalates in the double-stranded DNA and the emission of the fluorescent signal is measured by the cycler. Therefore, the increase in fluorescence is proportional to the increasing amounts of amplified gene of interest. The threshold describes the value (Ct value) at which the fluorescence signal significantly exceeds the background noise. The Ct value of the gene of interest was normalized on the Ct values of two house-keeping genes (GNB2L1 and HPRT1), which then results in the ΔCt value. A melting curve analysis was performed as quality control after the PCR was completed, to determine the specificity of the amplificates in comparison to the values of the housekeeping genes. The primers that were used for qRT-PCR were previously tested as described in 2.2.6.3 and are listed in the table 2.1.11. A 384-well plate was used to perform the qRT-PCRs and each sample was measured in triplicates. For each gene, 8 µl of the qRT-PCR master mix were mixed with 2 µl cDNA (10 ng) in a 384-well plate. The plate was covered with a sealing foil, spun down (5 min, 750 g) and the qRT-PCR was run according to the following protocol in the 7500 Fast Real-Timer PCR system (Applied Biosystems):

<u>10× PCR buffer:</u>

- 0.75 M Tris-HCl pH 8,8
- 0.2 M Ammonium Sulfate
- 0.1% (v/v) Tween-20

SYBR-Green master mix:
The trehalose solution was prepared in 10 mM Tris-HCl (ph 8.0)

- 10x PCR buffer 2.5 ml
- 25 mM MgCl2 3 ml
- SYBR green (1:100) 31.3 µl
- 20 mM dNTP mix 250 µl
- 5 U/µl Taq polymerase 100 µl
- 10% Triton X-100 652 µl
- 1 M trehalose 7.5 ml

PCR reaction mix:

- SYBR green master mix 5,6 µl
- fw-primer (10 µM) 0.3 µl
- rv-primer (10 µM) 0.3 µl
- nuclease-free water 1.8 µl

PCR protocol:

1. 12 min at 95 °C
2. 15 s at 95 °C
3. 1 min at 60 °C
4. 15 s at 95 °C
5. 2°C/min at 60-95°C
6. Hold at 4°C

Steps 2-4 were repeated 40 times.

## 2.2.7 Protein biochemistry

### 2.2.7.1 Protein extraction

In order to study the expression of proteins, $1 \cdot 10^6$ cells were seeded into 6-well plates and incubated overnight at 37 °C. Cells were washed once with PBS and then lysed in 80 µl RIPA lysis buffer per well with a cell scraper on ice. The lysates were transferred to a 1.5 ml reaction tube and incubated at 4 °C for at least 30 minutes under constant shaking. Samples were cleared for 5 min at 20.000 g, 4 °C and the supernatant transferred to a new tube for storage at -20 °C.

RIPA lysis buffer:

| | |
|---|---|
| 50 mM Tris | 1.514 g |
| 150 mM NaCl | 2.1915 g |
| 0,1% SDS | 0.25 g |
| 0,5% Na-deoxycholat | 1.25 g |
| 1% Triton X-100 | 2.5 ml |
| | Ad 250 ml MilliQ $H_2O$ |
| | adjust to pH 7.2 |

To isolate proteins from LV, MV or Exo preparations, the pellets were resuspended in PBS and the EV protein concentration was determined as described in 2.2.7.2.

**2.2.7.2 Lowry assay**

The Lowry assay is a biochemical method to quantify proteins and is based on two reactions. In the first step, the formation of a blue-violet dye complex based on a peptide bond of copper (II) ions in an alkaline solution takes place. In the second step, the copper ions are reduced to monovalent cations and react with the yellow Folin-Ciocalteu reagent, which then turns into a blue color that can be measured by a photometer at 750 nm (Lowry *et al*, 1951). The Lowry protein assay (DC™ Protein Assay Kit II, #500-0223, Bio-Rad) consist of the aqueous stock solutions A and a second solution B that were mixed with the protein samples according to the manufacturer's protocol. The cell lysates or LV were diluted 1:20 and MV or EXO 1:10 in MilliQ water and mixed with 50 µl reagent A. Subsequently, 400 µl reagent B were added and after vortexing, the samples were incubated for 15 min at room temperature. The absorbance was measured in duplicates at 750 nm in a plate reader (TECAN or Victor X3) and the values were correlated to the values of a BSA standard curve (0-1 mg/ml BSA).

**2.2.7.3 SDS-PAGE**

The "SDS polyacrylamide gel electrophoresis" (SDS-PAGE) is a method to separate proteins according to their molecular weight. For this purpose, SDS-containing polyacrylamide gels were prepared, consisting of a separating gel (8-12%) and a stacking gel (5%). The gel was inserted into the vertical electrophoresis chamber which was filled with running buffer. Cell lysates or EV samples (up to 50 µg of protein) were diluted 1:4 in 4x Laemmli loading buffer

(Bio-Rad) containing ß-mercaptoethanol (1:10 dilution) and heated for 5 min at 95 °C to denature secondary and tertiary structures of the proteins. The ß-mercaptoethanol in the Laemmli buffer reduces protein disulfide bonds and the anionic detergent SDS quantitatively binds to proteins resulting in a negative charge and allowing their separation in an electric field according to their mass. Dithiothreitol (DTT) served as protein stabilizer by preventing the oxidation of sulfhydryl groups of the proteins to disulfide bridges. Bromophenol blue was used as a dye for visualizing the sample in the gel. As some antibodies (FZD6, CD9, Alix and CD63) were not able to detect denatured proteins, to analyze the expression of these proteins, cell lysates and EV samples were prepared in 4x Laemmli buffer without ß-mercaptoethanol and heated 10 min at 70 °C. The protein samples and a molecular weight marker (Precision Plus Protein™ - Bio-Rad) were loaded onto the gels and first collected in the stacking gel for about 30 minutes at 90 V and then separated for 60 to 90 minutes at 140 V.

Separating gel buffer:

| | |
|---|---|
| 1,5 M Tris | 181.71 g |
| 2% SDS | 100 ml 20% SDS |
| | Ad 1l MilliQ $H_2O$ |
| | Adjust pH to 8.8 |

Stacking gel buffer:

| | |
|---|---|
| 1,5 M Tris | 181.71 g |
| 2% SDS | 100 ml 20% SDS |
| | Ad 1 l MilliQ $H_2O$ |
| | Adjust pH to 6.8 |

Separating gel

| | | **8x** | **10X** | **12%** |
|---|---|---|---|---|
| MilliQ $H_2O$ | ml | 2.38 | 2.03 | 1.7 |
| Separating gel buffer | ml | 1.25 | 1.25 | 1.25 |
| Acrylamid | ml | 1.32 | 1.67 | 2 |
| TEMED | µl | 5 | 5 | 5 |
| APS | µl | 50 | 50 | 50 |

Stacking gel

| | |
|---|---|
| MilliQ $H_2O$ | 2.13 ml |
| Sammelgelpuffer | 380 µl |
| Acrylamid | 500 µl |
| TEMED | 3 µl |
| APS | 30 µl |

10x Tris-Glycine Buffer

| | |
|---|---|
| Tris base (25mM) | 30 g |
| Glycine (192mM) | 144 g |
| | Ad 1 l MilliQ $H_2O$ |

Electrophoresis buffer (10x)

| | |
|---|---|
| Tris-Base | 30 g |
| Glycine | 144 g |
| SDS | 10 g |
| | Ad 1 l MilliQ $H_2O$ |

**2.2.7.4 Western Blot**

Next, proteins are transferred to a nitrocellulose membrane using the wet blot method. For this purpose, the gel was removed from the electrophoresis chamber and put on top of a membrane, which was then placed in the middle of a holder with two layers of fabric and two sheets of Whatman paper in transfer buffer. After removing all air bubbles, the holder was closed and placed in a blotting chamber filled with transfer buffer. The protein transfer was conducted for 3 hours at 80V and 4°C. Afterwards, the membrane was stained in 0.5 % Ponceau S (PanReac AppliChem) under constant shaking. The Ponceau S is a red, negatively charged dye, which binds reversibly to positively charged amino acids of the proteins. Therefore, it was used as loading control. The membrane was unstained in TBST and blocked for 60 min at room temperature in 3-5 % BSA (Roth) or milk powder (ChemCruz) in TBST to reduce unspecific binding sites. The primary antibodies (see 2.1.5) in 3-5% BSA or milk powder in TBST were incubated for 2 h at room temperature or overnight at 4 °C. Then, the membrane was washed three times with TBST for 5 min each at room temperature and subsequently incubated with horseradish peroxidase (HRP)-labeled secondary antibodies for 1

h at RT followed by three washing steps in TBST for 5 min each. A catalytic enzymatic reaction of the HRP elicits a chemiluminescent signal by oxidizing luminol. To detect the protein signals, ECL prime (GE Healthcare) or SuperSignal™ West Pico Plus chemiluminescent substrate (Thermo Scientific) were used. In case of insufficiently strong signals, either SignalFire ECL Reagent (Cell signaling) or Clarity Max™ Western ECL substrate (Bio-Rad) were used as more sensitive reagents. After incubating the membrane with the respective ECL substrates, the signals were detected in a chemiluminescence imager (Amersham Imager600, GE Healthcare or Intas ECL Chemostar). The relatively quantification of protein bands from Western blots with FIJI, enables to analyze the relative amounts as a ratio of each protein band in comparison to the loading control.

Protocol 10x TBS:

| | |
|---|---|
| Tris base | 24 g |
| NaCl | 88 g |
| | Ad 900 ml MilliQ $H_2O$ |
| | Adjust pH to 7.6 with HCl |
| | Ad 1000ml MilliQ $H_2O$ |

For 1x TBST:

| | |
|---|---|
| TBS 10x | 100 ml |
| MilliQ-$H_2O$ | 900 ml |
| Tween-20 | 1 ml |

10x Blotting buffer

| | |
|---|---|
| Tris-Base: | 30.28 g |
| Glycin: | 144.14 g |
| | Ad 1 l MilliQ $H_2O$ |

**2.2.7.5 Co-immunoprecipitation**

Co-immunoprecipitation (Co-IP) is a technique to identify protein–protein interactions by using a target protein-specific antibody to capture proteins that are bound to the captured protein. These protein complexes can then be analyzed by Western Blot to identify new interaction partners. For Co-IP experiments, $6 \cdot 10^6$ MCF-7 cells were seeded into 10 cm Petri

dishes and allowed to adhere overnight. Then, the cells were transfected according to the protocol described in 2.2.4.1 with either FZD6-Flag, V5-Wnt11 and pCMV control vectors or with pROR2, V5-Wnt11 and pcDNA3.1 control vectors. 24 h post transfection, the cells were carefully washed twice with ice-cold PBS and then crosslinked by using 1 mM disuccinimidyl suberate (DSS, Thermo Scientific) in 1 ml PBS + 1 mM $MgCl_2$ for 30 minutes at room temperature. DSS is a non-cleavable, membrane-permeable crosslinker that consists of an amine-reactive N-hydroxysuccinimide (NHS) ester at each end of an 8-carbon spacer arm that reacts with primary amino groups to form stable amide bonds resulting in crosslinked proteins. After crosslinking, the cells were washed twice with ice-cold PBS and lysed on ice with a cell scraper and Co-IP RIPA buffer:

Co-IP lysis buffer

- 50 mM Tris/HCl pH 8,0
- 150 mM NaCl
- 1 % NP-40
- 1:100 Protease-Inhibitor-Cocktail (Sigma)

For efficient cell lysis, the lysates were incubated for at least 30 min at 4°C under constant shaking and then cleared by centrifugation for 20 min at 4°C at 16060 g. The supernatant was transferred to a new reaction tube and the protein concentration was determined by Lowry assay as described in 2.2.7.2. For each Co-IP sample, 20 µl of the A / G agarose beads (#sc-2003, Santa Cruz) were washed five times with 1 ml ice-cold PBS. 500 µg of protein lysate per sample were adjusted to a volume of 1 ml with ice-cold PBS. The 20 µl purified beads were then added and incubated for 1 h at 4 °C under constant shaking in order to deplete unspecific binding sites in the lysates. The samples were spun down at 4 °C and 1700 x g for 5 min. The supernatant was carefully transferred into a new tube and 1 µg of the V5 antibody (#13202, cell signaling and #SAB2702199, Sigma) or IgG control (#2729, cell signaling and #M5284, Sigma) was added to the samples. After 16 h at 4 °C under constant agitation, 20 µl of previously washed A/G agarose beads were added and incubated at 4 °C for 2 h under constant shaking. The samples were centrifuged at 4 °C and 1700 x g for 5 min to pellet the antibody-bead-complexes. To reduce background signals, the supernatant was removed and the complexes were washed five times with 1 ml ice-cold PBS. Finally, the samples were resuspended in 15 µl Laemmli loading buffer (4x) and heated for 5 min at 95 °C to elute the antibodies and their bound targets from the beads. The samples were centrifuged for 1 min at 11.000 g and the supernatants were loaded onto a SDS-PAGE gel for detection of protein

signals by Western Blot as described above. As control, up to 50 µg of the input cell lysates were loaded onto the same gel.

## 2.2.8 EV techniques

### 2.2.8.1 EV isolation

EVs were isolated from cell culture supernatants. LV, MV and EXO differ in their size so that they can be separated by differential ultracentrifugation. $6 \cdot 10^6$ cells per 10 cm Petri dish were cultured overnight in media supplemented with 10 % vesicle-depleted FCS at 37 °C. Vesicle-depleted FCS was generated by first heat-inactivating the FCS for 30 min at 56 °C and then centrifuging it for 16 h at 153700 g. The supernatant was then sterile-filtered (0.2 µM diameter), aliquoted in 50 ml and finally stored at 4 °C. The supernatants were collected and centrifuged at 500 x g for 5 min to remove residual cells and debris, followed by 1.500 g for 15 min to pellet the LV. The MV were pelleted from the supernatant by ultracentrifugation at 17.000 x g for 30 min at 4 °C. In order to isolate EXO, the supernatant of the MV centrifugation step was transferred to small ultracentrifugation tubes and then ultracentrifuged at 143.000 g, 4 °C for 1.5 h. All pelleted EVs were washed once in PBS and resuspended in 20-50 µl PBS for subsequent analysis by NTA or western blotting.

### 2.2.8.2 EV characterization

In the first step, the modified cells were counted and the same number of cells were seeded equally into 10 cm petri dishes, to guarantee isolation of EV from the same number of cells in all conditions. In order to measure and compare the cell confluence, five pictures of one representative dish per condition were taken with a light microscope (4x or 10x magnification). FIJI (ImageJ) (Schindelin *et al*, 2012) was used to analyze the picture by using the plugin “trainable weka segmentation“, allowing the software to distinguish between cells and background and thus calculating the area of the cells in the image in relation to the remaining background. This percentage value then gives the cell confluence and the values of the five images were averaged. To analyze the EVs further, western blots, flow cytometry and Nanoparticle Tracking Analysis (NTA) were performed as described below.

#### 2.2.8.3 Nanoparticle Tracking Analysis (NTA)

In order to analyze EV concentration and size the ZetaView device (ZetaVIEW PMX120-S, Particle Metrix) was used for NTA. NTA is a method based on the principles of Brownian molecular movement for determining particle sizes and concentrations in liquid media. The Brownian molecular movement depends on the particle size under constant temperature conditions. Small molecules move faster than big molecules and the particles can then be tracked by a camera in the ZetaView, which allows the software to determine the sizes and concentrations of different particles. For measurement, each sample was diluted in 1 ml PBS and then injected into the flow cell of the instrument. Depending on the EV type and the concentration, the dilution factor varied between 1:250 and 1:5000. The ZetaView device filmed and measured at eleven positions for 1 s with a previously adjusted sensitivity the concentrations, size distributions, particles per frame, total number of measured particles and particle sizes with the ZetaView 8.05.05 SP2 software.

### 2.2.9 Microscopy

#### 2.2.9.1 Fluorescence microscopy

In order to show that the MDA-MB231 ROR1 knockout cells do not differ morphologically from the MDA-MB231 CRISPR control cells, their cytoskeleton was stained by F-Actin labeling via Phalloidin and the staining analyzed under a fluorescence microscope. First, $5 \cdot 10^4$ cells were seeded onto glass coverslips in RPMI + 10% FCS into a 24-well plate and incubated overnight at 37 °C to allow the cells to adhere. After incubation, the cells were washed twice with PBS and fixed with 4% PFA for 15 min at room temperature on a shaker. After fixation, the cells were washed twice with PBS and then blocked with PBS+0.3%BSA+0.05% saponin for 20 min at room temperature to prevent unspecific antibody binding and to permeabilize the cell membranes ng. Cells were stained with FITC-labeled Phalloidin for at least 1h at room temperature. Afterwards, the cells were washed twice with PBS and the coverslips were dried. Then, the coverslips were mounted in medium with DAPI onto microscopy slides which were stored at 4 °C until fluorescence microscopy with the Olympus IX83.

### 2.2.9.2 Confocal microscopy

To ensure that the MCF-7 pROR2 deletion constructs were still located at the cell membrane, the cells were analyzed by confocal microscopy. The MCF-7 pROR2 modified cells were seeded at a concentration of $1 \cdot 10^5$ cells onto glass coverslips and allowed to adhere overnight at 37 °C. Then, the cells were washed twice with PBS and fixed with 4% PFA as described in 2.2.9.1. In order to permeabilize the cell membrane the cells were incubated with PBS + 0,2 % Triton-X for 10 min at room temperature and then blocked in 1% BSA with PBS for 1 h at room temperature to prevent unspecific antibody binding. Afterwards, the cells were stained with 5 µl mouse anti-ROR2 antibody (#FAB20641G, R&D) in 5 µl PBS + 0,2 % Triton-X +1 % BSA solution for at least 1 h at room temperature. After washing and drying the cells, Mowiol solution was dropped on the coverslips for mounting and the coverslips were stored at 4 °C in the dark. The fluorescent images were taken on the confocal microscope (Olympus, FV 1200).

### 2.2.10 Flow cytometry

In order to analyze the proliferation of the MCF-7 knockout FZD6 cells and the cells expressing ROR2 deletion constructs, as well as to confirm the CRISPR ROR1 KO and to characterize MVs, flow cytometry was used. For each sample, $5 \cdot 10^5$ cells were pelleted at 500 x g for 5 min and the pellet was resuspended in PBS + 1 % EV-depleted FCS for 20 min in order to block unspecific bindings of the antibodies. For MV, 4 µg of MVs were blocked for 20 min in PBS + 1% EV-depleted FCS. The cells and MVs were then incubated for 20 min at RT in the dark with the respective fluorescently-labeled antibodies listed in 2.1.5. As controls, matched isotype controls and unstained cells were included in the analysis at the Attune Nxt Acoustic Focusing Cytometer. The percentage of fluorescent-positive single cells was then analyzed by FlowJo software (FlowJo 10.6.1).

As shown in Figure 9, the MV (A) and the cells (B) in this work were measured differently by flow cytometry and evaluated using FlowJo. Since the MVs are significantly smaller than cells, the threshold was reduced so that the MVs could be separated from the cell debris. To this end, 10.000 events were measured in the MV gate. The values were then compared with the respective isotype control. The cells (B) were gated according to single cells in two steps, also based on their size and granularity, so that 10.000 events were measured here too and could also be compared in comparison to the corresponding isotype control.

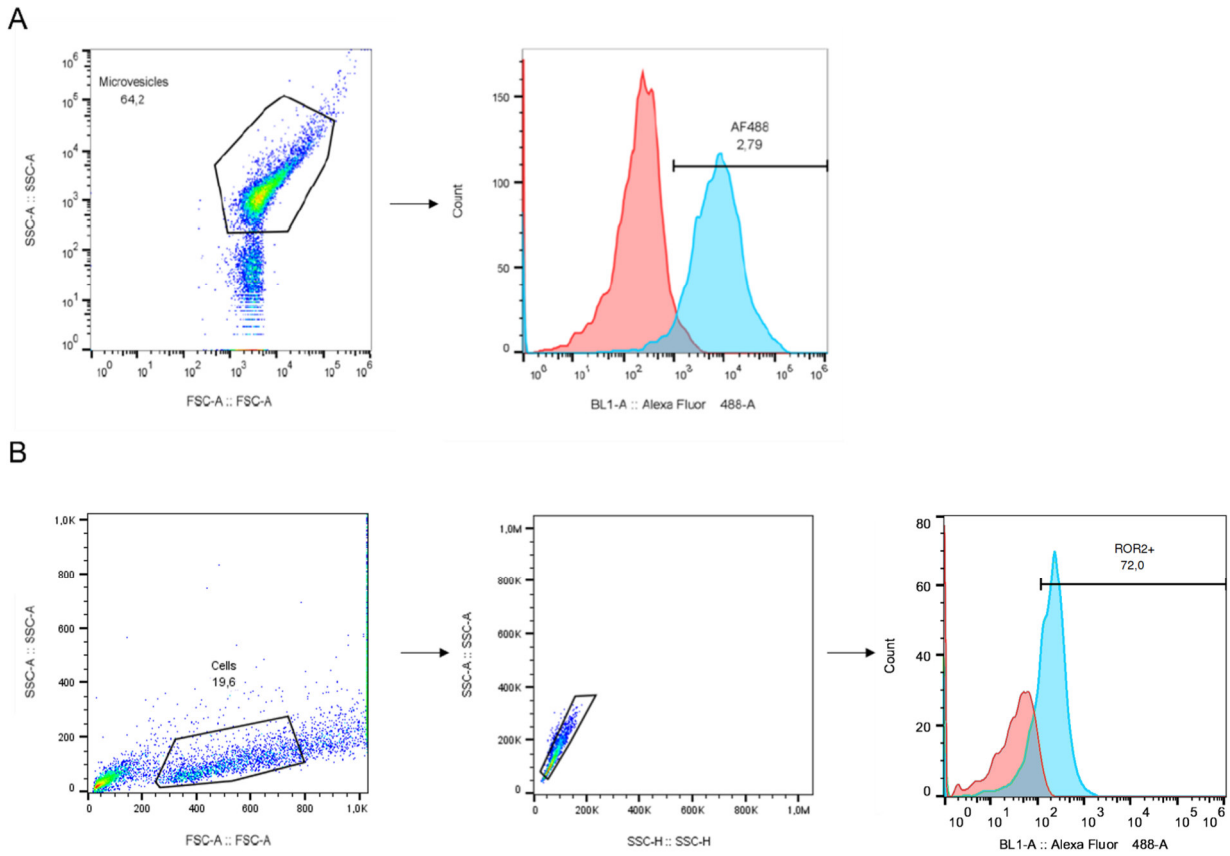


***Figure 9*: Flow cytometry:** Gating strategy of MV (A) and cells (B), according to their size, granularity and fluorescence signals. A: MVs were gated based on their size and granularity and separated from the cell debris. A total number of 10.000 events was measured in the MV gate and later analyzed using FlowJo. B: The cells were gated from cells to single cells. The evaluation was also carried out using FlowJo.

### 2.2.11 Bioinformatics and statistics

The data were analyzed with the Graphpad Prism software, calculating means ± standard deviation (SD) and significance by using a two-sided student's t-test or one-way ANOVA test, unless indicated otherwise. P-values $< 0.05$ were considered significant. All performed experiments were executed in at least three independent biological replicates.

The bioinformatic analyses were performed as part of the MyPathSem consortium in cooperation with the bioinformatics department (Institute Medical Bioinformatics) and the group of Prof. Tim Beißbarth, Darius Wlochowitz and Dr. Maren Sitte. Further survival analysis was performed with the online tool kmplot.com (Győrffy, 2021). (https://kmplot.com/analysis/index.php?p=service&cancer=breast).

# 3. Results

## 3.1 ROR receptors in breast cancer cells

### 3.1.1 ROR1/2 expression in different breast cancer cell lines

The ROR receptor family was shown to be overexpressed in different cancer entities (Zhou *et al*, 2020; Hasan *et al*, 2017; Liu *et al*, 2020). Based on preliminary results, the ROR receptor family moved into the center of attention. It has been shown that ROR receptors play an important role in embryonic development, but are often associated with cancer diagnoses (Menck *et al*, 2021; Yamada *et al*, 2010; Borcherding *et al*, 2014; Zhang *et al*, 2012c; Debebe & Rathmell, 2015). In 2017, RNA-seq revealed an upregulation of Wnt11 in ROR2 overexpressing MCF-7 cells, indicating a possible interaction of those proteins (Bayerlová *et al*, 2017). Based on this background, a cell line screening of various human breast cancer cell lines was carried out, in which the ROR1/2 gene and protein expression was analyzed using qRT-PCR and Western blot. As shown in Figure 10, the Luminal A breast cancer cell line MCF-7 does not express ROR1 or ROR2, which makes it a good model system for studying the function of ROR1 and ROR2 through overexpression experiments. T47d, on the other hand, showed a relatively high expression of ROR2, although ROR1 is hardly expressed. This makes T47d an ideal cell line for the knockdown of ROR2. In contrast to T47d, the basal-like breast cancer cell line MDA-MB231 does not express ROR2, but instead rather high levels of ROR1, which makes it a suitable model for ROR1 knockout.

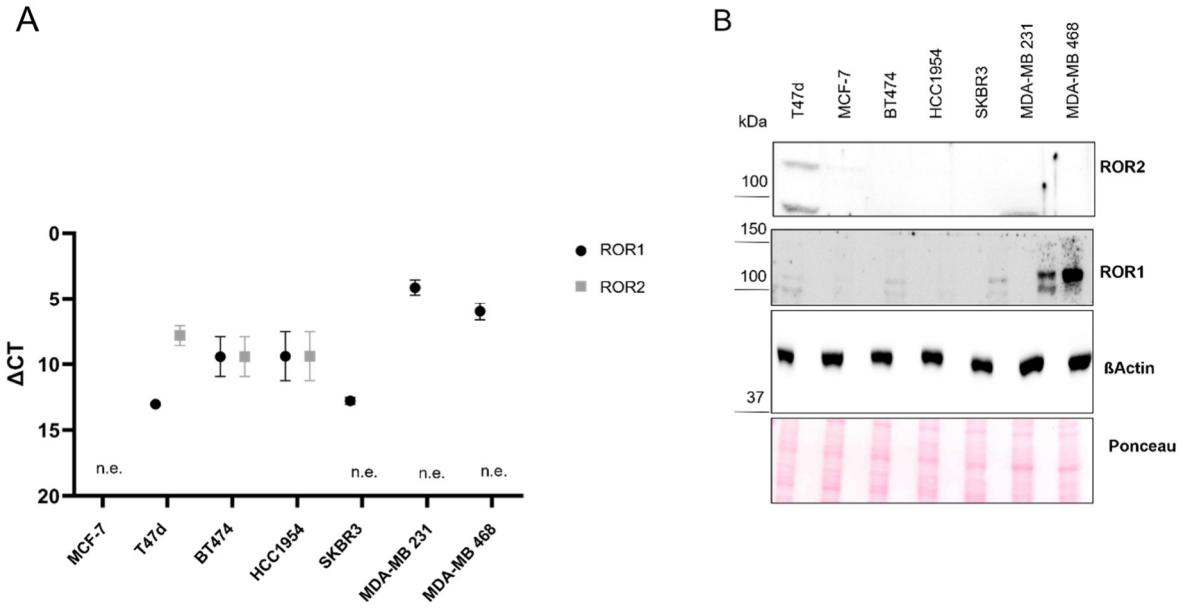


***Figure 10*: ROR1 and ROR2 expression in human breast cancer cell lines*:*** A, Gene expression of ROR1 and ROR2 in different breast cancer cell lines was measured by qRT-PCR (mean±SD, n=3,

n.e.= not expressed; CT values <30 marked as not expressed). B, Various human breast cancer cell lines showed different ROR1 and ROR2 protein expression in western blot. ß-Actin is shown as housekeeper and Ponceau staining was used as loading control.

### 3.1.2 ROR2 overexpression increases breast cancer invasion, but not migration

To investigate the role of ROR2 in breast cancer regarding tumor progression, ROR2 was overexpressed in MCF-7 cells and the cells were then examined in functional assays focusing on cell invasion and migration as two key features required for cell spreading. The ROR2 overexpression was first confirmed by using Western blots (Fig.11 A). The ROR2 overexpression led to a significantly increased invasion rate in Boyden chamber experiments compared to empty vector cells, confirming previous results (Bayerlová *et al*, 2017). Despite the fact that studies found a link of ROR2 knockdown to decreasing migration rates in osteosarcoma cells (Dai *et al*, 2017), no difference between the MCF-7 empty vector and ROR2 overexpression cells was detected in the previously established migration assays (Fig.11 C). On the one hand the effect on cancer cell invasion could be cell line-specific; on the other hand the migration assay might not be sensitive enough for revealing weak effects.

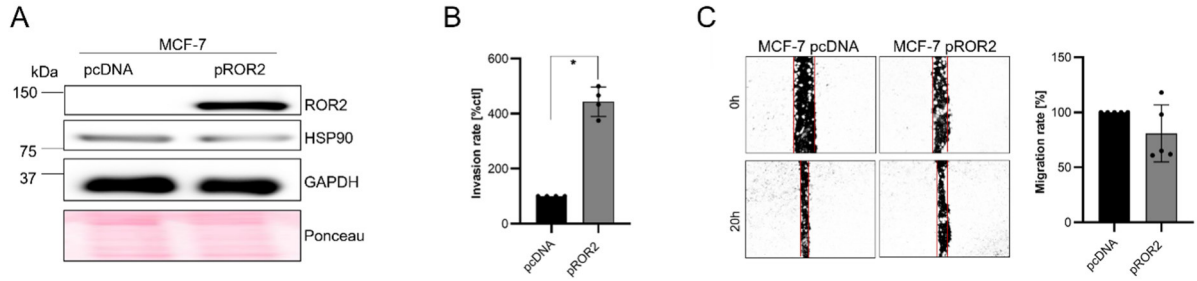


***Figure 11*: ROR2 overexpression increases breast cancer invasion, but not migration*:*** A, MCF-7 cells were transfected with either empty vector (pcDNA) or a human ROR2 overexpression plasmid (pROR2). HSP90 was used as loading control. B, Invasion assay: The invasion rates of MCF-7 pROR2 and pcDNA cells were measured in Boyden chambers over 96 h (mean±SD, n=3, *p<0.05), C, Migration of MCF-7 pcDNA and pROR2 cells was studied in wound healing assays over 20 h. Representative images are shown on the left, the corresponding quantification on the right (mean±SD, n=5).

### 3.1.3 Wnt11 is a novel ligand for ROR2

Up to date, Wnt5a was claimed to be the sole ligand for ROR2 (Fukuda *et al*, 2008; Oishi *et al*, 2003). Whether ROR2 binds other non-canonical Wnt ligands was unclear. Based on an RNA sequencing (RNA-seq) analysis, an upregulation of Wnt11 in ROR2 overexpressing MCF-7 was found (Bayerlová *et al*, 2017), which indicated that Wnt11 is a possible new ligand for ROR2. To answer this question, MCF-7 pROR2 cells were transiently transfected with V5-tagged Wnt11 and its interaction with ROR2 studied by Co-IP (Fig.12).

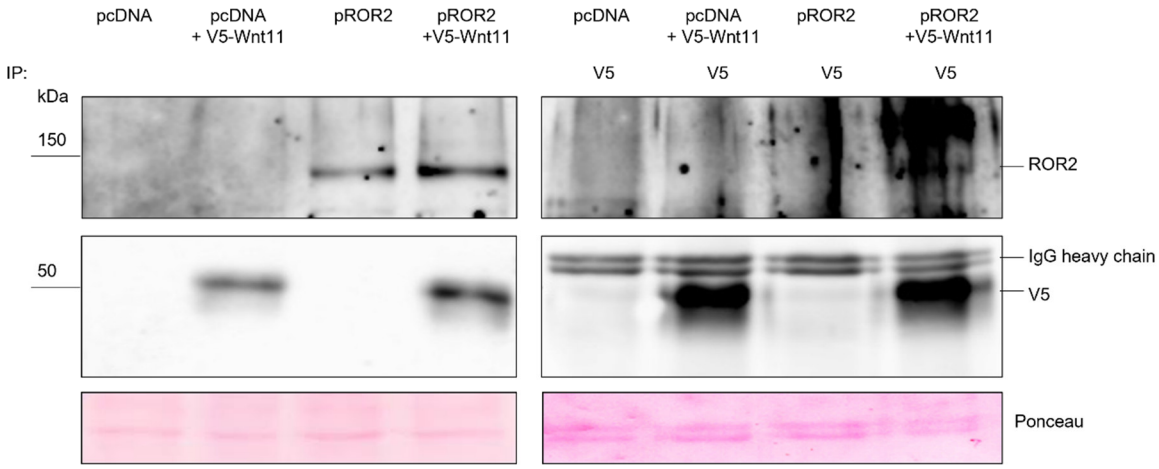


***Figure 12*: Wnt11 interacts with human ROR2*:** MCF-7 pcDNA or pROR2 cells were transiently transfected with V5-tagged Wnt11 and its interaction with ROR2 studied by Co-IP with a V5 antibody. Ponceau staining was used as loading control.

Indeed, the V5 antibody successfully pulled down ROR2, and thus confirming its interaction with Wnt11 in human MCF-7 cells in the Co-IP.

### 3.1.4 TKD and CRD are important for ROR2-mediated cell invasiveness

Wnt5a was identified for this purpose as a ligand for ROR receptors, with the CRD domain of ROR receptors identified for binding with Wnt5a (Xu & Nusse, 1998; Oishi *et al*, 2003). The question now arises whether the same domain is also responsible for interaction with Wnt11 and whether it mediates the effects of Wnt11 on tumor invasion. Furthermore, since ROR2 is a potential tyrosine kinase, the question arises whether the TKD, or rather the PRD, which mediates protein-protein interactions, is important for the transduction of Wnt11 signaling. For this purpose, serial deletions of the individual domains were generated which are shown

schematically in Figure 13 A. In order to prove the successful overexpression of the cloned ROR2 deletion constructs in ROR2-negative MCF-7 wildtype cells, both Western blots (Fig13 B) and flow cytometry (Fig 13 C) were performed. and the deletion constructs with the expected sizes could be verified. Interestingly, the antibody used for the expression analysis by Western blot failed to detect some ROR2 constructs, therefore flow cytometry was used to ensure the expression of ROR2 ΔIg-like domain, as well as the intracellular deletion constructs, as shown in Figure 13 C.

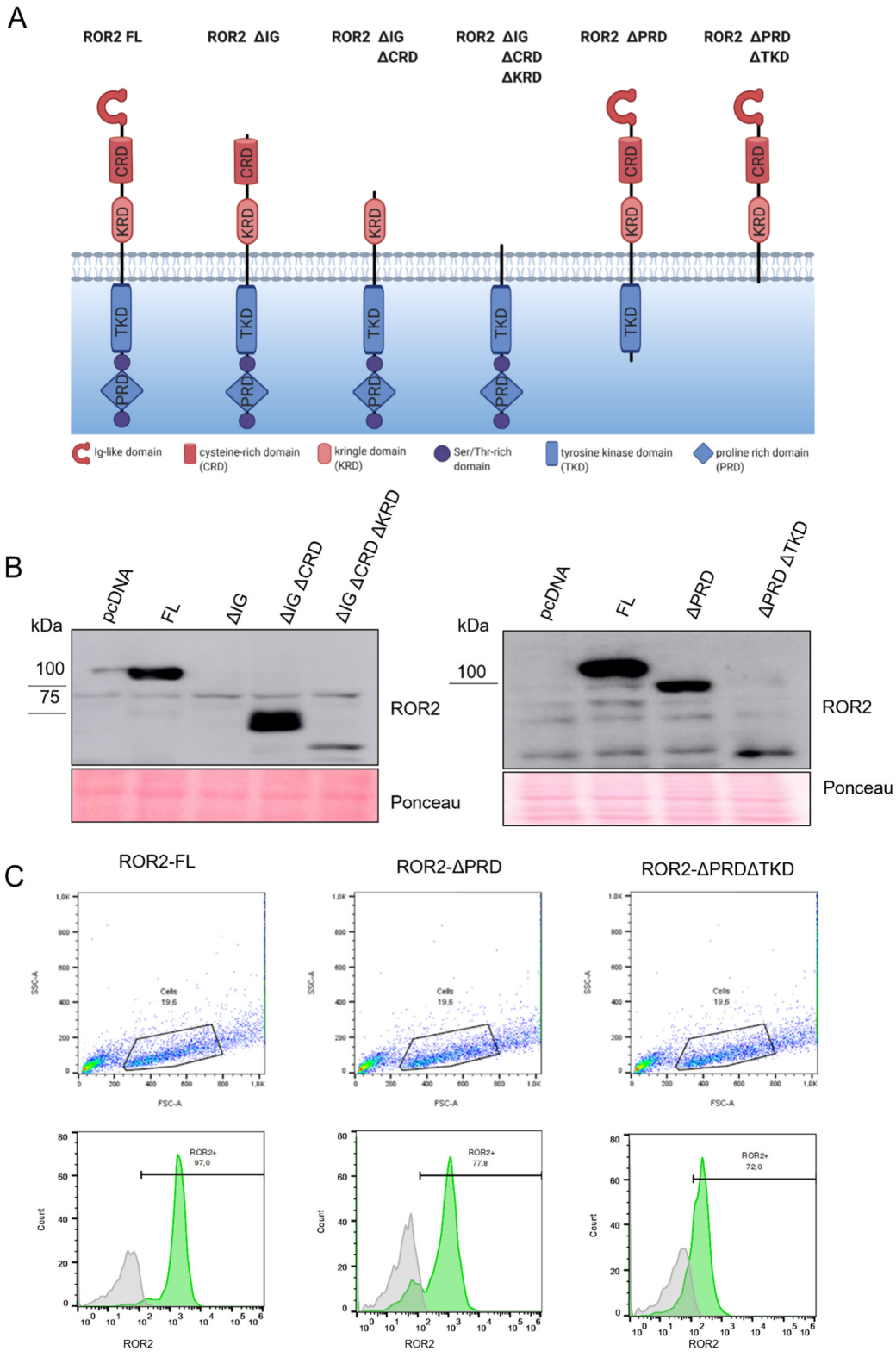


***Figure 13*: Generation of ROR2 C- and N-terminal deletion constructs:** A, Schematic overview of pROR2 C- and N-terminal deletion constructs (created with biorender.com, adapted from (Menck *et al*, 2021)). B, MCF-7 cells were stably transfected with either the empty vector (pcDNA), ROR2 full length (ROR2 FL ~130 kDa) or the deletion constructs (ΔIg ~90 kDa, ΔIg ΔCRD ~72 kDa, ΔIg

ΔCRD ΔKRD 62 kDa). C, MCF-7 cells were transfected with either ROR2 FL or with the deletion constructs missing PRD (~90 kDa) or PRD and TKD (~75 kDa). Flow cytometry confirmed the expression of ROR2 (green) in the deletion constructs. The IgG control is shown in grey.

In order to confirm that the deletion of the distinct domains did not affect the intracellular localization of ROR2, immunofluorescence stainings with a fluorescently-labeled ROR2 antibody were carried out. As shown in Figure 14, all ROR2 constructs were overexpressed in MCF-7 cells and indeed still localized at the cell membrane.

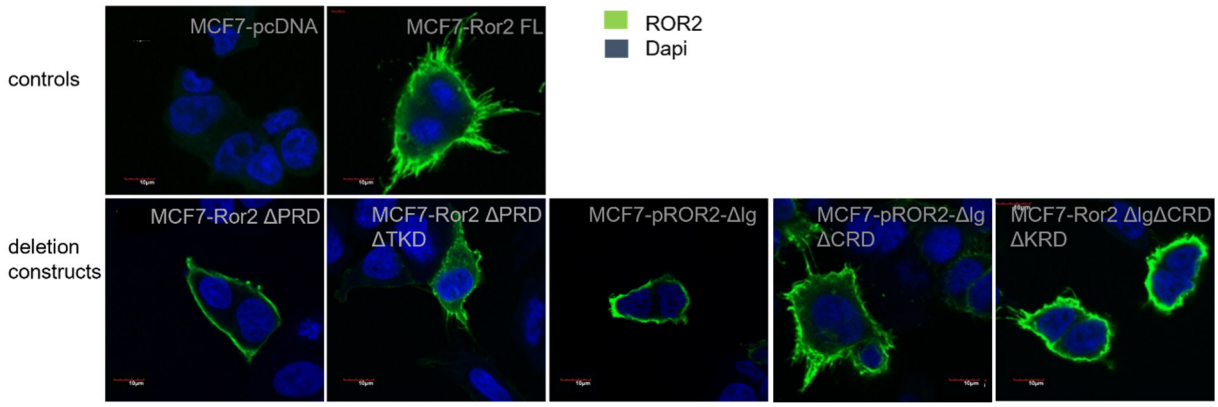


***Figure 14*: ROR2 deletion constructs are still located at the cell membrane*:*** MCF-7 cells were transfected with the different ROR2 deletion constructs or with the ROR2 full length (FL) or pcDNA empty vector plasmid and stained with an AlexaFluor488-labeled ROR2 antibody. The nuclei were counterstained with DAPI. Expression was analyzed by confocal microscopy. (Scale bar 10 µm)

In order to find out which domains of the ROR2 receptor then provide information about which functions of ROR2 might be relevant for mediating the increased invasiveness of ROR2 overexpressing MCF-7 cells, invasion assays were carried out. The Boyden chamber experiments revealed a significant reduction in the cell invasiveness of the N-terminal CRD deletion constructs, as well as the ROR2 constructs lacking PRD and TKD, indicating that these domains are important for cell invasion, as can be seen in Figure 15. The CRD domain has already been identified for binding of other Wnt ligands, suggesting that the CRD domain is also important for Wnt11 binding, indicated by the significant reduction in invasiveness after deletion of this domain. Furthermore, the considerable decrease of cell invasiveness by the loss of the TKD domain hints at its substantial role in mediating cell invasion

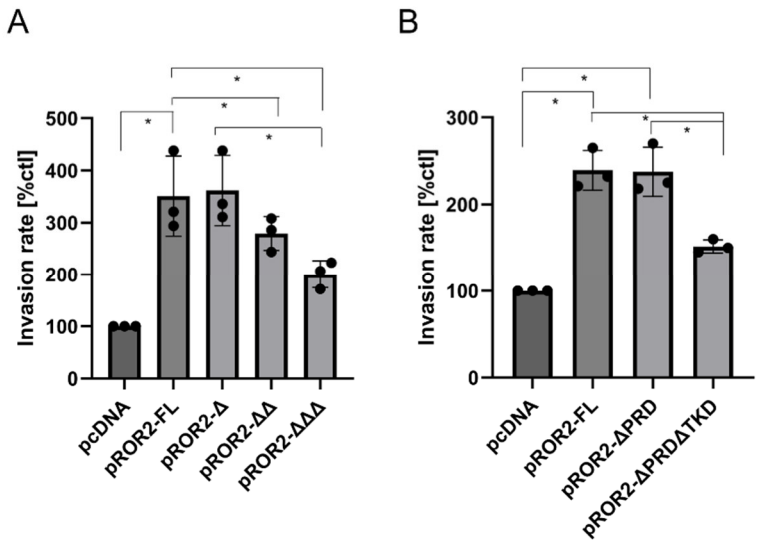


***Figure 15*: Loss of TKD, CRD and KRD of ROR2 significantly reduces ROR2-induced breast cancer invasion*:*** The invasion rates of MCF-7 breast cancer cells expressing either pcDNA, pROR2-FL or pROR2 deletion constructs of extracellular domains (A) or intracellular domains (B) were assessed by Boyden chamber assays over 96 h (mean±SD, n=3, *p<0.05).

### 3.1.5 High ROR expression is prognostic in breast cancer patients

The data demonstrated here show that ROR2 mediates a tumor-promoting aggressive phenotype in breast cancer. Furthermore, ROR2 has been shown to interact with the non-canonical Wnt ligand Wnt11. The CRD and TKD domains were found to be important for the functionality of ROR2 in relation to tumor invasion, as the CRD domain is required for Wnt interaction and the TKD domain is thought to be important for signal transduction. ROR1 has already been identified as an oncogene by various studies in breast cancer (Zhang *et al*, 2012), whereas the role of ROR2 has been discussed controversially (Tseng *et al*, 2020; Guo *et al*, 2020). Various studies have found that ROR1 was highly expressed in breast cancer and linked to an aggressive phenotype.

In line with these results also linking ROR2 to an aggressive phenotype and published data demonstrating that non-canonical Wnt signaling might be linked to metastasis formation, by promotion cell invasion, migration, adhesion, motility and proliferation (Chen *et al*, 2021), the question now arises whether high expression of ROR receptors in breast cancer patients is also associated with poorer metastasis-free survival. For this purpose, a microarray data set with 2075 primary breast cancer patients was analyzed for the influence of ROR1 and ROR2 on distant metastasis-free survival (DMFS) in the four distinct molecular subtypes. Among

them, ROR1 was only prognostic in the aggressive basal-like subtype in which high ROR1 expression in the primary tumor was associated with shorter DMFS (Fig. 16 A). In the remaining subtypes, high ROR1 expression had no effect on DMFS. This result obtained here fits with those of other studies in which ROR1 was also expressed highly in the basal-like subtype and therefore might function as a biomarker for this subtype (Pandey *et al*, 2019). To investigate the influence of increased ROR2 expression on breast cancer patients, the same data set was used for following analysis as can be seen in Figure 16 B Especially in the Her2 subtype a high ROR2 expression led to significantly worse DMFS compared to the other subtypes. High ROR2 expression in the remaining subtypes did not show any impact on the DMFS of the patients. Interestingly, a high ROR2 expression in the basal-like subtype showed the opposite effect of ROR1 with a high ROR2 expression resulting in better clinical outcome for the breast cancer patients.

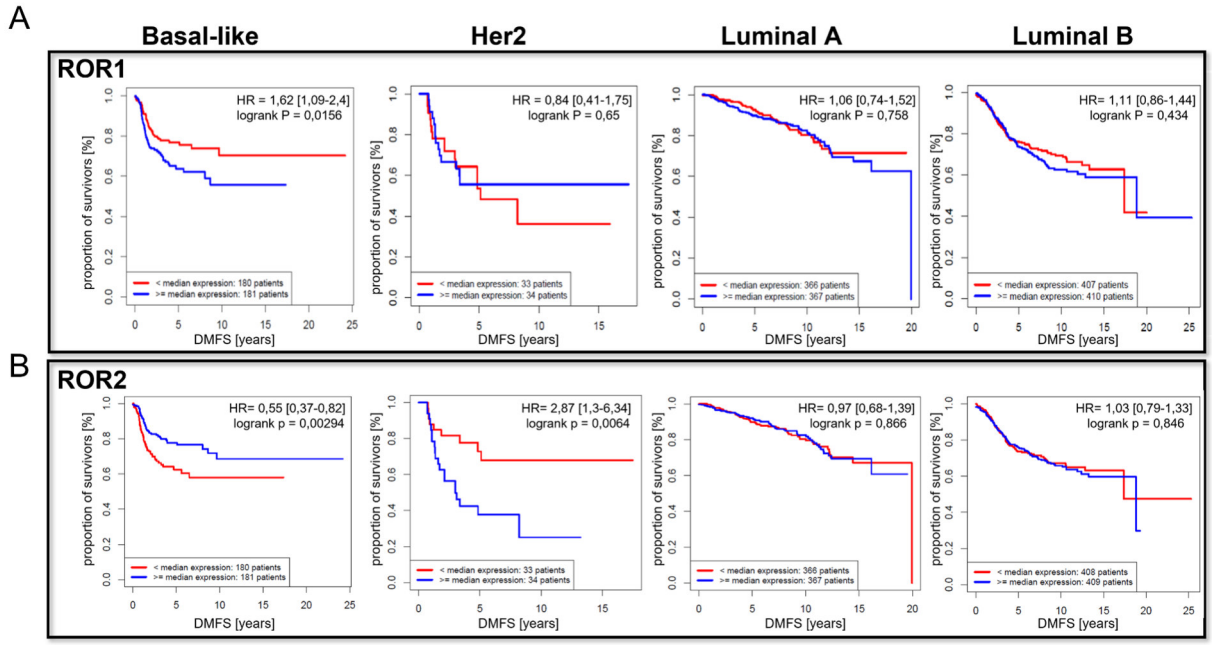


***Figure 16*: A high expression of ROR1/2 is prognostic in distinct breast cancer subtypes*:*** A+B, Survival analysis based on ROR1 gene expression data of primary breast cancers divided by their molecular subtype. Red: <median ROR1 expression, blue: >median ROR1 expression. Statistical significance was assessed by log-rank test (A). B, the same data set of primary breast cancer patients was used to analyze the DMFS depending on the expression of ROR2 in the distinct breast cancer molecular subtypes. Red: <median ROR1 expression, blue: >median ROR1 expression. Statistical significance was assessed by log-rank test.

In summary, a high ROR2 expression was linked to a poorer DMFS for Her2 subtype and for basal-like subtype a high ROR2 expression led to a better clinical outcome although the

immunohistochemical stainings and moreover a study from 2015 found high ROR2 expression in basal-like subtypes (Henry *et al*, 2015b). Nevertheless, it could be shown that ROR2 interacts with Wnt11 and triggers an aggressive phenotype in breast cancer. This suggests that ROR receptors play an important role in tumor progression in breast cancer.

## 3.2 Non-canonical Wnt11 mediates breast cancer invasion and migration via FZD6

### 3.2.1 Cell line screening

After it had been shown that ROR2 acts as a novel receptor for Wnt11 signaling, the question arose whether Wnt11 can additionally interact with other Wnt receptors, since MCF-7 does not express ROR2. Therefore, the first step was to perform a cell line screen to elucidate which WNT receptors and co-receptors are highly expressed in different breast and colorectal cancer cells, since Wnt signaling plays a central role in tumor progression in both breast cancer and CRC. Different cell lines, including a colorectal cancer cell line (SW48) and three breast cancer cell lines (MCF-7, T47d, SKBR3) were examined for the expression of all currently known WNT receptors and co-receptors using qRT-PCR (Fig. 17). The receptors vary in their expression levels depending on the respective cell lines. For example *FZD8* and *FZD10* were also not expressed in MCF-7 and T47d and only very weakly in SKBR3 and SW48. *FZD2* and *FZD5* were expressed in all cell lines examined. The non-canonical co-receptor *PTK7* was also expressed in all investigated cell lines, although the expression in SKBR3 was very low. A relatively high expression of *FZD1, FZD4* and *FZD6* and *RYK* was found in all four cell lines, whereas *FZD9* was consistently not expressed.

*FZD1*, on the one hand, is well-known for its role in the canonical Wnt signaling pathway and has been shown to bind the canonical Wnt ligands Wnt3 and Wnt3a (Chacón *et al*, 2008; Gazit *et al*, 1999). *FZD6*, on the other hand, appears to play a central role in both canonical and non-canonical Wnt signaling, although *FZD6* was mainly associated with non-canonical Wnt signaling (Corda & Sala, 2017). Therefore, FZD6 was selected as the most promising non-canonical Wnt receptor because it was the most highly expressed in the cell lines studied here

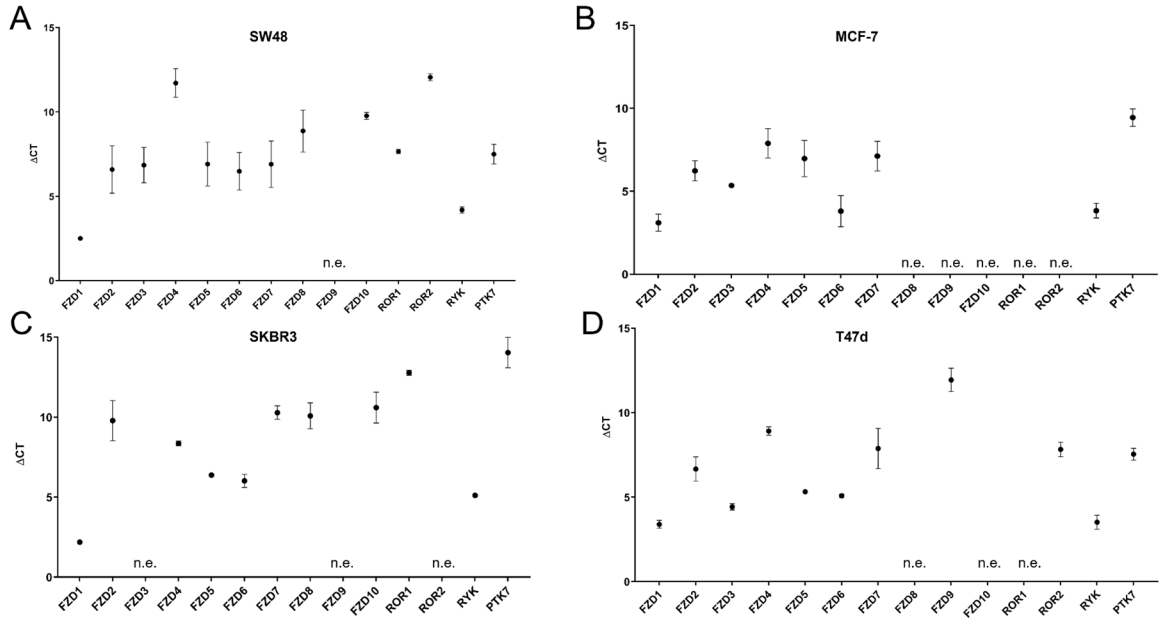


***Figure 17*: Characterization of the WNT receptor profile in distinct human breast and CRC cells*:*** The expression of different Wnt receptors and co-receptors was measured by qRT-PCR in the human colorectal cancer cell line SW48 (A), as well as the human breast cancer cell lines MCF-7 (B), SKBR3 (C) and T47d (D) (mean±SD, n=3). All genes with Ct values >30 were considered as not expressed (n.e.).

### 3.2.2 WNT11 interacts with non-canonical Wnt receptor FZD6 in breast cancer cells

To investigate whether the knockout of Fzd6 antagonizes WNT11-induced tumor invasion and migration, FZD6 knockout was first established in the breast cancer cell line MCF-7 by using the CRISPR / Cas9 method to generate two single-strand breaks in the second exon of FZD6 and thereby a knockout of FZD6. Two clones were picked for subsequent experiments. The Western blot showed a complete knockout of FZD6 in comparison to the control cells (Fig.18 A). First, a migration assay as shown in Figure 18 B was established. For this assay, 6-well plates coated with ECM were prepared and cells were seeded into Ibidi inserts. After removal of the inserts, microscopic images were taken after 0 h and 20 h and the migration rate was determined by measuring the area occupied by the migrating cells. Knockout of FZD6 resulted in a significant reduction in the migration rate in MCF-7 cells compared to control cells (Fig.18 C). In a second step, the invasion rate was measured in Boyden chamber experiments. MCF-7 FZD6 knockout and control cells were stimulated with recombinant Wnt11 for 96h and the invasion rate was determined (Fig.18 D). Knockout of FZD6 resulted

in a significant reduction in the migration rate in MCF-7 cells compared to control cells. Stimulation of Wnt11 led to a significant increase in migration in control cells, whereas FZD6 knockout cells showed no increase in migration despite Wnt11 stimulation. In order to exclude that the observed effects were caused by an influence of the FZD6 knockout on cell proliferation, dye dilution assays were carried out (Fig.18 E). As shown in Figure 18, there was no significant reduction in cell proliferation in the two FZD6 knockout clones compared to the control cells, suggesting indeed that FZD6 mediates Wnt11-induced breast cancer invasion and migration.

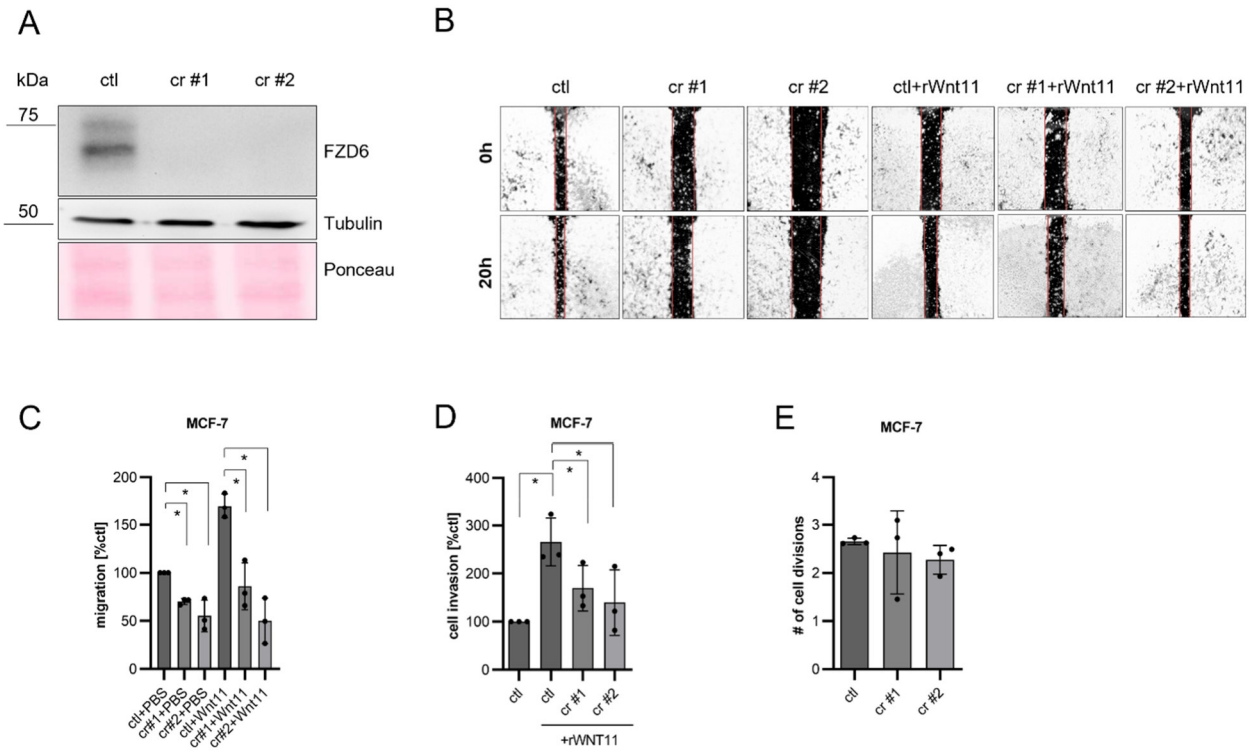


***Figure 18*: FZD6 mediates Wnt11-induced breast cancer invasion and migration*:*** A, Western blot of MCF-7 CRISPR FZD6 knockout cells (Cr #1,2 = two clones, ctl = empty vector control) shows a complete knockout of FZD6. B, Experimental setup of wound healing assay with MCF-7 control or CRISPR FZD6 cells either stimulated for 96 h with PBS (ctl) or rWnt11 (100 ng/ml, mean±SD, n=5). C, Migration rate of FZD6 knockout in MCF-7 cells in comparison to the control cells, either stimulated with PBS or with rhWnt11 in the wound-healing assay as shown in B (*p<0.05). D, Invasion assay: MCF-7 control or CRISPR FZD6 cells treated with rWNT11 (mean±SD, n=3, *p<0.05). D, MCF-7 CRISPR FZD6 and control cells were stained with celltrace violet. The cell divisions were then measured by flow cytometry according to the dye distribution over 72h.

### 3.2.3 WNT11 is a novel ligand of FZD6

The question now arose whether there is an interaction between Wnt11 and FZD6. Based on these results, it was hypothesized that FZD6 might act as a novel receptor for WNT11. In order to confirm a potential interaction, Co-IP experiments were conducted. To this end, MCF-7 cells were transfected to express V5-tagged Wnt11 and FLAG-tagged FZD6. 24 h post transfection, the cells were treated with a membrane-permeable crosslinker and lysates were subjected to pull-down with the V5 antibody. Indeed, FZD6 precipitated with V5-Wnt11 suggesting an interaction between both (Fig.19).

As FZD receptors often engage with distinct co-receptors to relay Wnt signals, the question arose whether this is also the case for Wnt11-Fzd6. Preliminary data from our group (not shown here) suggested that the overexpression of Wnt11 in MCF-7 cells upregulated the expression of PTK7, while the other known Wnt co-receptors (Ryk, ROR1 and ROR2) remained unaffected. Furthermore, it had been shown that the combined expression of Wnt11, FZD6 and either PTK7 or Ryk led to increased 5-year mortality rates in human colorectal cancer (Gorroño-Etxebarria *et al*, 2019). Taken together, these data supported the hypothesis that PTK7 might act as a possible co-receptor for Wnt11. Indeed, it was demonstrated that PTK7 was co-immunoprecipitated with Wnt11 (Fig.19), thereby confirming FZD6 and PTK7 as novel interaction partners for Wnt11.

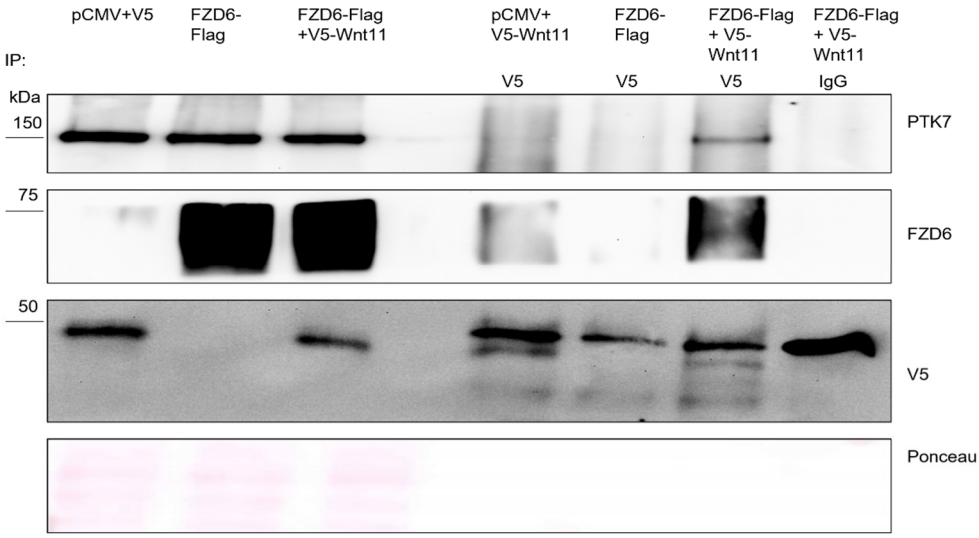


***Figure 19*: Co-immunoprecipitation of FZD6 with Wnt11 and PTK7*:*** MCF-7 cells were transiently transfected with pCMV, pFZD6-Flag or V5-tagged Wnt11 and used for Co-immunoprecipitation of V5-Wnt11 or IgG control. Successful pull-down was visualized by western blot for V5, FZD6 and PTK7. Ponceau staining is shown as loading control.

### 3.2.4 High FZD6 expression is prognostic in breast cancer patients

Having identified FZD6 as a receptor for Wnt11 and demonstrated that both Wnt11-mediated invasion and migration are initiated via its interaction with FZD6, the next step was to investigate whether FZD6 has a prognostic impact on breast cancer patients. A microarray data set of 2075 primary breast cancer patients was analyzed (Fig. 20) (Bayerlová *et al*, 2017). First, based on our preliminary results (unpublished) and previously published data, a Wnt11 gene signature of non-canonical Wnt signaling genes including receptors and downstream targets, as well as genes from associated signaling pathways such as PI3K signaling, was generated. As can be seen in Figure 20 A, the signature clustered patients into two groups that differ in distant metastasis-free survival. Here, the group with the worse clinical outcome is the one in which Wnt11 is highly expressed. *FZD4, FZD9, mTOR, GSK3, ROCK2, RORA* and *PIK3C* clustered together with Wnt11. Interestingly, *FZD6* did not cluster with *Wnt11*, but instead clustered with *FZD1, FZD2, FZD5, FZD7, FZD10, RYK, ROCK1, FZD5, RASGRP1* and *ROR1/2*. The group with high gene expression of these genes showed a better clinical outcome in comparison. In addition, Kaplan-Meier survival curves showed the influence of high or low *FZD6* or *FZD4* gene expression alone on the distant metastasis-free survival (DMFS) of the patients. It was found that a high *FZD6* expression was associated with a significantly reduced DMFS, while the opposite was true for *FZD4* (Fig.20 B). Another data set was used to confirm these data and therefore the public online tool kmplot.com was utilized for this purpose. The online tool uses various public datasets for the analyses, which then include data from 2675 breast cancer patients (Győrffy, 2021). In fact, the prognostic influence of *FZD6* on the metastasis-free survival of breast cancer patients was also confirmed in this independent dataset (Fig.20 C).

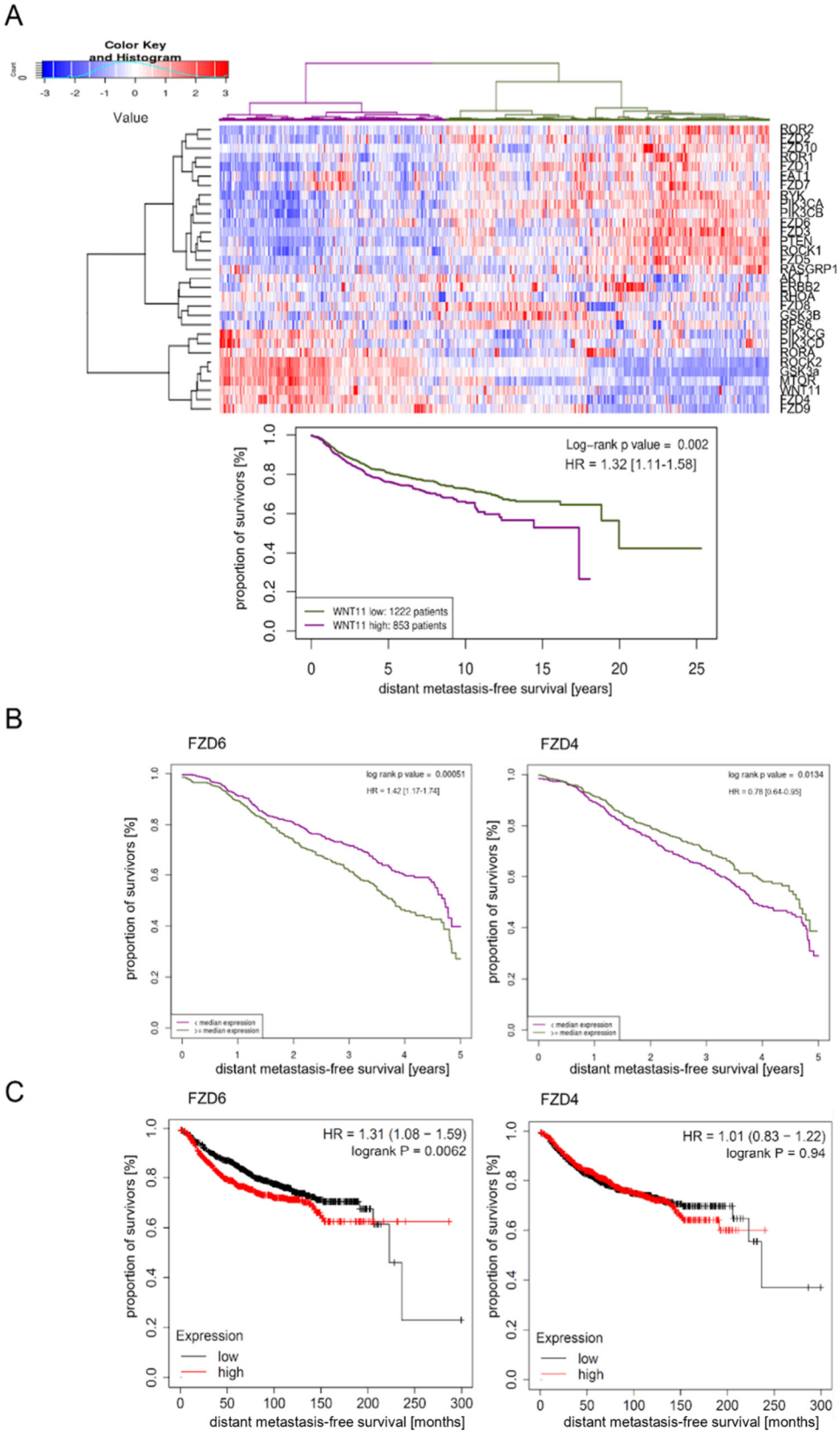


***Figure 20*: High FZD6 expression is prognostic in breast cancer patients*:*** A, Gene expression data of 2075 primary breast cancer patients were analyzed based on a preliminary defined Wnt11 signaling

signature with associated genes. The signature clustered the data set into two patient groups, among which the group with high Wnt11 expression (violet curve) is associated with poor distant metastasis-free survival. B, Kaplan-Meier plot of distant-metastasis free survival (DMFS) in the cohort depending on the FZD6 or FZD4 expression level. Violet: <median expression, green: >median expression. Statistical significance was calculated by log-rank test. C, the online tool kmplot.com was used to additionally analyze the distant metastasis-free survival of 2765 breast cancer patients based on their median FZD6 and FZD4 expression. black = low expression, red = high expression.

### 3.2.5 High FZD6 expression is prognostic in colorectal cancer patients

Although canonical Wnt signaling is predominantly active in colorectal cancer and is known to be a main driver of CRC, non-canonical Wnt members are also found to be highly expressed in colorectal cancer. For instance *Wnt11* was characterized as an oncogene in CRC and furthermore found to be highly expressed in CRC (Ouko *et al*, 2004; Kirikoshi *et al*, 2001; Nie *et al*, 2020). Therefore, the Wnt11 signature, which was used before, was extended to all Wnt ligands and also Norrin, as a known non-canonical ligand for FZD4 (Bang *et al*, 2018). Since Norrin and other Wnt ligands trigger Wnt signaling in the CRC and are therefore of central importance for CRC progression, they were considered important for the generation of this signature, as Norrin-triggered Wnt signaling, for example, has been linked to angiogenesis in the CRC (Planutis *et al*, 2014).

This signature was used to analyze a patient cohort with public microarray data of 290 primary CRC patients (Fig.21). The hierarchical cluster analysis yielded four patient clusters. The Kaplan-Meier curves display the DMFS according to the four clusters, generated on the basis of this gene expression analysis. Interestingly, *Wnt11* clusters with *Norrin* and other Wnt ligands, with most of the ligands being highly expressed in the CRC patient data. *Wnt11* does not cluster here either with *FZD6*, which in turn clustered in a group *with FZD5, GSK3, Wnt10, Wnt8A, RYK, Wnt16, Wnt7b, mTOR* and *AKT*. A patient group with high gene expression of this *FZD6* cluster showed a significantly worse distant-metastasis free survival. In comparison to *FZD6, FZD4* showed contrary expression levels in the CRC patients and clustered with *ROR1, RORA, ROR2, FZD8, Wnt3a, Wnt2* and *Wnt5a*. Nonetheless, non-canonical Wnt signaling appears to play a greater role in breast cancer.

Both the in vitro data and the patient data showed greater effects in breast cancer with regard to Wnt11-mediated non-canonical Wnt signaling and its impact on tumor progression and metastasis. Therefore, the focus of this work remains on breast cancer.

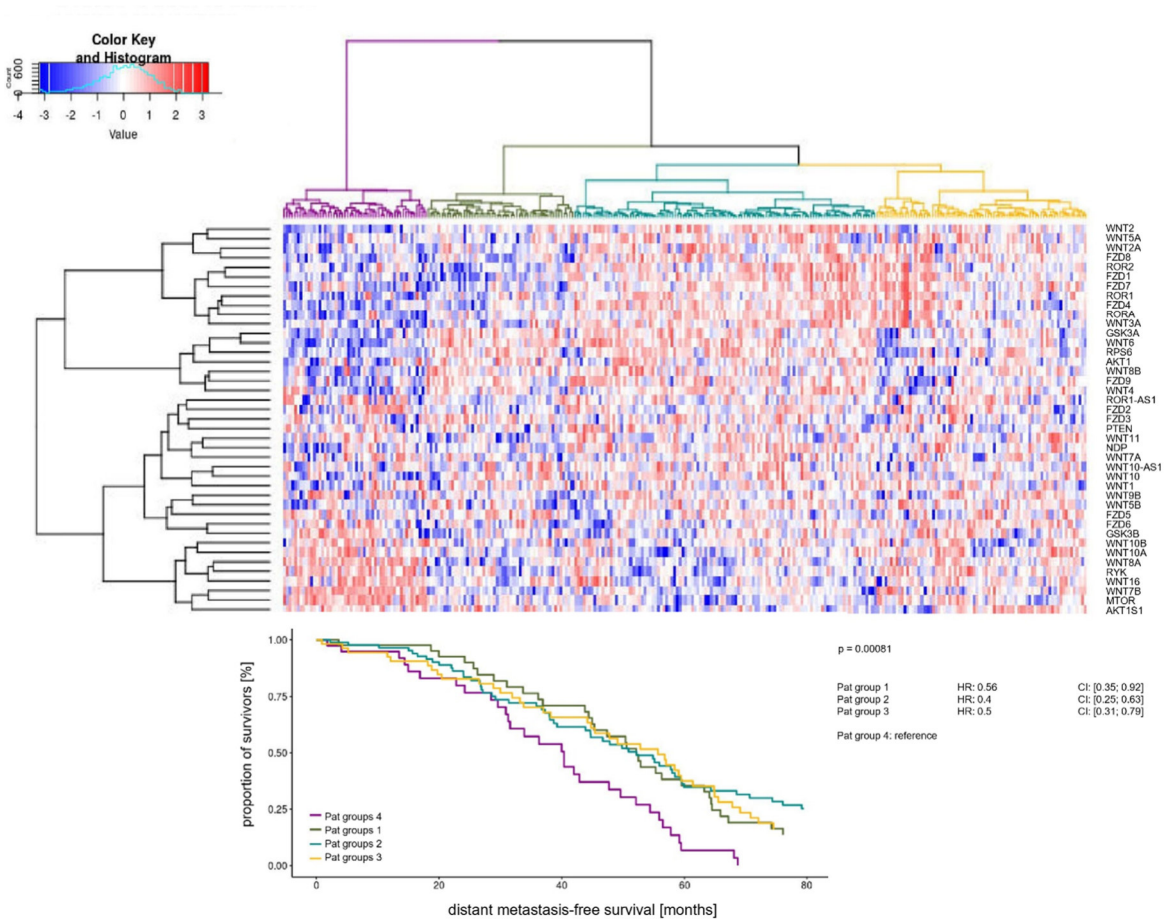


***Figure 21*: Gene expression and survival analysis of primary CRC patients*:*** Microarray data of 290 primary colorectal cancer patients were analyzed and a signature of Wnt signaling associated genes subdivided the patients into four groups. Kaplan-Meier survival curves showed distant metastasis-free survival of the four groups. Statistical significance was calculated by log-rank test.

## 3.3 The role of the ROR receptors in EV biogenesis

### 3.3.1 ROR1 is expressed on MDA-MB231 EVs

Various studies have shown that Wnt proteins are transported on EVs to neighboring cells in which they can trigger Wnt signaling responses (Gross *et al*, 2012; Menck *et al*, 2013). In order to investigate whether the same is true not only for WNT ligands, but also for WNT receptors, the expression of ROR1 was investigated on LV, MV and EXO. To this end, EVs

were isolated from the TNBC cell line MDA-MB231 by differential ultracentrifugation, because ROR1 was shown to be highly expressed in MDA-MB231 breast cancer cells. To confirm successful EV isolation, the vesicles were characterized according to the MISEV criteria (Théry *et al*, 2018) by NTA and Western blot.

First, the isolated EVs were characterized by NTA, to confirm the isolation of different EV populations that differ in their sizes. Therefore, mean sizes and concentrations of the isolated vesicles were measured and they concurred with the expected values for EVs (Menck *et al*, 2020), with a mean size for LVs of 212 µm, MVs 205 µm and EXOs 171 µm. MDA-MB231 cells show a very low secretion of LVs and predominantly secrete MVs, as can be seen in Figure 22. A Western blot was used to investigate whether MDA-MB231 EVs actually express ROR1 and, if so, on which vesicle subpopulation. Various vesicle markers were used as controls to ensure that the isolated vesicle populations are not contaminated and that the results are valid. As can be seen in Figure 22 A, ROR1 is expressed specifically on MV and EXO, but not on the larger LV populations. Rgap1, α-Actinin4 and CK18 were used as LV markers, Rgap1, α-Actinin4 and Kif4 functioned as MV markers, whereas CD9, CD63, Syntenin and Alix displayed EXO markers. GM130 is a membrane protein localized at the Golgi matrix (Nakamura, 2010). Calregulin, on the other hand, is a $Ca^{2+}$-binding chaperone protein and is localized at the endoplasmic reticulum or other cellular compartments (Varricchio *et al*, 2017). Since neither of the proteins are involved in vesicle biogenesis, they act as negative markers here.

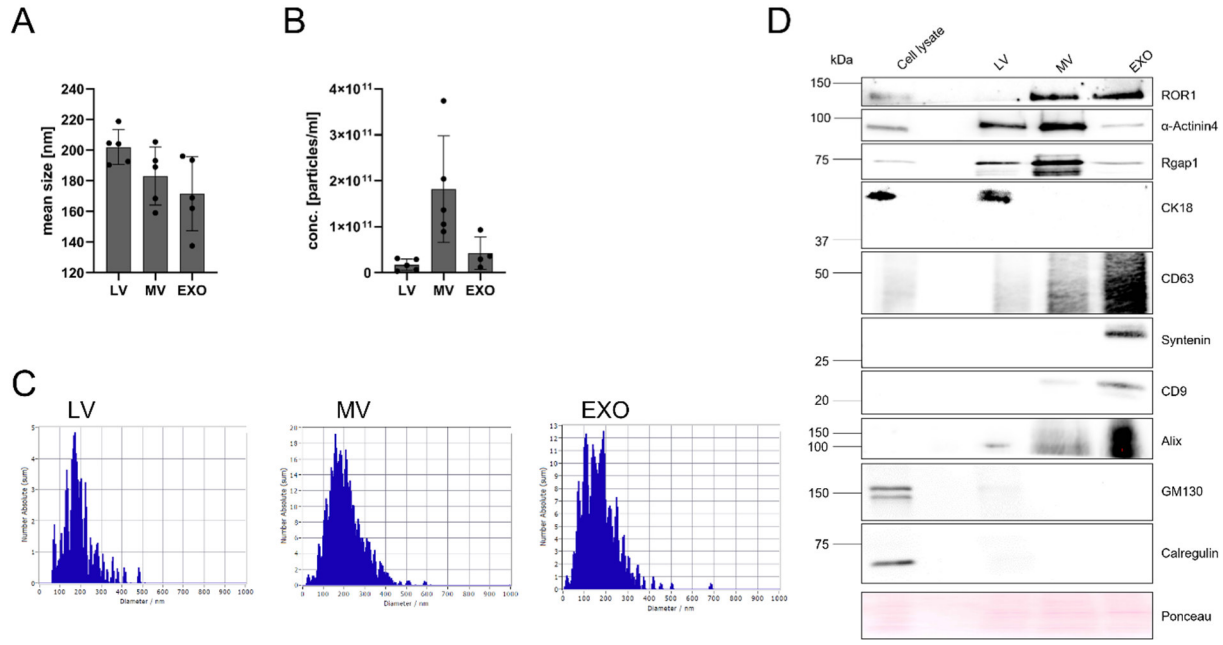


***Figure 22*: ROR1 is expressed on MV and EXO of MDA-MB231 cells*:*** A+B, Characterization of the extracellular vesicles of MDA-MB231 cells by using NTA, according to their sizes (A) and concentrations (B). C, Size distribution of LVs, MVs, and EXOs in nm. D, Characterization of MDA-MB231 wildtype cells and EVs by western blot with different EV markers and ROR1. GM130 and Calregulin were used as negative markers.

### 3.3.2 ROR1 affects protein composition of breast cancer cell-derived EVs

After it was found that ROR1 is expressed on MDA-MB231 MV and EXO, ROR1 was knocked out in MDA-MB231 wild-type cells to investigate whether ROR1 only functions as a cargo molecule on EVs, or whether it is itself involved in their biogenesis. For this purpose, two knockout clones (#1 and #2) were generated using the CRISPR/Cas9 method targeting either exon one (clone #1) or exon two (clone #2). Successful knockout was validated by Western blot in comparison to empty vector cells. (Fig.23 A). To ensure that the loss of ROR1 would not be compensated with ROR2 and thereby affect subsequent results, qRT-PCR was performed with the MDA-MB231 ROR1 knockout cells. No upregulation of ROR2 was found, ruling out possible compensation (data not shown).

In order to investigate the influence of ROR1 on vesicle biogenesis, the same number of ROR1 knockout and control cells were subjected to EV isolation. Equal cell numbers were confirmed by measuring the cell confluence (Fig.23 B) and allowed to draw quantitative conclusions about EV release. NTA demonstrated no significant effect of the ROR1 knockout on the concentrations or size of the released vesicles (Fig.23 C). To ensure that knockout of

ROR1 did not cause cells to differ from control cells and might affect vesicle biogenesis, phalloidin staining of ROR1 knockout cells and control cells was prepared and compared by immunofluorescence microscopy. As shown in Figure 23 D, no morphological differences were found that would account for possible differences in vesicle biogenesis.

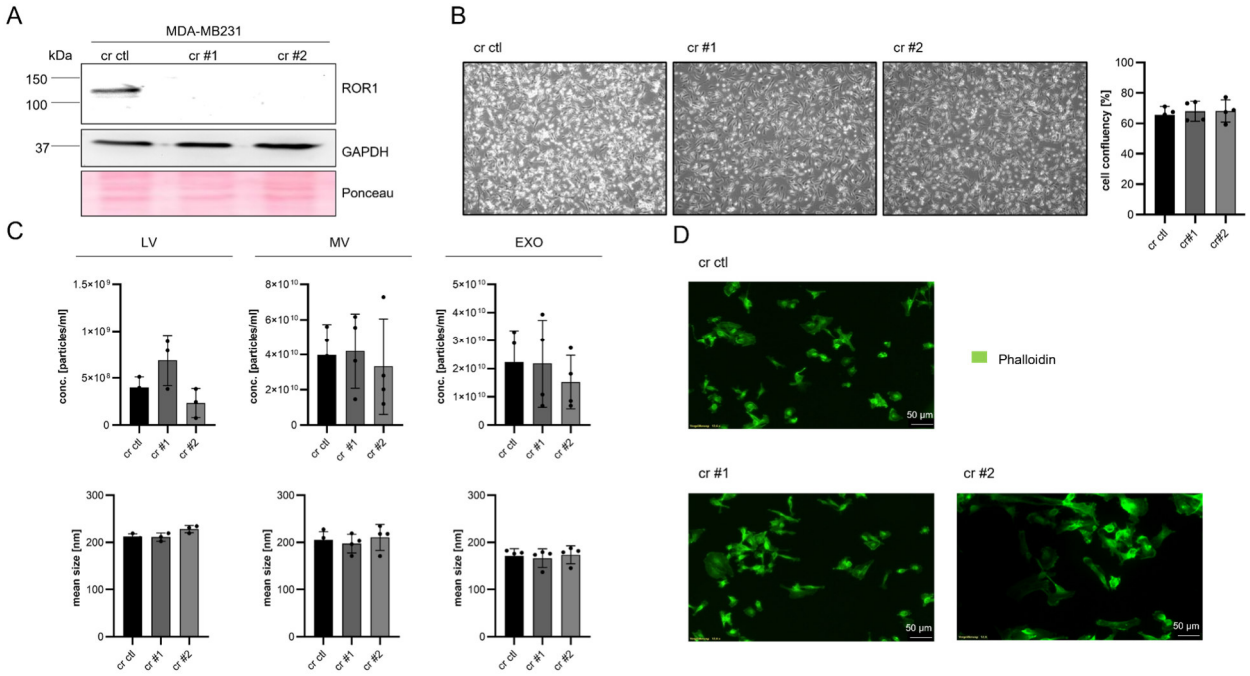


***Figure 23*: Knockout of ROR1 does not affect the size or concentration of MDA-MB231 EVs*:*** A, Western Blot of ROR1 expression in MDA-MB231 CRISPR ROR1 knockout cells (cr #1,2 = two clones, cr ctl = empty vector). GAPDH is shown as housekeeper protein, Ponceau staining as loading control. B, Cell confluency measurement: The same number of MDA-MB231 cr ctl or cr ROR1 cells were seeded into petri dishes and grown overnight for EV isolation. The cell confluence was determined based on microscopic pictures. C, EV concentration and mean size: NTA analysis of concentration and mean size of the different EV populations released by cr ctl or cr ROR1 cells. D, Immunofluorescence microscopy: Phalloidin staining of MDA-MB231 CRISPR ROR1 cells in comparison to empty vector cells (scale bar 50 µm).

As shown in Figure 24, the knockout of ROR1 indeed affected the protein composition of all three investigated EV populations, i.e. LV, MV, and EXO. In the LVs Rgap1 expression was significantly reduced by the knockout of ROR1, as well as Kif4 and Rgap1 expression on MVs of the CRISPR ROR1 clone #2. Interestingly, Kif4 and Rgap1 expression were not decreased in clone #1. This should be analyzed in more detail in further experiments, in order to determine which clone reflects the effects of ROR1 on the EV composition more accurately. Furthermore, expression of the EXO markers CD63 and CD9 was significantly

reduced by the knockout of ROR1 in both knockout clones. Interestingly, knockout of ROR1 affected vesicle composition of Rgap1 expression on LVs in both ROR1 knockout clones, suggesting a stable effect, although ROR1 per se was not expressed on the LVs. Indeed, it is not entirely clear which of the ROR1 knockout clones now reflects the most accurate results for the effect of ROR1 on vesicle composition. All in all, clone #2 often seems to have the stronger effects on vesicle composition, whereas α-Actinin4 does not appear to be affected by the ROR1 knockout. The effect on CD9 in EXOs is significant for both ROR1 knockout clones, suggesting a strong consistent effect of ROR1 on CD9.

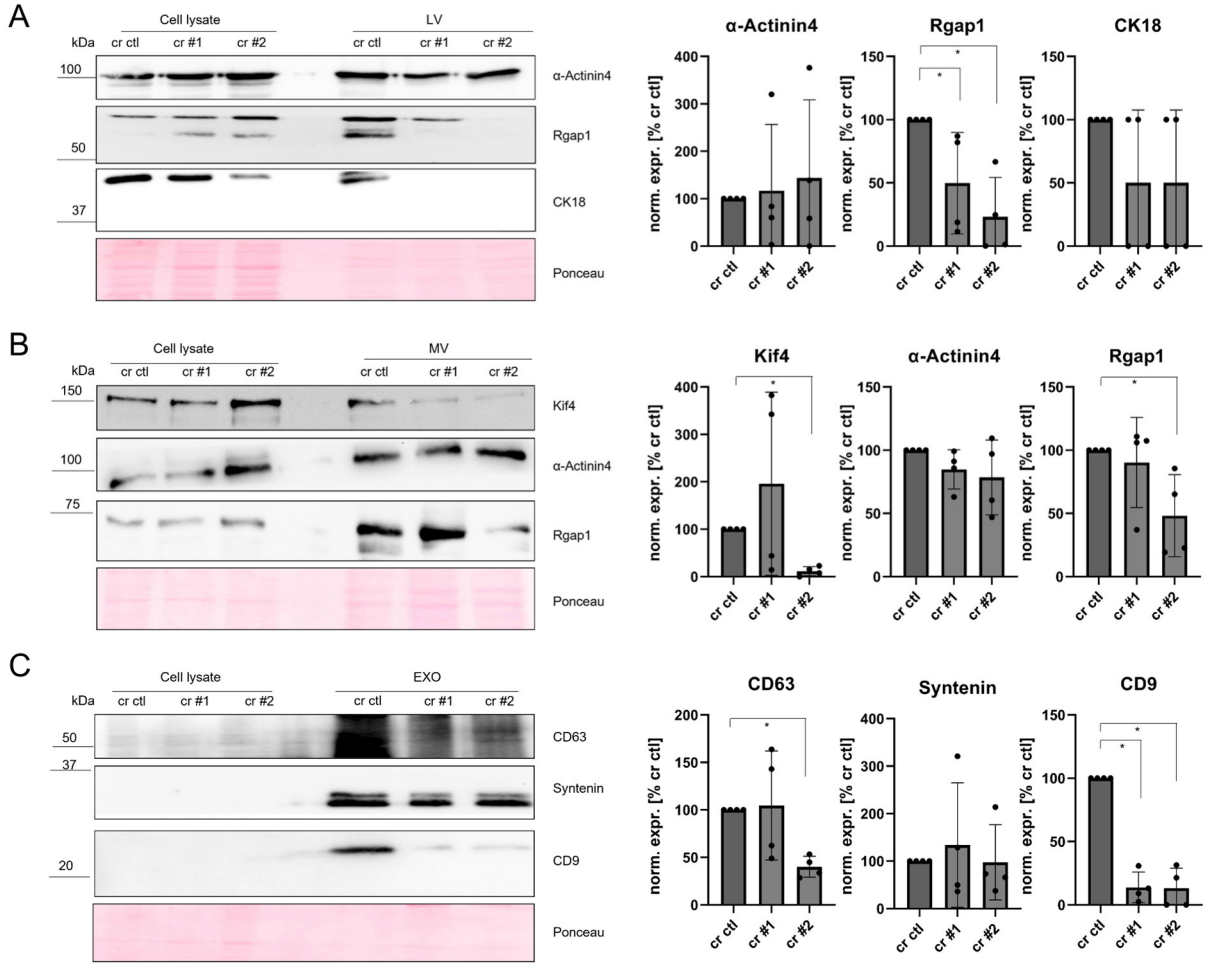


***Figure 24*: The knockout of ROR1 altered EV protein composition*:*** A-C, EVs isolated from MDA-MB231 ROR1 knockout (cr #1,2 = two clones) and control (cr ctl) cells were characterized by Western blot for the expression of characteristic markers for the distinct EV populations. The corresponding cell lysates are shown for comparison. Densitometric quantification of the selected marker proteins is shown below and was normalized on the EV isolated from cr ctl cells (mean±SD, n=4, *p<0.05).

ROR1 overexpression allows the study of ROR1 regarding its role in vesicle composition, as well as its role on the concentration of released vesicles and their sizes. Thereby, overexpression allows a different perspective compared to the knockout of ROR1 and may further support these results. Since MCF-7 wild-type cells do not express ROR1, ROR1 overexpression was performed in MCF-7 cells. The ROR1 overexpression in comparison to empty vector cells was confirmed by Western blot (Fig.25A). The same number of cells were seeded in EV-free medium and the cell confluence was determined by microscopic images quantified with FIJI, revealing no significant difference (Fig.25 B). The EVs were then isolated by differential ultracentrifugation and quantified by NTA (Fig.25 C). While there was a non-significant increase in the concentration of MVs secreted by ROR1-overexpressing MCF-7 cells, the effect was not observed for EXO. In line, the overexpression of ROR1 did not affect the size of the secreted EVs. Unfortunately, not enough LV could be isolated from the ROR1 overexpression cells to ensure a valid NTA measurement, since the NTA analysis requires sufficient amounts of EVs. Therefore, LV measurements were not included in this work.

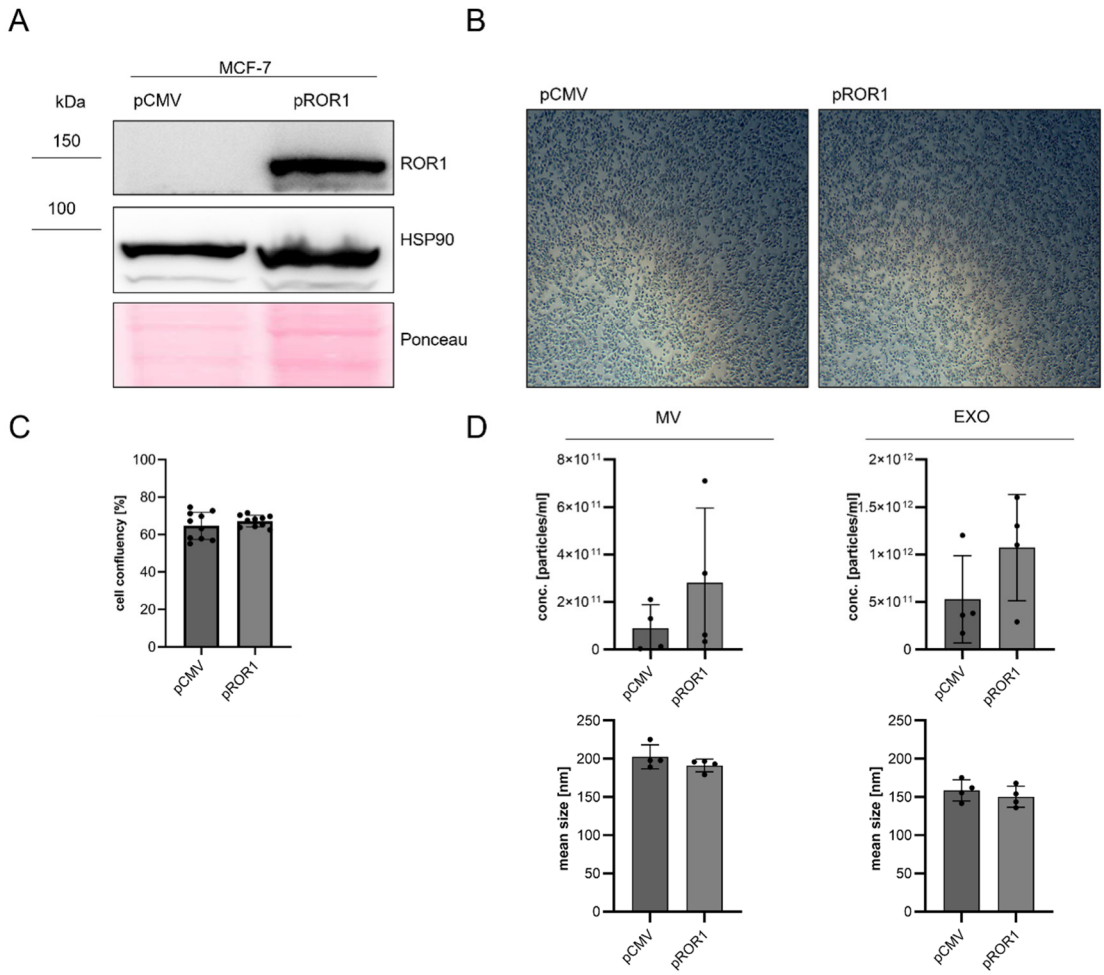


***Figure 25*: Overexpression of ROR1 has no major effects on the size or concentration of MCF7-EVs:** A, ROR1 overexpression (pROR1) in MCF-7 cells in comparison to the empty vector control (pCMV) was confirmed by Western blot. HSP90 was used as housekeeper protein. B, Microscopic pictures: the same number of MCF-7 pROR1 and pCMV cells were sown overnight in petri dishes for EV isolation. C, Cell confluency measurement of the microscopic pictures with the FIJI software. D, Concentration and mean sizes of EVs: NTA measurement of size and concentration of the different EV subpopulations isolated from MCF-7 pCMV and pROR1 cells.

Next, the previously isolated vesicles were analyzed for the various EV markers by Western blot (Fig.26).

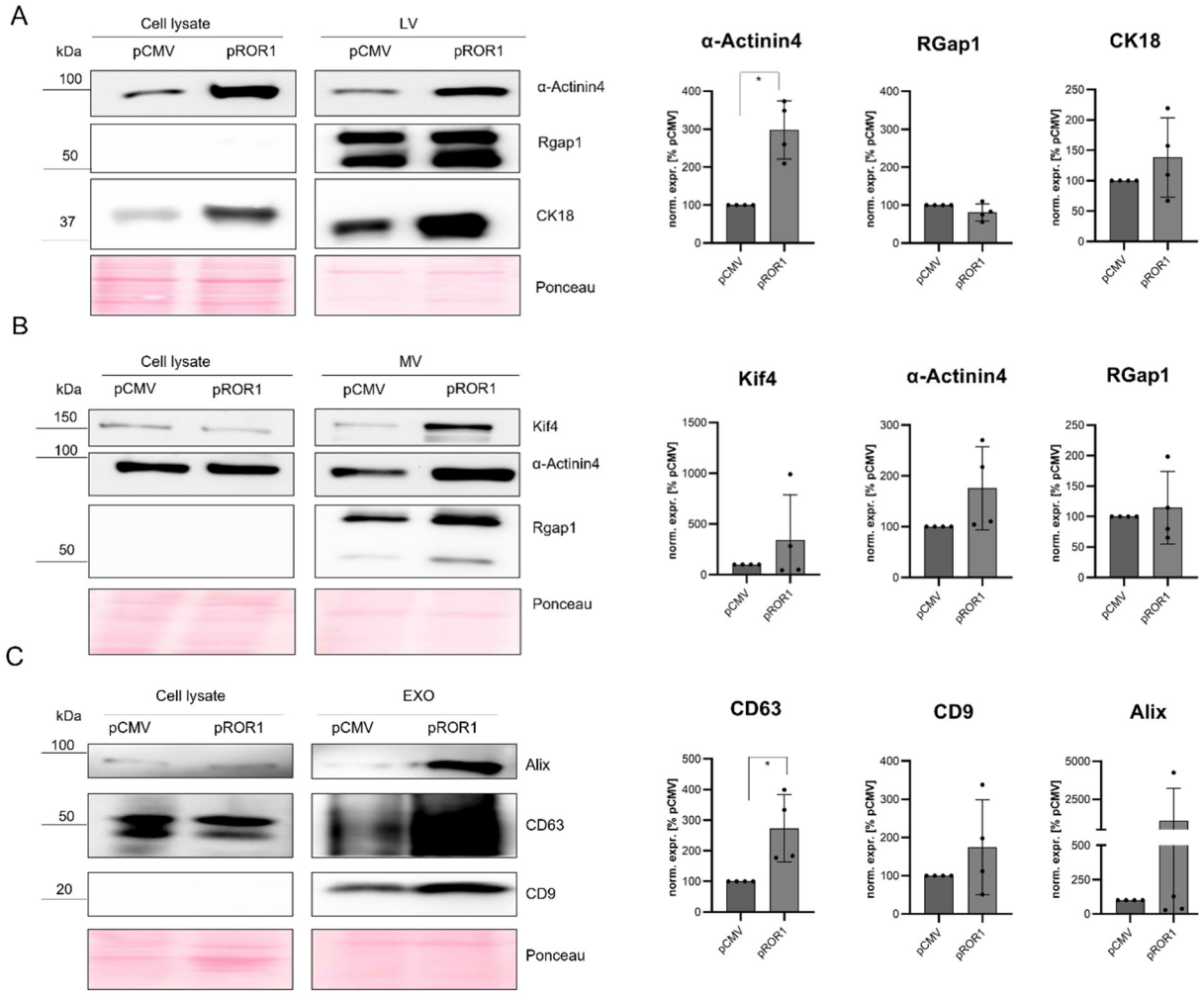


***Figure 26*: ROR1 overexpression leads to increased vesicle marker expression on EVs*:** A-cC, Western blot of LV (A), MV (B) and Exo (C) released by the same number of MCF-7 pCMV or pROR1 cells. The expression of the proteins was quantified by densitometry (mean±SD, n=4, *p<0.05).

Although not all effects of the ROR1 knockout on the EV protein composition fit to the results of ROR1 overexpression, the obtained results of ROR1 overexpression led to a significantly increased CD63 expression, which matches the results of the ROR1 knockout clone #2. Furthermore, the α-Actinin4 protein expression levels were increased by ROR1 overexpression in the LVs In addition, ROR1 overexpression resulted in a non-significant increase in the levels of the two EXO markers Alix and CD9. The significant reduction of Rgap1 under the loss of ROR1 did not match to the results obtained from the overexpression of ROR1 with no changes in the protein expression of Rgap1, suggesting a non-specific off-target effect of the ROR1 KO. The results for Kif4 and CD9, although not significant here,

show a trend that both proteins with ROR1 overexpression are more highly expressed on EVs, which again fits the results from the ROR1 knockout.

Although ROR1 was found only on MVs and EXOs, ROR1 overexpression and knockout in breast cancer cell lines led to changes in EV composition in all EV subpopulations. It is possible that there could be a direct interaction of ROR1 with EV markers altered here. Indeed, it has recently been shown that the deletion of ROR1 deletion inhibits the formation of CD63-positive MVEs, thereby reducing EXO release (Yamaguchi *et al*, 2020). All these results indicate a possible interaction of those proteins.

### 3.3.3 Loss of vesicular ROR1 on MDA-MB231 EVs affects MCF-7 cell invasion

Preliminary data demonstrated that the stimulation of EVs from aggressive cells such as MDA-MB231 on less aggressive cells such as MCF-7 could increase their invasiveness in vitro (Menck *et al*, 2015). Moreover, it had already been shown that the stimulation of Wnt5a positive EVs led to increased breast cancer cell invasiveness (Menck *et al*, 2013). In a subsequent step, the influence of the isolated vesicles on the invasion of the less aggressive MCF-7 breast cancer cells was investigated by stimulating MCF-7 cells in modified Boyden chambers with 1 µg EVs from the various EV populations of MDA-MB231 ROR1 knockout cells in comparison to empty vector cells (Fig.27). The results show that the invasiveness of the MCF-7 cells can be increased by stimulation with EVs of the MDA-MB231 empty vector cells which confirms previous data (Menck et al, 2015). Stimulation with the EVs of MDA-MB231 control cells resulted in a strong invasion increase of MCF-7 cells. Upon loss of ROR1, the invasion rate of MCF-7 cells under EV stimulation decreased at least back to control levels, and even below for MVs. Subsequently, knockout of ROR1 and thus ROR1-negative MVs slightly inhibited MCF-7 cell invasion.

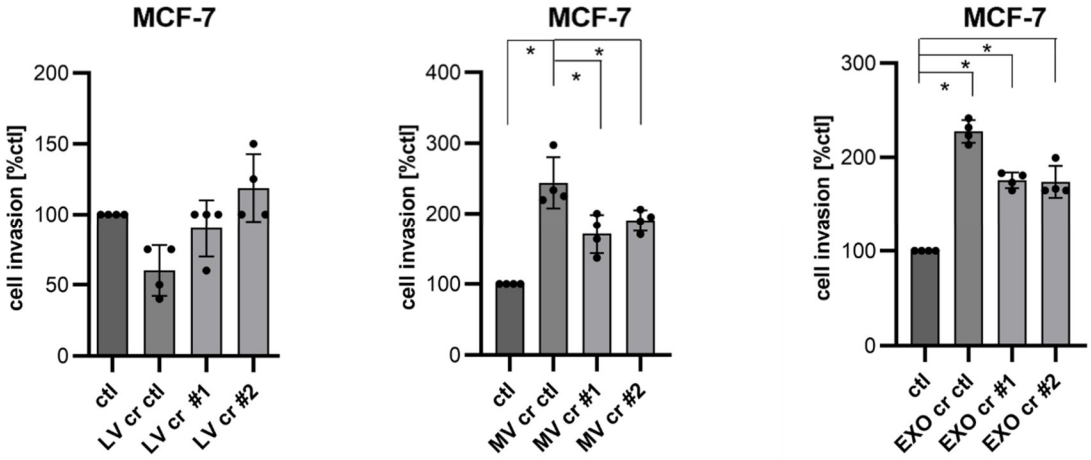


***Figure 27*: Loss of vesicular ROR1 on MDA-MB231 EVs affects MCF-7 cell invasion*:** Invasion assay of MCF-7 cells stimulated with 1µg EVs of MDA-MB231 CRISPR ROR1 or CRISPR control cells over 96h. (mean±SD, n=3 *p<0.05).

### 3.3.4 The role of ROR2 on breast cancer cell-derived EVs

Due to the similarities of both receptors and the results from ROR1 the question arose whether ROR2 also has an effect on EV composition. To answer this question, ROR2 knockdown and overexpression breast cancer cells were generated as model cell lines. ROR2 knockdown was performed in the Luminal A breast cancer cell line T47d, which had previously shown a relatively high gene and protein expression of ROR2 in the cell line screening (Fig.10). As an initial screening of the EV concentration and sizes as quality control, the vesicles of T47d were characterized in the NTA (Fig.28).

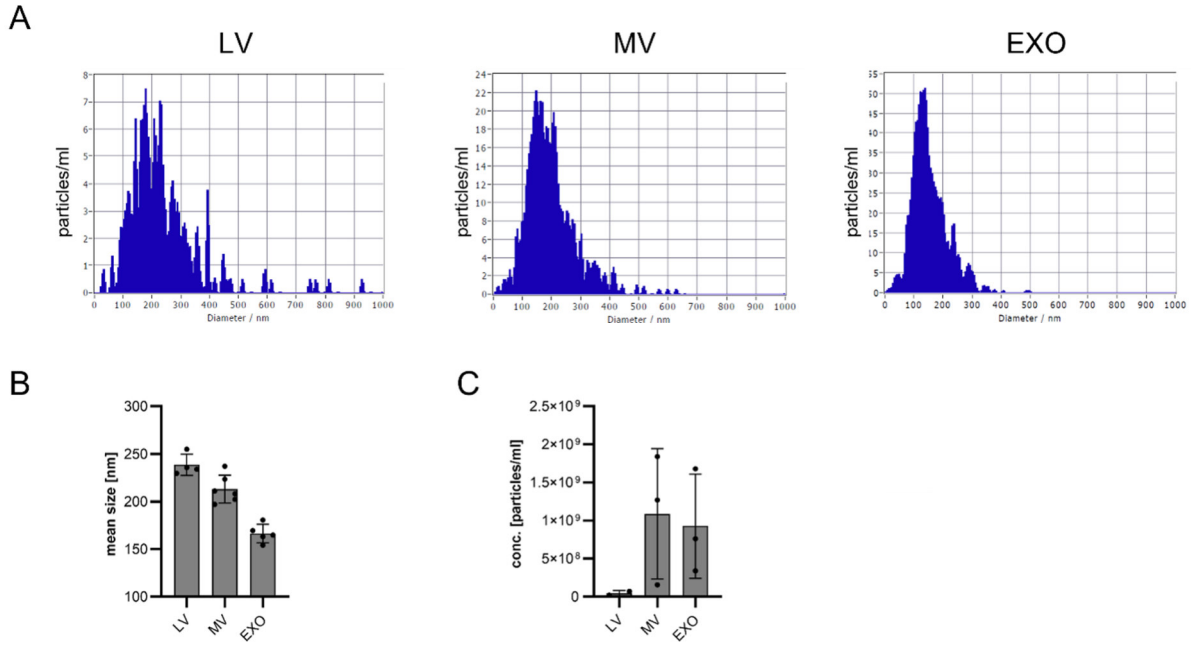


***Figure 28*: Extracellular vesicles of T47d wildtype cells*:*** A, NTA measurement: size distribution of T47d EVs. B, NTA measurement of mean sizes of EVs from T47d cells. C, Concentration of the isolated EVs from T47d breast cancer cells and characterized by NTA.

Overall, the mean sizes and concentrations of T47d vesicles were as expected, although T47d cells secrete few LVs, suggesting that these cells predominantly transmit signals via MVs and EXOs (Fig.29 C) The mean sizes of MVs with a size of 216 µm and EXOs with a mean size of 169 µm were in line with the expected size for these EV populations, suggesting that MVs and EXOs could indeed be isolated (Menck *et al*, 2020). Overall, T47d cells appear to secrete a little higher MV concentrations than the EXOs, although the difference in concentration is very small. Subsequently, ROR2 was knocked down in T47d cells using an siRNA pool. Successful knockdown was confirmed by Western blot (Fig.29 A). To study the influence of ROR2 on EV biogenesis, equal numbers of T47d cells transfected with either a control siRNA or a siRNA targeting ROR2 were seeded for EV isolation (Fig.29 B). Then, the EVs were isolated by differential ultracentrifugation and quantified by NTA (Fig.29 C). Comparable to the results observed for ROR1, the knockdown of ROR2 did not lead to a reduction in EV concentration or size.

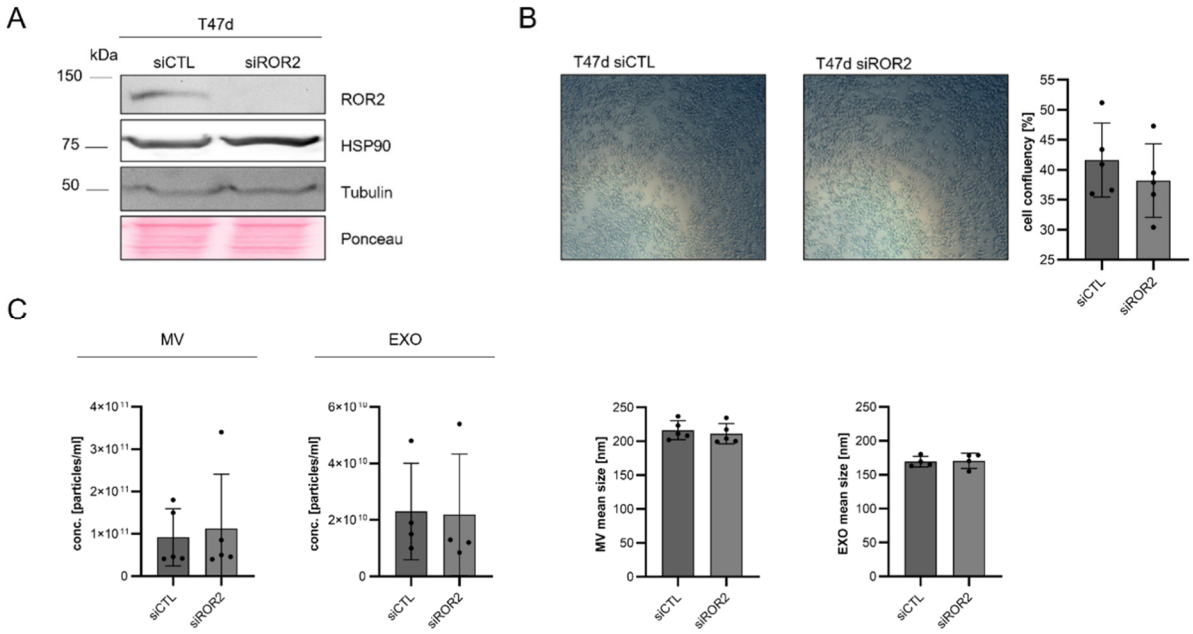


***Figure 29*: Knockdown of ROR2 in T47d does not affect the concentration or size of the released EVs*:*** A, T47d breast cancer cells were transfected with a control siRNA (siCTL) or a siRNA targeting ROR2 (siROR2). The knockdown efficiency was confirmed 72h post transfection by Western blot. Ponceau staining was used as loading control. B, Cell confluency: The same number of T47d siROR2 and siCTL cells were seeded into petri dishes for EV isolation and the cell confluence was determined by quantification of microscopic pictures with FIJI. C, NTA measurement of EV concentration and mean sizes: different EV populations of T47d cells treated with siCTL or siROR2 were measured by NTA.

Next, the composition of EVs released by T47d cells treated with a siRNA for ROR2 was analyzed by Western blot. Like ROR1, ROR2 affected the vesicle composition. In particular, the knockdown of ROR2 caused a significant reduction in Rgap1 protein expression on LVs, α-Actinin4 and Rgap1 expression on MVs and Alix expression on EXOs (Fig. 30). Interestingly, after knockdown of ROR2 the other marker proteins also showed a slight reduction in expression on LVs, MVs and EXOs, although these effects were not significant, indicating that these effects are either small or not biologically relevant.

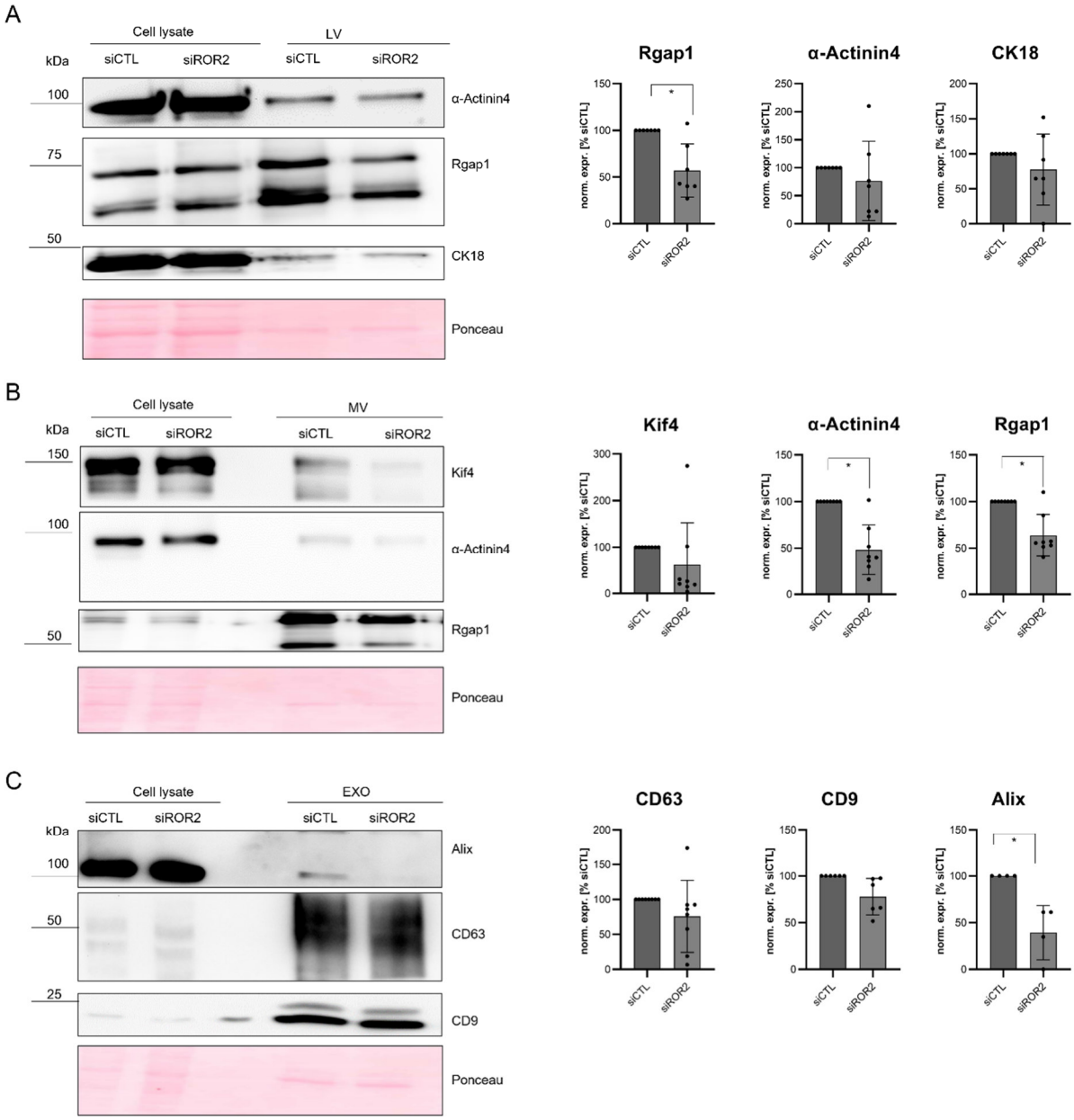


***Figure 30*: Knockdown of ROR2 leads to altered EV composition*:*** A-C, Characterization of the different EV subtypes released by T47d siCTL or siROR2 cells for the expression of respective markers was performed by Western blot. Ponceau staining was used as loading control. Densitometric quantification of the signals is shown below (mean±SD, n=4, *p<0.05).

As with ROR1, ROR2 overexpression should provide a second perspective on the results collected from the loss of ROR2 to EV composition, concentration of secreted EVs and their sizes. Therefore, ROR2 overexpressing MCF-7 cells were generated (Fig. 11). The same number of ROR2 overexpression or empty vector control cells were seeded in EV-free medium in order to subsequently isolate the EVs by differential ultracentrifugation. The ROR2 overexpression seemed to slightly increase cell proliferation as observed in the

measurement of the confluence (Fig.31A). However, since the effect was not significant, quantitative conclusions about the concentration of the secreted EVs can still be drawn. NTA analysis revealed a slight, but non-significant, increase in number of all three EV populations released by ROR2-overexpressing cells (Fig.31B). There was no effect on EV size.

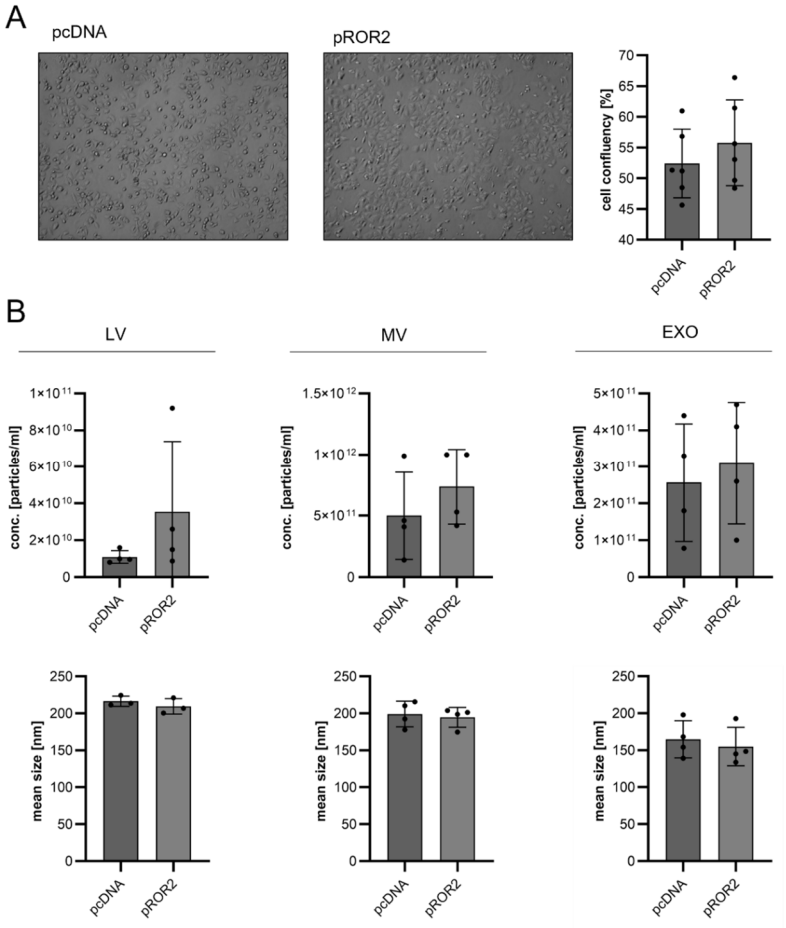


***Figure 31*: ROR2 overexpression leads to higher EV concentrations*:*** A, Microscopic pictures: The same number of MCF-7 empty vector (pcDNA) or ROR2 overexpressing (pROR2) cells were seeded into petri dishes and grown overnight for EV isolation. The cell confluence was measured by the analysis of *microscopic* pictures with FIJI. B, NTA measurements: The EVs secreted by MCF-7 pcDNA and pROR2 cells were analyzed by NTA with regard to mean size and concentration.

In the next step, the effects of ROR2 overexpression on the EV composition were examined using Western blot. Surprisingly, the overexpression of ROR2 led to a reduction of all EV marker proteins (Fig.32).

All LV marker proteins were significantly reduced upon ROR2 overexpression (Fig.32 A). Likewise, Kif4 and Rgap1 expression was reduced on MVs (Fig.32B). A reduction was also

observed for the selected EXO marker proteins, although it did not reach statistical significance.

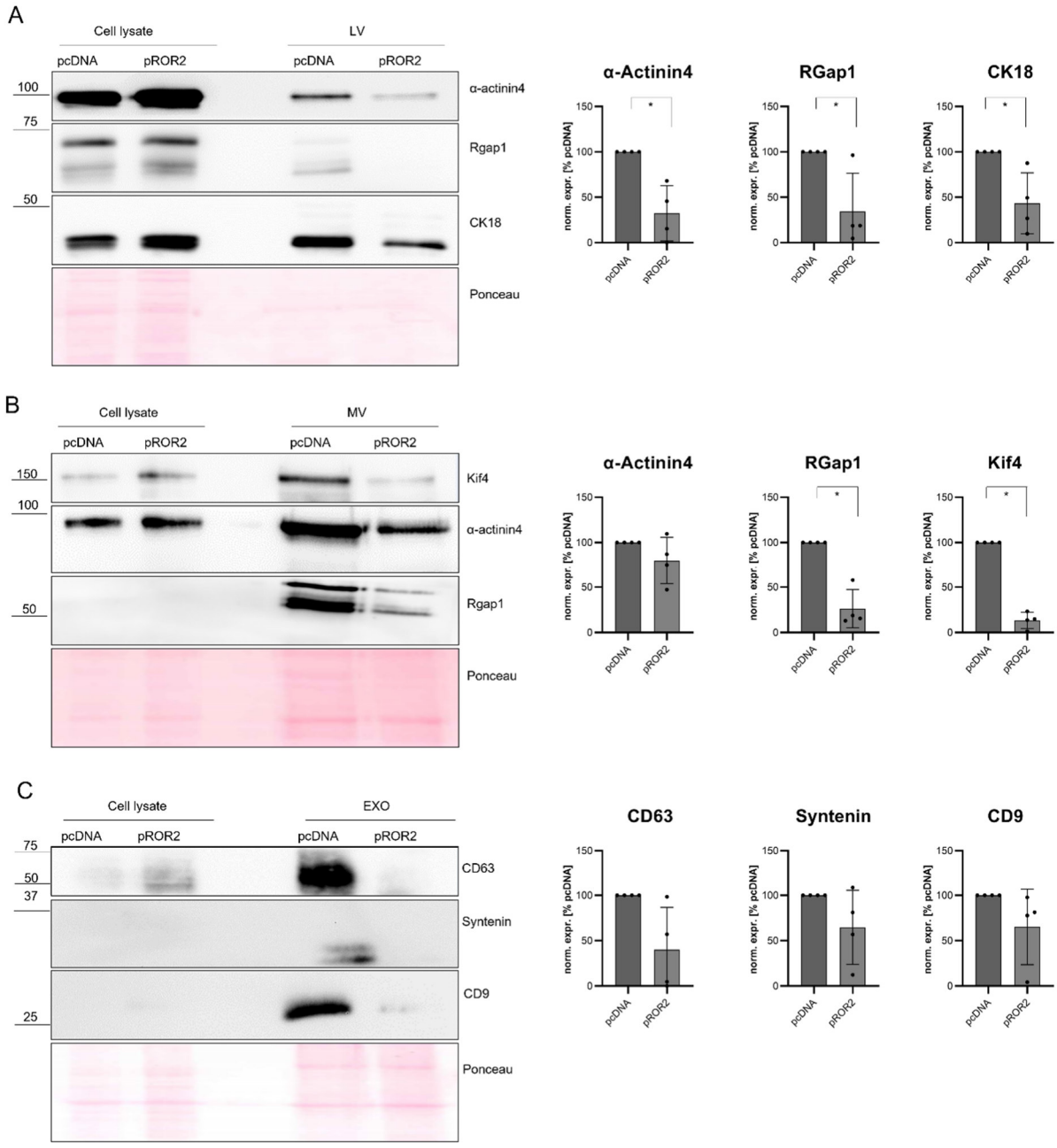


***Figure 32*: ROR2 overexpression significantly reduces EV protein expression*:*** A-C, The EVs of MCF-7 pcDNA or pROR2 cells were analyzed by Western blot, using typical protein markers for either LV, MV or EXO. Ponceau staining is depicted as loading control. Protein expression was quantified by densitometry and is shown below (mean±SD, n=4, *p<0.05).

Indeed, both ROR1, and ROR2 appear to play a role in vesicle composition. In all three EV populations studied, modifications of the ROR receptors in the cells could lead to a change in EV composition, although ROR1 and ROR2 have so far only been found on MVs and EXOs. This effect of ROR receptors on EV composition was shown in this work. All in all these results indicate that ROR receptors may be involved in MV and EXO biogenesis.

## 3.4 ROR1 and ROR2 as breast cancer biomarkers?

Based on previous results of Dr. Kerstin Menck, EMMPRIN could be found on MVs of metastatic breast cancer patients (Menck *et al*, 2015). Based on these findings, the question arose whether ROR1 and ROR2 can also be found on patient MVs and whether there is a difference in the expression of ROR1 and ROR2 according to the clinical status. Thus, ROR1 or ROR2 could function as biomarkers for breast cancer, as the MVs can be easily obtained from patient blood and the expression of ROR1 and ROR2 can then be measured by flow cytometry. For this purpose, blood samples were collected from healthy controls and breast cancer patients with the different subtypes (Luminal A, Luminal B, TNBC/basal-like and HER-2 positive). The EVs were isolated using differential ultracentrifugation (Menck et al, JOVE, 2017). The EVs were then stained and analyzed by NTA (Table below, Fig. 33).

***Table 14: List of breast cancer patient and control data:*** *Overview of patients and control samples isolated so far with subtype, age, mean sizes and concentrations of LVs, MVs, EXOs.*

| **Subtype** | **Age** | **LV Mean size** | **MV Mean size** | **EXO mean size** | **LV conc.** | **MV conc.** | **EXO conc.** |
|---|---|---|---|---|---|---|---|
| Luminal-B | 54 | 233.1 | 224.9 | 144.9 | 9.45E+09 | 8.25E+08 | 65250000 |
| TNBC | 35 | 232.9 | 177.1 | 155 | 4.5E+09 | 9.5E+08 | 1.18E+08 |
| Her2-enriched | 61 | 210.4 | 217.7 | 135.4 | 7.25E+08 | 6.75E+08 | 1.95E+08 |
| Luminal B | 52 | 234.5 | 214.7 | 143 | 9.5E+08 | 1.5E+08 | 1.88E+08 |
| Luminal B | 51 | 217.7 | 204.5 | 194.4 | 6.67E+09 | 1.08E+09 | 8.5E+06 |
| Luminal B | 43 | 197.9 | 154.6 | 129.2 | 6.4E+09 | 2.16E+09 | 2.33E+08 |
| TNBC | 59 | 227.5 | 220.9 | 123.2 | 2.97E+08 | 3.92E+08 | 8.67E+08 |
| Luminal B | 57 | 194 | 210.8 | 140.6 | 1.29E+09 | 5.86E+08 | 4.75E+08 |
| Luminal B | 37 | 235 | 252.0 | 137.6 | 4E+08 | 98181818 | 2.04E+08 |
| Luminal A | 48 | 238 | 195.2 | 139.7 | 2.07E+09 | 4.67E+08 | 5.4E+6 |
| TNBC | 52 | 259.7 | 224.9 | 126.9 | 1.28E+09 | 6.28E+08 | 1.73E+08 |
| TNBC | 64 | 239.6 | 208.3 | 136.6 | 7.2E+08 | 1.23E+09 | 1.06E+08 |

| | | | | | | | |
|---|---|---|---|---|---|---|---|
| Luminal B | 56 | 241.5 | 215.0 | 157.6 | 1.2E+09 | 2.75E+09 | 5.7E+06 |
| Her2-enriched | 38 | 246 | 209.1 | 157.8 | 1.2E+08 | 8.8E+08 | 1.09E+08 |
| Luminal B | 61 | 249.7 | 217.1 | 170.5 | 9.71E+08 | 4.38E+08 | 30857143 |
| Luminal B | 56 | 175.6 | 181.5 | 142.5 | 1.29E+10 | 1.12E+09 | 33430769 |
| Her2-enriched | 57 | 174.2 | 196.7 | 148.2 | 5.59E+09 | 1.07E+09 | 35573529 |
| Basal-like | 43 | 167 | 190.1 | 162.8 | 2.49E+08 | 1.85E+09 | 22076923 |
| Luminal B | 43 | 303.3 | 224.5 | 152.9 | 28000000 | 3.91E+08 | 3E+08 |
| Basal-like | 49 | 186.8 | 252.6 | 145.1 | 2.39E+08 | 3.16E+08 | 3.86E+08 |
| Her2-enriched | 63 | 197.8 | | 118.6 | 5.43E+09 | 4.78E+08 | 1.7E+08 |
| TNBC | 59 | 206.4 | 190.7 | 123.7 | 3.78E+09 | 5.8E+08 | 1.7E+08 |
| Luminal B | 59 | 204.1 | 159.8 | 120.5 | 3.37E+09 | 1.5E+09 | 2.83E+08 |
| Luminal B | 49 | 193.7 | 207.1 | 175 | 2.31E+08 | 5.07E+08 | 52622222 |
| Luminal A | 40 | 162.5 | 194.3 | 152.7 | 2.06E+09 | 7.43E+08 | 86153846 |
| TNBC | 69 | 202.4 | 192.7 | 183 | | 5.32E+08 | 1.7E+08 |
| Luminal A | 51 | 223.8 | 210.1 | 161.7 | 3.85E+08 | 1.79E+08 | 3.72E+08 |
| Luminal B | 51 | 195.2 | 154.4 | 113.7 | 1.45E+10 | 7.2E+08 | 2.18E+08 |
| Basal-like | 36 | 177.7 | 204.1 | 132.5 | 93333333 | 3.62E+08 | 2.8E+08 |
| Luminal A | 53 | 215.9 | 184.8 | 141.2 | 1.33E+08 | 2.13E+08 | 86666667 |
| Luminal B | 56 | 196.9 | 196.2 | 116.3 | 1.64E+09 | 2.66E+08 | 4.5E+08 |
| Her2-enriched | 39 | 195.5 | 187.5 | 125.3 | 1.13E+09 | 2.19E+08 | 3.05E+08 |
| Basal-like | 52 | | 187.2 | 161.1 | | 3.24E+08 | 1.3E+08 |
| Luminal B | 30 | 185.9 | 197.8 | 157.7 | 4.13E+08 | 2.49E+08 | 2.67E+08 |
| Her2-enriched | 70 | 206.1 | 183.6 | 137.3 | 2.17E+09 | 5.33E+08 | 2.6E+08 |
| Her2-enriched | 48 | 190.7 | 197.5 | 130 | 1.89E+09 | 4.69E+08 | 1.54E+08 |
| TNBC | 53 | 218.5 | 203.6 | 139.3 | 1.07E+09 | 3.84E+08 | 3.12E+08 |
| Luminal B | 61 | 151.8 | 180.9 | 127.3 | 1.82E+08 | 8.27E+08 | 2.53E+08 |
| Luminal A | 47 | 162.6 | 177.4 | 143.3 | 91428571 | 1.58E+09 | 3.4E+08 |
| Luminal B | 39 | 202.6 | 175.8 | 143.9 | 2.69E+08 | 3.19E+08 | 2.27E+08 |
| Luminal B | 59 | 183.6 | 174.4 | 144.6 | 4.8E+09 | 9.41E+08 | 2.39E+08 |
| Luminal B | 44 | 183.4 | 178.9 | 132.6 | 2.66E+09 | 52800000 | 1.96E+08 |
| Controls | 74 | 197.5 | 180.4 | 136 | 4E+09 | 1.75E+09 | 2.54E+08 |
| Controls | 22 | 219.9 | 216.8 | 162.7 | 1.75E+09 | 4.38E+08 | 4.69E+08 |
| Controls | 37 | 172.1 | 185.7 | 154.2 | 6.4E+09 | 5.67E+08 | 57333333 |
| Controls | 33 | 201.1 | 196.2 | 155.6 | 3.38E+09 | 6.36E+08 | 1.49E+08 |
| Controls | 53 | 211.4 | 202.6 | 172.1 | 4.36E+09 | 2.4E+09 | 62545455 |
| Controls | 55 | 201.5 | 177.7 | 144.5 | 7.46E+09 | 1.88E+09 | 2.51E+08 |
| Controls | 52 | 204.5 | 183.4 | 132 | 7E+09 | 2.21E+09 | 4.5E+08 |
| Controls | 58 | 214.3 | 193.1 | 148.4 | 7.56E+09 | 2.77E+09 | 2.3E+08 |
| Controls | 52 | 220.2 | 200.9 | 136.8 | 1.24E+09 | 2.62E+08 | 2.62E+08 |
| Controls | 53 | 212.7 | 194.6 | 145.9 | 4.33E+09 | 5.22E+08 | 3.97E+08 |
| Controls | 35 | 201.3 | 171.8 | 149.8 | 2.06E+09 | 1.22E+09 | 2.69E+08 |
| Controls | 30 | 201.9 | 189.8 | 160 | 3.38E+09 | 4.62E+08 | 4.86E+08 |
| Controls | 30 | 191.6 | 185.5 | 151.3 | 2E+09 | 1.16E+09 | 2.01E+08 |
| Controls | 52 | 203.4 | 187.3 | 150.1 | 1.43E+10 | 1.37E+09 | 1.14E+08 |

| | | | | | | | |
|---|---|---|---|---|---|---|---|
| Controls | 39 | 196.9 | 191.7 | 135.4 | 1.31E+09 | 1.42E+08 | 2.69E+08 |
| Controls | 32 | 185.9 | 213.3 | 152 | 1.16E+09 | 4.8E+08 | 86956522 |
| Controls | 22 | 187.4 | 181.8 | 146.1 | 1.04E+10 | 1.23E+09 | 1.52E+08 |
| Controls | 22 | 179.8 | 190.6 | 157.1 | 3.95E+10 | 98684211 | 96184211 |
| Controls | 27 | 178 | 182.8 | 159.6 | 8.38E+09 | 8.65E+08 | 60810811 |
| Controls | 24 | 203.9 | 174.4 | 152.3 | 3.64E+09 | 1.04E+09 | 1.31E+08 |
| Controls | 23 | 200.2 | 194.6 | 155 | 1.68E+09 | 4.32E+08 | 1.6E+08 |
| Controls | 30 | 198.2 | 180.5 | 147.2 | 1.71E+09 | 6.08E+08 | 3.74E+08 |
| Controls | 81 | 191.4 | 196.3 | 147.1 | 1.3E+10 | 8.27E+08 | 2.2E+08 |
| Controls | 49 | 189.3 | 183.5 | 168.3 | 4E+10 | 1.24E+09 | 5.33E+08 |
| Controls | 55 | 192.5 | 184.8 | 134.7 | 2.97E+09 | 7.86E+08 | 2.91E+08 |
| Controls | 38 | 191 | 172.6 | 134.5 | 3.67E+09 | 1.1E+09 | 2.17E+08 |
| Controls | 39 | 184 | 144.6 | 128.5 | 1.31E+10 | 2.43E+09 | 1.87E+08 |
| Controls | 26 | 202 | 163.0 | 119.3 | 3.73E+09 | 8E+08 | 73333333 |
| Controls | 33 | 185.9 | 170.0 | 138.5 | 2.02E+09 | 6.71E+08 | 3.9E+08 |
| Controls | 29 | 199.2 | 169.4 | 139.3 | 4.29E+09 | 2.1E+09 | 2.79E+08 |
| Controls | 69 | 193.8 | 179.8 | 152.6 | 2.9E+09 | 1.79E+09 | 1.65E+09 |
| Controls | 61 | 207 | 206.0 | 142.1 | 5.37E+08 | 4.79E+08 | 78780488 |
| Controls | 60 | 212.7 | 193.6 | 148.3 | 2.11E+09 | 6.64E+08 | 1.12E+08 |
| Controls | 69 | 195.4 | 214.6 | 144.3 | 6.85E+09 | 16438356 | 4.88E+08 |
| Controls | 55 | 199 | 185.1 | 142 | 1.65E+10 | 8.61E+08 | 1.76E+08 |

The table above shows the age, subtype of the patients or control status, and the data obtained in NTA on E V mean size and EV concentration. The collection of patients is still ongoing and currently only includes early tumor stages. As can be seen in Figure 33, there could be no difference between the control groups and the patients obtained in mean size (A) and concentration (B). This aspect in particular seems interesting, as it has already been shown that tumor cells secrete higher amounts of EVs (Baran *et al*, 2010; Tesselaar *et al*, 2007; Galindo-Hernandez *et al*, 2013; König *et al*, 2017). Possibly, there could be no difference be obtained because the patient samples were collected from very early stages.

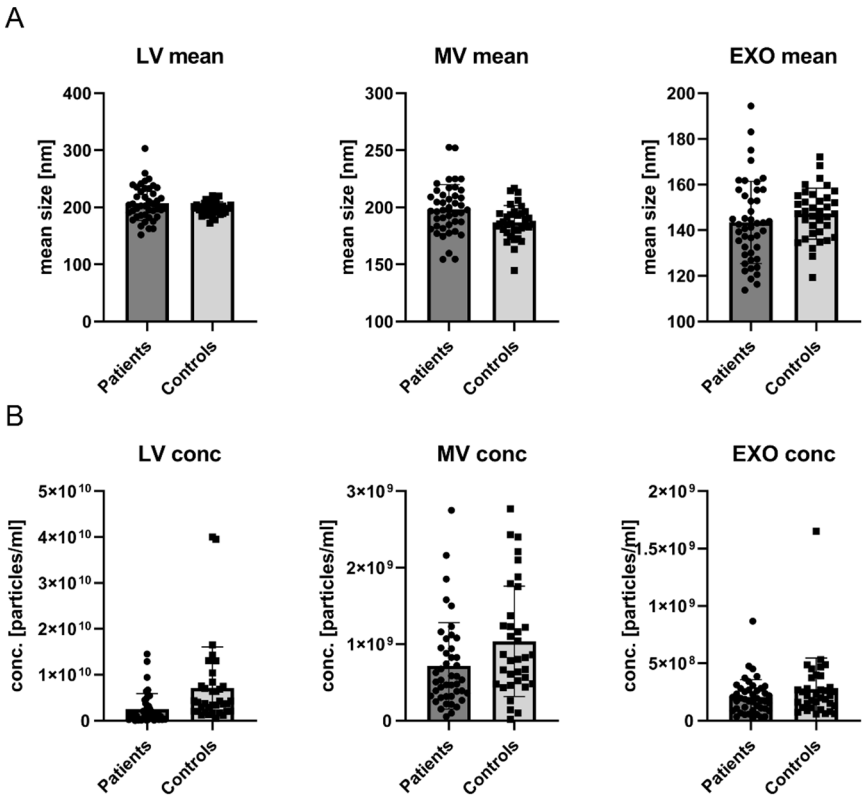


***Figure 33*: EVs from patients with early breast cancer stage compared to control EVs do not differ in size or concentration*:*** A+B, NTA measurements of 42 breast cancer patients and 35 healthy controls. A, mean sizes of LVs, MVs and EXOs of breast cancer patients with early stages compared to healthy controls. B, Concentration of LVs, MVs, EXOs from the same patients and controls.

In the second step, the isolated MVs should then be examined for the expression of ROR1, ROR2, EMMPRIN and Her2 by flow cytometry, as can be seen in Figure 33. First, EMMPRIN and Her2 flow cytometry antibodies were established using MVs of SKBR3 cells and ROR1 antibody by staining of MDA-MB231 MVs (Fig. 33A). Isotype staining served as a control. Thereby, 52% of the SKBR3 MVs were EMMPRIN positive, 55% of MDA-MB231 MVs were ROR1 positive, and 98% of the SKBR3 MVs were Her2-enriched (Fig. 33A). The ROR2 antibody was established in previous projects using MCF-7 pROR2 cells (data not shown) and subsequently transferred to the MVs. Since Her2 plays a major role in breast cancer, as approximately 15-20% of all breast cancer patients exhibit elevated Her2 expression and are thus assigned to this subtype (Exman & Tolaney, 2021). Therefore, Her2 was selected as a biomarker. Whether ROR1/2 could function as a biomarker could not be conclusively determined in this study, as not many patient samples have been analyzed for ROR1/2 expression to date. Moreover, the samples collected so far are predominantly early

stages, for which it is questionable whether and to what extent they can be distinguished from control samples at all. The MVs of the patient samples were then measured by flow cytometry. Figure 33 B shows a representative result of the gating strategy of MVs based on EMMPRIN staining and IgG control. Figure 33 C shows the analyses with the line indicating the median of the values. So far, only the first four patient samples and three control samples could be analyzed.

For ROR2, the median value of the fluorescence intensity for the breast cancer patients of 25.62 was higher than that of the control patients of 13.24, which represents a slight trend and thus confirms the preliminary results of Dr. Kerstin Menck, in which it was shown that a breast cancer patient group had increased ROR2 expressions on MVs. This trend was not visible for ROR1, where the median values of patients (4.5) and controls (9) hardly differed. For EMMPRIN, the values of the breast cancer patients were also slightly higher than those of the controls at 86.82 with a median value of 80.74. Her2 was not expressed in the control patients with a median value of 0, whereas there was increased Her2 expression on MVs (26.7). However, because the other patient samples also had very low Her2 expression, this is reflected in the low median value of 1.32. Presumably, however, Her2 could be a promising marker for Her2-enriched patients, but this would need to be validated in further experiments using later stages. All in all, no difference in the expression of the four markers could be seen between controls and patients, with a slight tendency for ROR2 and EMMPRIN to show slightly increased expression of the markers in the tumor patients, although one patient had a low EMMPRIN expression. Interestingly, the patients chosen for this study were all assigned to the Her2 subtype, although only one patient showed higher Her2 expression compared to the control samples.

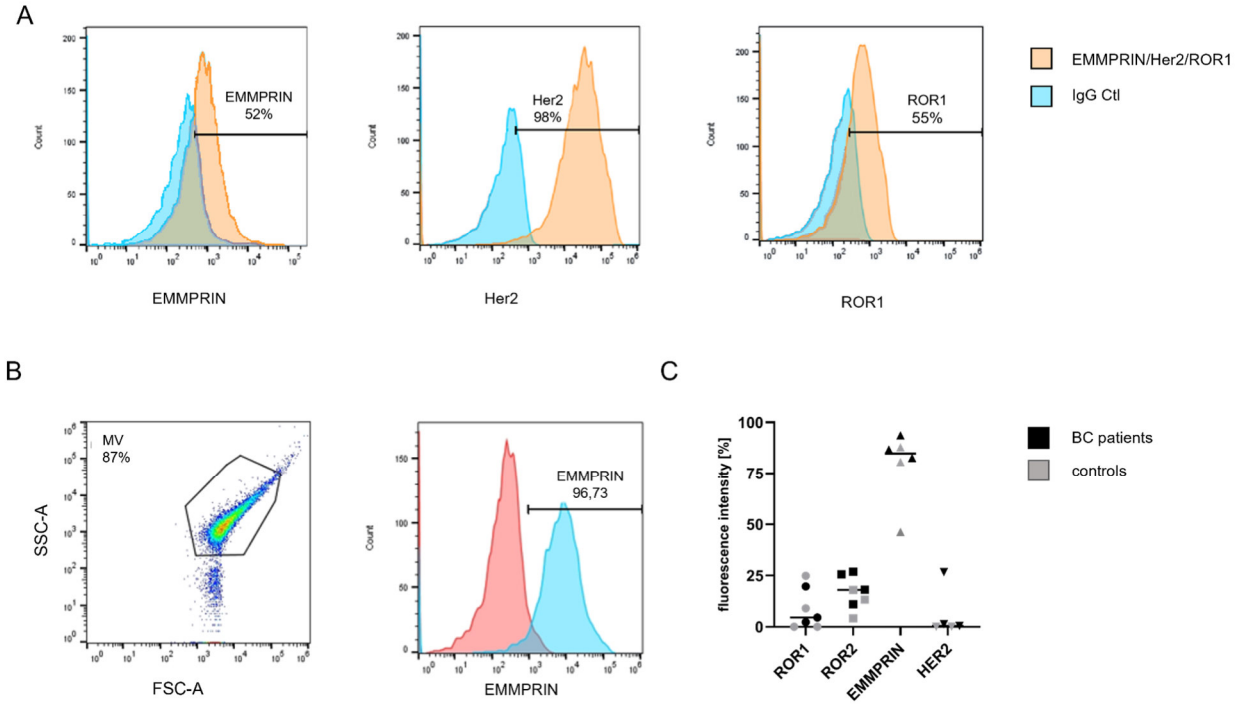


***Figure* 34: Flow cytometry of EVs from peripheral blood of breast cancer patients:** A, Antibody establishment of EMMPRIN, HER2 and ROR1 by flow cytometry. For EMMPRIN (orange) and Her2 (orange) SKBR3 MVs were utilized. For ROR1 antibody establishment MDA-MB231 MVs were used (orange). The isotype control (IgG Ctl) is portrayed in blue. B, Flow cytometry: A representative gating strategy of MVs and a histogram of EMMPRIN (blue) and IgG control (red) of blood-derived MVs from Her2-enriched breast cancer patient. B, Flow cytometry measurement of Patient MVs: ROR1, ROR2, EMMPRIN and HER2 expression on MV isolated from four breast cancer patients (black) and four healthy controls (grey) was analyzed by flow cytometry.

In the future, more samples will be collected and measured by flow cytometry and NTA. In particular, breast cancer patients with metastases and in general later stages will then also be included in the measurements to elucidate whether ROR1/2 can function as biomarkers for breast cancer.

# 4. Discussion

## 4.1 Wnt11 is as a novel ligand for ROR2

### 4.1.1 Functional impact of ROR2 on breast cancer invasion

In several cancer entities the ROR receptor family was found to be overexpressed and linked to tumorigenic processes (Zhou *et al*, 2020; Hasan *et al*, 2017). In this study, it could be demonstrated that ROR2 overexpression led to an increased invasion in breast cancer cells which confirms previous data (Bayerlová *et al*, 2017). Several studies clearly demonstrated a linkage of ROR2 expression to enhanced migration rates of tumor cells (Yang *et al*, 2017; Henry *et al*, 2015a). However, no effect of ROR2 overexpression on migration could be found in breast cancer cells. This can also be due to the fact that the migration assay developed here might not be sensitive enough and therefore minor effects cannot come into play.

ROR2 and its role in tumor development are discussed controversially, as some groups showed that ROR2 acts as a tumor suppressor (Tseng *et al*, 2020) and at the same time other groups found that ROR2 can induce tumor-promoting effects (Guo *et al*, 2020; Wright *et al*, 2009). One possible explanation could be that the knockdown of ROR2 induces a compensatory upregulation of ROR1 which might mask the effects of the ROR2 loss. For example, in epithelial ovarian cancer it has been shown that only the double knockdown of ROR1 and ROR2 was able to inhibit cell migration and invasion (Henry *et al*, 2015a). This indicates that the two ROR receptors may be able to compensate for each other. Another possibility could be that the cellular background may play a fundamental role and additionally determines which FZD and co-receptors are present, thereby determining the function of ROR2. Interestingly, ROR2 has been identified predominantly in breast cancer as an oncogene (Bayerlová *et al*, 2017; Henry *et al*, 2015b; Guo *et al*, 2020), whereas for example in prostate cancer, ROR2 primarily was determined as a tumor suppressor (Tseng *et al*, 2020). In addition, various studies have shown that ROR2 can initiate both canonical and non-canonical signaling, thereby affecting the downstream targets and finally the effects on tumor progression (Henry *et al*, 2015b).

### 4.1.2 Wnt11 as novel ligand for ROR2

In the past, Wnt ligands and their influence on signaling pathways were investigated. For ROR1 and ROR2, Wnt5a was identified as the corresponding ligand (Oishi *et al*, 2003;

Fukuda *et al*, 2008). Interestingly, several experiments recently indicated Wnt5b, as well as Wnt16 as novel ligands for ROR1 (Janovska *et al*, 2016; Karvonen *et al*, 2019) and Wnt5b as a ligand for ROR2 in osteosarcoma cells (Morioka *et al*, 2009). ROR receptors gain an extracellular and an intracellular part, consisting of several domains. The intracellular domains of ROR receptors comprise a TKD and a PRD domain framed by two serine-threonine-rich domains (Menck *et al*, 2021). The extracellular part contains the Ig-like domain, the CRD and the KRD, that might mediate the interaction with Wnt ligands. It has been shown that Wnt proteins can bind to the CRD domain of ROR receptors and therefore initiate the Wnt signaling pathway (Oishi *et al*, 2003; Mikels & Nusse, 2006; Enomoto *et al*, 2009; Fukuda *et al*, 2008). In addition to Wnt5a, Wnt11 in particular is classified as a non-canonical Wnt ligand (Pandur *et al*, 2002). Nonetheless, Wnt11 can also induce ß-catenin-independent signaling responses and has been far less studied (Baarsma & Königshoff, 2013; Bisson *et al*, 2015). In fact, several receptors for Wnt11 have already been identified, including FZD4 (Ye *et al*, 2011), FZD5 (Cavodeassi *et al*, 2005), FZD7 (Djiane *et al*, 2000) and FZD8 (Murillo-Garzón *et al*, 2018). In zebrafish, it has been demonstrated that Wnt11 can bind to ROR2 (Bai *et al*, 2014), but whether this is also the case in human cells has never been investigated. An RNA sequencing analysis showed that ROR2 overexpression led to increased gene expression of *Wnt11* in breast cancer cells (Bayerlová *et al*, 2017), suggesting a possible interaction of the two proteins also in humans. Indeed, in this work Co-IP experiments demonstrated an interaction of ROR2 and Wnt11. Nevertheless, a Co-IP can not prove direct binding. Thus, there is a possibility that both interact only indirectly. To detect direct binding, different methods like surface plasmon resonance (SPR) should be considered (Drescher *et al*, 2009).

The next step was to investigate which domains are important for the interaction with Wnt11 and which functional influence the various ROR2 domains have on ROR2-induced tumor invasion. Therefore, deletion constructs were first generated, with sequential deletions of the respective domains. It is possible that ROR2 undergoes shedding and therefore exhibits multiple banding patterns in the Western blot (Yu *et al*, 2016). For Wnt5a it was shown that the CRD domain is important for the binding with Wnt5a and therefore for initiating the non-canonical Wnt signaling pathway (Oishi *et al*, 2003; Mikels & Nusse, 2006; Enomoto *et al*, 2009; Fukuda *et al*, 2008; Hikasa *et al*, 2002). Recently, the importance of the CRD domain for the interaction with Wnt11 discovered in this work could also be validated through further Co-IP experiments by Dr. Kerstin Menck (Menck *et al,* 2020). In line with this finding, the

deletion of the CRD led to a significant reduction of the cell invasiveness of the MCF-7 ROR2 overexpressing cells, probably due to the fact that Wnt ligands can then no longer bind to ROR2. Deletion of the Ig-like domain had no effect on MCF-7 cell invasion. In contrast, loss of CRD and KRD also showed a reduction in invasiveness compared with deletion of the CRD domain. This suggests that the KRD domain is also important for mediating the invasiveness of MCF-7 cells.

This ultimately leads to the question of why the invasiveness of the deletion constructs is still higher than that of the control. One possibility could be that other receptors besides ROR2 play a role in the Wnt signaling pathway (e.g. FZDs) and that ROR2 could function as a co-receptor despite the deletion of the extracellular domain. The C-terminal deletion constructs of ROR2 lacking either the TKD or the PRD were analyzed in modified Boyden chamber assays to determine which domain mediates the signal conductions induced by the interaction of ROR2 with its Wnt ligands. The loss of the PRD did not affect the cell invasiveness at all, indicating that the PRD is not required for the functionality of ROR2 in mediating cancer cell invasiveness. The results show that the double deletion of both domains led to a significant reduction in ROR2-induced cancer cell invasiveness, suggesting that the TKD is important for the functionality of ROR2 regarding the invasive phenotype. To date, the functionality of the TKD has been controversial in the literature (Mikels *et al*, 2009; Artim *et al*, 2012). The data shown here may suggest possible functionality of the domain, although this assay is not sufficient to definitively address the question of its functionality. All in all, however, the TKD domain is important for ROR2-mediated invasion in MCF-7 cells. Indeed, it has also been shown that the TKD is also required to mediate Wnt5a signaling in HEK293 cells (Mikels *et al*, 2009). Whether ROR2 acts as the sole receptor for Wnt11 or whether it is a co-receptor of an FZD receptor remains unanswered and would be worth analyzing further.

## 4.2 The non-canonical Wnt receptor FZD6 as a novel receptor for Wnt11

### 4.2.1 The functional impact of FZD6 on breast cancer invasion

FZD6 belongs to the FZD family and is a receptor for Wnt ligands. This interaction can trigger either canonical or non-canonical Wnt signaling and thus influence tumor progression in different tumor entities. An important aspect of tumor progression and metastasis is the ability of cells to migrate. It has been demonstrated that in breast cancer cells, the ablation of

FZD6 resulted in decreased cell motility and invasiveness (Corda *et al*, 2017). However, a different study showed that FZD6 represses gastric cancer cell proliferation as well as migration (Yan *et al*, 2016a). In this work, examining the migration properties of FZD6 knockout breast cancer cells in a wound-healing assay revealed FZD6's importance in breast cancer cell migration. The migration of the FZD6 knockout cells under rhWnt11 stimulation was significantly reduced, indicating that FZD6 is important to mediate the pro-migratory function of Wnt11. Accordingly, this finding contrasts with the previous study, which showed a contrary effect of FZD6 on migration, demonstrating that FZD6 suppresses migration, indicating that the cellular context plays a major role in the function of the various FZD receptors.

In order to demonstrate that this effect was not caused by a changed proliferation rate of the FZD6 knockout cells compared to the empty vector cells, a proliferation assay was performed. The FZD6 knockout cells showed the same proliferation rate as the control cells, indicating no connection between FZD6 knockout and proliferation in this study. However, MCF-7 cells showed a relatively high gene expression of other FZD receptors in the cell line screening, which in turn might trigger other functions in the cells. For example, in metastatic lung, liver, colon, and breast cancer cell lines it has been demonstrated that FZD2 influences migration via non-canonical Wnt signaling. Moreover, a reduced cell migration, invasion and also reduced metastasis formation was observed in xenograft models by using a specific antibody targeting FZD2 (Gujral *et al*, 2014).

The invasion assay performed in this study with FZD6 knockout cells compared with empty vector cells under Wnt11 stimulation and led to a significant reduction in invasiveness of FZD6 knockout cells, indicating a possible interaction between Wnt11 and FZD6. Further studies have equally observed a correlation of FZD6 and cancer cell invasiveness, as shown in a study by Corda and colleagues, in which the ablation of FZD6 expression led to inhibited breast cancer cell motility, invasion and repressed metastasis *in vivo* (Corda *et al*, 2017).

### 4.2.2 Identification of FZD6 as novel receptor for Wnt11

The interaction of FZD6 with several Wnt ligands, such as Wnt4 or Wnt5a, has already been shown (Lyons *et al*, 2004; Hirano *et al*, 2014; Kamino *et al*, 2011). But whether FZD6 also interacts with the non-canonical Wnt11 has been controversially discussed. In a study by Kilander et al, possible Wnt ligand binding to FZD6 was investigated using a FRAP assay. In

this assay FZD6 was stimulated with different Wnt ligands and the surface mobility of FZD6 was then measured to identify WNT-FZD interactions. The results revealed a direct or indirect interaction of FZD6 with Wnt1, Wnt3a, Wnt4, Wnt5a, Wnt9b, Wnt10b and Wnt16b. Interestingly, Wnt5b and Wnt11 had no effect on FZD6 mobility, indicating no interaction of those Wnts with FZD6 (Kilander *et al*, 2014). However, another study has shown that cancer-associated fibroblast-derived EXOs can trigger a motile phenotype in breast cancer cells through Wnt/PCP signaling via FZD6, DVL1, VANGL1, PK1 and Wnt11. Interestingly, the association of Wnt11 and FZD6 was investigated by using immunofluorescence and confirmed a colocalization of both (Luga *et al*, 2012). Therefore and moreover due to the high gene expression of *FZD6* revealed by the cell line screening, FZD6 moved into the focus of this work as an interesting, possible receptor for Wnt11. It might also be possible that the cellular context plays a major role in the interaction between FZD receptors and Wnt ligands. Not all identified Wnt ligands and receptors are equally expressed in every cell line, as the cell line screening shown here also illustrated. Therefore, the choice of cell line may be crucial when investigating possible interactions between Wnt ligands and FZD6. Indeed, the study by Luga *et al* was performed using breast cancer cells, whereas the study by Kilander *et al* utilized HEK293T/17 cells.

Furthermore, it was not clear with which CO receptors FZD6 interacts. A recent study showed an interaction between Wnt5a, FZD6 and ROR1, and between Wnt10b, FZD6 and LRP6 in prostate cells (Neuhaus et al, 2021). Results of synergistic in-vivo effects in zebrafish experiments suggest a possible interaction of Wnt11 with Ryk (Macheda *et al*, 2012). Whether FZD6 is involved in this possible interaction is unclear. However, a study demonstrated that Wnt11 is highly expressed in colorectal cancer and moreover showed a correlation of WNT11 expression with the expression of FZD6, RYK, and PTK. The combined expression of WNT11 with FZD6 and RYK or PTK7 was linked to an increased risk of 5-year mortality, suggesting a possible interaction of those proteins (Gorroño-Etxebarria *et al*, 2019). In line with these findings, an interaction between FZD6, Wnt11 and PTK7 was shown in this work by Co-IP.

### 4.2.3 High FZD6 expression and its prognostic values in breast cancer

Considering that *FZD6* was identified as a receptor for *Wnt11*, the question remained whether there is a correlation between the expression of both genes and whether high expression of both would have an influence on the survival of the patients.

To address this question, a non-canonical Wnt signature was created that included key members of the non-canonical Wnt pathway. In addition, associated pathways were also included, as non-canonical Wnt signaling has already been shown to be linked to PI3K signaling (Landin Malt et al, 2020; Dai et al, 2017). This signature clustered the patients into two groups that differed significantly in their DMFS. Thereby *Wnt11* clustered with *FZD4, FZD9 mTOR, GSK3, ROCK2, RORA* and *PIK3C* and a high expression of those genes was associated with significantly worse DMFS in breast cancer patients. Interestingly, the RNA-seq analysis of TNBC patients demonstrated also a clustering of *Wnt11* with *FZD4. FZD5* and *FZD9* (Koval & Katanaev, 2018), thereby supporting the findings in this study. In the second step, *FZD4* and *FZD6* were then further investigated to determine the impact of high expression of these genes on patients' DMFS. Various studies displayed a connection between increased *FZD6* expressions and a poor clinical outcome in various cancer entities (Zhang *et al*, 2020). For instance, the loss of FZD6 led to less leukemia development and furthermore to a prolonged survival in mice (Wu *et al*, 2009). One study found that the gene encoding *FZD6* is frequently highly amplified in breast cancer. Moreover, an increased incidence was identified particularly in TNBC. The loss of *FZD6* expression inhibited both bone and liver metastasis *in vivo* in this study (Corda *et al*, 2017).

Previous data from this work and previous published studies suggest a possible correlation of FZD6 expression on DMFS of breast cancer patients. Indeed, analysis of 2000 primary breast cancer patients could establish a correlation between high FZD6 gene expression and a significantly worse DMFS rate. For FZD4, however, the opposite effect was shown. In pancreatic cancer, recently a similar observation could also be made, as high FZD4 expression was also associated with better overall and recurrence-free survival (Li et al, 2021). However, FZD6 has been frequently discussed in the literature as a tumor suppressor in prostate and gastric cancer (Yan *et al*, 2016a; Han *et al*, 2018), although the observed data shown here clearly suggest that FZD6 may play an important role in breast cancer progression and might represent a promising target for therapeutic interventions. A major challenge in designing small molecules targeting FZD receptors appears in the analysis of the crystal structure of FZD4. The structure represents a ligand-free receptor, thereby giving the impression that the

development of small molecules targeting FZDs might be impossible, due to the hydrophilic nature of the binding pocket (Yang *et al*, 2018). Nevertheless, there are already intensive efforts to design small molecules targeting FZD receptors. One example is the small molecule SAG1.3 tested for targeting FZD6. It has recently been shown that SAG1.3 was able to successfully bind to FZD6 and thereby induce conformational changes in the receptor that affect Dvl recruitment and activation (Kozielewicz *et al*, 2020).

### 4.2.4 Role of non-canonical Wnt members in primary CRC

Indeed, Wnt signaling plays a central role in CRC. In particular, mutations in the APC gene are common (Morin *et al*, 1997). Most studies suggest an association between CRC and canonical-Wnt signaling (Yoshida *et al*, 2015; Morin *et al*, 1997). Several FZD receptors have been associated with CRC invasion, survival and metastasis (Ueno *et al*, 2008; He *et al*, 2011). For example, overexpression of FZD7 in CRC patients was associated with poorer overall survival (Ueno et al, 2009). Another study demonstrated that high mRNA expression of Wnt11 in CRC tumor tissue was significantly increased and moreover strongly linked to recurrence in patients (Nishioka *et al*, 2013). The Wnt11 receptor FZD7 has been shown to be involved in the progression of colorectal cancer, and activation of the Wnt11/FZD7-mediated Wnt signaling pathway triggers CRC proliferation, migration, and invasion through the phosphorylation of JNK and c-Jun (Ueno *et al*, 2008; Nishioka *et al*, 2013). Thus, to further investigate the effects of non-canonical Wnt signaling in CRC patients and to determine whether the signature has an impact on CRC patients' DMFS compared with the prior data, the data set of primary colorectal cancer patients was analyzed in this study. For this purpose, a gene signature was also created that entirely encompassed the previously used signature and supplements it with all remaining Wnt ligands. In addition, Norrin was added as an important FZD4 ligand (Bang *et al*, 2018). This signature divided the patient cohorts into four groups. The group in which *FZD6* clustered with *FZD5, GSK3, Wnt10, Wnt8A, RYK, Wnt16, Wnt7b, mTOR* and *AKT.* The patient group with a high expression of those genes showed an overall reduced DMFS compared to the other three. Overall, for CRC, little has been published on FZD6 as a relevant receptor. FZD7, on the other hand, seems to be more in the spotlight of scientific attention as both a canonical and non-canonical Wnt receptor. This is also reflected in efforts to therapeutically target FZD receptors (Ueno *et al*, 2008). In one study, a monoclonal antibody simultaneously targeting five different FZD receptors (FZD1, FZD2,

FZD5, FZD7, and FZD8) by structural similarities was found and resulted in decreased tumor growth (Gurney *et al*, 2012). This antibody was further investigated for solid tumor entities in a phase 1b clinical trial in breast, colorectal, pancreatic, sarcoma, neuroendocrine cancer and NSCLC (Gurney *et al*, 2012). Overall, targeted therapeutics against FZD receptors need to be investigated further, since the relationships between the receptors and the various signaling pathways are very complex.

## 4.3 ROR receptors on tumor-derived EVs

### 4.3.1 ROR receptors in cancer cell communication via EVs

EVs play a remarkable role in cell-cell communication, and different types of vesicles can be differentiated based on their size and biogenesis. Previously published data suggest that Wnt proteins can be transferred via EVs and can induce Wnt signaling in target cells (Gross *et al*, 2012; Menck *et al*, 2013). Therefore, it was hypothesized that ROR proteins might also be transferred via EVs.

The cell line screening revealed a relative high expression of *ROR1* in MDA-MB231 breast cancer cells. Accordingly, the MDA-MB231 wild type cells were used to isolate potentially ROR1-positive EVs. Indeed, Western blot analysis revealed ROR1 to be expressed on MVs and EXOs. This matches with a recently published study showing that ROR1 is localized on EXOs (Daikuzono *et al*, 2021). Surprisingly, no ROR1 was detected on LVs.

Members of the Rho family have been linked to play an important role in EV release. RhoA had been shown to be important for MV release, by regulating cytoskeletal movement (Li *et al*, 2012a). In nucleus pulposus cells (NPCs), the RhoC/ROCK2 signaling pathway was associated with exosome release via autophagic pathways (Hu *et al*, 2020). Since ROR receptors can initiate the non-canonical Wnt signal

ing pathway or ROR/PCP signaling pathway and thus influence Rho/Rock signaling (Martinez *et al*, 2015; Karvonen *et al*, 2019), it is reasonable to assume that they are thereby also involved in EV biogenesis. This led to the question of the role of ROR receptors in this process and whether they are also functionally actively transferred to target cells.

Tumor EV can increase tumor invasion of neighboring cells. However, the factors underlying this effect have not yet been conclusively determined. Since RORs can increase tumor invasion, the question arises whether RORs can have a similar effect on EVs in target cells. It was shown that stimulation of MCF-7 cells with EVs from MCF-7 cells or MDA-MB231

wild-type cells could increase cell invasiveness in Boyden chamber assays (Menck *et al*, 2015). In the next step it was then investigated whether the knockout of ROR1 from MDA-MB231 vesicles has an influence on their pro-invasive function on MCF-7 cells. Therefore, MDA-MB231 ROR1 knockout cells were generated by using CRISPR/Cas9. Two clones showing a complete knockout of ROR1 in Western blot and flow cytometry as well as no morphological differences in comparison to the empty vector cells were used for further investigations. A qRT-PCR demonstrated no increased *ROR2* expression after the knockout, which excludes a compensation of *ROR2*. The wild-type MDA-MB231 vesicles induced a significantly increased invasive behavior of the MCF-7 cells which confirms previous data (Menck et al, 2015). Interestingly, this effect was decreased after the knockout of ROR1 in MVs and in EXOs. In prostate cancer cells an increase in invasiveness was observed after stimulation with LVs expressing αV-integrin by activating the AKT pathway (Ciardiello et al, 2019). Nevertheless, the stimulation of MCF-7 cells with MVs or EXOs resulted in significantly higher invasiveness of the cells compared to stimulation with LVs. The increase upon stimulation with LVs was barely present, while stimulation of both MDA-MB231 MVs and EXOs significantly increased invasiveness. This finding fits with previous data that ROR1 is particularly localized to MVs and EXOs. Interestingly, loss of ROR1 on MVs and EXOs resulted in a decrease in MV/EXO-induced invasiveness, although it still did not reach the control level. Additionally, the results that MDA-MB231 cells secrete predominantly MVs and EXOs and almost no LVs are consistent with this finding. The effects of MVs and EXOs are almost the same, which ultimately fits with the fact that ROR1 was found on both MVs and EXOs. Although ROR1 is strongly localized on MVs and EXOs, other proteins might also be transported on MVs and EXOs that may affect invasiveness. It can be concluded that ROR1 is transported on vesicles to target cells and can influence invasion there, but does not seem to be solely responsible for it. Possibly, other Wnt receptors are transported on the EVs, which can also trigger invasiveness in target cells.

### 4.3.2 ROR receptors and their impact on EV composition

The question that follows the above findings was then whether ROR receptors per se are involved in vesicle biogenesis. To answer this question, the influence of ROR receptors on vesicle composition, concentration and size was investigated. Whether ROR receptors have an

influence on the concentration of the excreted EVs could not completely be solved. There seemed to be a trend that ROR overexpression led to a slightly increased concentration, while the loss of the ROR receptors led to a slight decrease. Since the effects are only small and not significant, further measurements could be made here in order to achieve more valid results. When characterizing the T47d wildtype-derived EVs, it could be shown that T47d cells hardly secrete LVs.

Further investigation of the vesicle compositions with different markers for LVs, MVs and EXOs revealed that EV composition actually changes with the modification of ROR1/2. This effect can even be observed in LVs, although they do not carry ROR receptors themselves. In comparison to the protein expression in the cell lysate, Rgap1, Kif4, α-Actinin 4, CD63, CD9 and Alix showed significant changes on EVs upon ROR modulation. The knockout of ROR1 led to a significant downregulation of CD9 and CD63, while there were no such strong changes under ROR2 knockdown in the EXOs. Rgap1, on the other hand, was significantly reduced when the respective ROR receptors were not expressed. The knockout of ROR1 and also the knockdown of ROR2 led to a decrease in Rgap1 likewise in LVs and MVs, indicating a stable effect of ROR receptors on Rgap1 expression. All in all, the effect of ROR modulations on Kif4 seems to be valid as well, since the same trend appears in all modifications. Under loss of ROR receptors, there is a significant decrease in Kif4 expression on MVs, whereas under overexpression of ROR1, there is a trend towards increased Kif4 expression, although the trend is not significant here. That both Kif4 and α-Actinin4 are both affected does not seem surprising, since Kif4 has been shown to be directly involved in MV biogenesis and α-Actinin4 indirectly through binding of actin to the plasma membrane (Charras, 2008).

The knockdown of ROR2 leads to a significant reduction in α-Actinin4, while the overexpression of ROR1 led to a slight increase in expression, although this trend is also not significant here. Whether the effects on α-Actinin4 are valid would require further results. Taken all results together, the effects of Kif4, Rgap1, CD9 and CD63 appear to be valid, since the same trend seems to be emerging in all Western blots with the exception of ROR2 overexpression. The overexpression of ROR2 led to a contrary result than the ROR2 knockdown. However, since the knockdown is more physiological, these results remain more valid. To further validate the results, one could generate another knockdown in a second cell line to perform further experiments.

For the first time, the influence of ROR receptors on the protein composition of EVs was demonstrated. The observations fit to a recent report which showed that ROR1 acts as a scaffold protein for the two subunits of the ESCRT complex “hepatocyte growth factor-regulated tyrosine kinase substrate“ (HRS) and “Signal Transducing Adaptor Molecule 1“ (STAM1), that play a prominent role in EXO biogenesis. Furthermore, ROR1 enabled the association of HRS and STAM1 in the membranes of Rab5-induced early endosomes and thus regulated Rab5-induced MVE formation and EXO biogenesis in HeLa and lung cancer cells (Yamaguchi *et al*, 2020). These results therefore match the ones shown here, however, with ROR1 knockout, the markers for endosomal EXOs (syntenin) do not change, but CD9-positive EXOs are strongly reduced, which probably represent a separate EXO subclass. It is not yet clear to what extent ROR affects the mechanisms of LV and MV biogenesis and what function ROR2 plays in EV biogenesis. Here it could be shown that ROR receptors influence the vesicle compositions of all vesicle populations, although they are exclusively transferred via MVs and EXOs.

### 4.3.3 ROR1/2 positive EVs as breast cancer biomarkers

One of the challenges in modern cancer research is the search for novel biomarkers for breast cancer. Most studies postulate that the concentration of vesicles in the blood of cancer patients is increased compared to healthy controls (Galindo-Hernandez *et al*, 2013; Zhao *et al*, 2016; König *et al*, 2017). However, not only the number of EVs plays a role, but also the expression of certain proteins on the EVs. This could make them a valuable tool in order to possibly act as biomarkers for certain cancer entities.

In this work and also in various studies, the connection between a high ROR1 expression and a poor clinical outcome for TNBC patients could be established (Chien *et al*, 2016; Fultang *et al*, 2020). In addition, it has already been shown that ROR1 mediates various tumor-promoting effects, like enhanced cell migration, invasion and survival. Due to the fact that ROR1/2 are often overexpressed in breast cancer (Henry *et al*, 2015b; Fultang *et al*, 2020) and are also expressed on MVs and EXOs, the question arose whether they might serve as new biomarkers to identify circulating tumor MV in the blood of breast cancer patients. Unfortunately, the question whether ROR1/2 on EVs can function as a biomarker for breast cancer could not be conclusively clarified in this work, since firstly too few patient samples could be measured and secondly the establishment of the staining proved to be difficult, since

the patient samples obtained were primarily only from early stages. However, a slight trend could be shown for ROR2 and EMMPRIN, as the median values of fluorescence intensity were higher in the patient samples than in the control samples. For ROR2, a median value of 25.62 was slightly higher compared to the control patients with a median value of 13.24. This trend fits with the previous results of Dr. Kerstin Menck, where elevated ROR2 values could be measured compared to control values in a group of breast cancer patients. For EMMPRIN there was also a slight trend where the median value of 86.82 in breast cancer patients was higher than the control level of 80.74. Nevertheless, it remains unclear whether the trends observed here are valid, which is why later stages should be included into the measurement. As expected, the results showed no striking differences between the early stages and control samples, so no conclusion can be drawn about the markers themselves. Therefore, further samples need to be collected and, at best, samples from later stages where more significant differences from controls can be expected. All in all, while single markers may also show some prognostic evidence for cancer patient survival, the combination of different markers or even signatures are less subject to variation than single markers and may therefore provide more valid results.

So far, the quality of ROR1/2 and their function as cancer biomarkers is still unclear, since too few patient samples have been measured and evaluated, but nevertheless a promising trend of ROR2 and EMMPRIN as a potential EV biomarker could be discovered.

# 5. Summary and Conclusion

This work investigated the role of non-canonical ROR receptors and its interaction partners on breast and colorectal cancer progression. Wnt11 has been identified as a non-canonical Wnt ligand in various studies, but its receptors have not yet been fully identified. Co-IP experiments confirmed an interaction of Wnt11 with the Wnt co-receptor ROR2 which had not been shown in the human setting so far. Sequential deletions of ROR2 pinpointed the CRD and the TKD as important domains for Wnt11-induced pro-invasive Wnt signaling. Whether Wnt11 interacts with further receptors was not clear. This study revealed FZD6 and PTK7 as promising receptors in breast and colorectal cancer progression and furthermore as possible interaction partners for Wnt11. The knockout of FZD6 resulted in a significant reduction in Wnt11-induced invasiveness and migration, which could not be rescued by stimulation with rhWnt11, supporting the theory of an interaction between FZD6 and Wnt11. The interaction was confirmed by Co-IP experiments.

Since it was already known that Wnt proteins can be transported to target cells via EVs, where they can trigger Wnt signaling or increase cell invasiveness, it was subsequently investigated whether ROR1, as example for the ROR receptors, is also transported via EVs. The analysis identified ROR1 on MVs and EXOs, but not on LVs. Stimulation of MDA-MB231 vesicles significantly increased the invasiveness of less aggressive MCF-7 cells, whereas loss of ROR1 reduced this effect. Stimulation of ROR1-negative MVs and EXOs did not increase invasiveness as much as wild type MDA-MB231 vesicles.

EV protein composition upon ROR1 and ROR2 depletion was examined and revealed that both significantly affected protein expression on all three analyzed EV subpopulations. However, whether the ROR receptors can also function as biomarkers requires further investigation. In first experiments, promising results could be obtained, especially regarding ROR2 as a possible biomarker for breast cancer.

# 6. Literature


Abels ER, Maas SLN, Nieland L, Wei Z, Cheah PS, Tai E, Kolsteeg C-J, Dusoswa SA, Ting DT, Hickman S, *et al* (2019) Glioblastoma-Associated Microglia Reprogramming Is Mediated by Functional Transfer of Extracellular miR-21. *Cell Rep* 28: 3105-3119.e7

Aberle H, Bauer A, Stappert J, Kispert A & Kemler R (1997) beta-catenin is a target for the ubiquitin-proteasome pathway. *EMBO J* 16: 3797–3804

Acebron SP, Karaulanov E, Berger BS, Huang Y-L & Niehrs C (2014) Mitotic wnt signaling promotes protein stabilization and regulates cell size. *Mol Cell* 54: 663–674

Adler PN, Vinson C, Park WJ, Conover S & Klein L (1990) Molecular Structure of Frizzled, a Drosophila Tissue Polarity Gene. *Genetics* 126: 401–416

Alkabban FM & Ferguson T (2021) Breast Cancer. In *StatPearls* Treasure Island (FL): StatPearls Publishing

Al-Nedawi K, Meehan B, Micallef J, Lhotak V, May L, Guha A & Rak J (2008) Intercellular transfer of the oncogenic receptor EGFRvIII by microvesicles derived from tumour cells. *Nat Cell Biol* 10: 619–624

van Amerongen R, Fuerer C, Mizutani M & Nusse R (2012) Wnt5a can both activate and repress Wnt/β-catenin signaling during mouse embryonic development. *Dev Biol* 369: 101–114

Andre P, Wang Q, Wang N, Gao B, Schilit A, Halford MM, Stacker SA, Zhang X & Yang Y (2012) The Wnt coreceptor Ryk regulates Wnt/planar cell polarity by modulating the degradation of the core planar cell polarity component Vangl2. *J Biol Chem* 287: 44518–44525

Antonyak MA & Cerione RA (2014) Microvesicles as mediators of intercellular communication in cancer. *Methods Mol Biol Clifton NJ* 1165: 147–173

Antonyak MA, Li B, Boroughs LK, Johnson JL, Druso JE, Bryant KL, Holowka DA & Cerione RA (2011) Cancer cell-derived microvesicles induce transformation by transferring tissue transglutaminase and fibronectin to recipient cells. *Proc Natl Acad Sci U S A* 108: 4852–4857

Arraud N, Linares R, Tan S, Gounou C, Pasquet J-M, Mornet S & Brisson AR (2014) Extracellular vesicles from blood plasma: determination of their morphology, size, phenotype and concentration. *J Thromb Haemost JTH* 12: 614–627

Artim SC, Mendrola JM & Lemmon MA (2012) Assessing the range of kinase autoinhibition mechanisms in the insulin receptor family. *Biochem J* 448: 213–220

Ataseven B, Angerer R, Kates R, Gunesch A, Knyazev P, Högel B, Becker C, Eiermann W & Harbeck N (2013) PTK7 expression in triple-negative breast cancer. *Anticancer Res* 33: 3759–3763

Baarsma H & Königshoff M (2013) WNT5A antagonizes canonical WNT/β-catenin signaling in lung epithelial cells. *Eur Respir J* 42

Bai Y, Tan X, Zhang H, Liu C, Zhao B, Li Y, Lu L, Liu Y & Zhou J (2014) Ror2 receptor mediates Wnt11 ligand signaling and affects convergence and extension movements in zebrafish. *J Biol Chem* 289: 20664–20676

Baietti MF, Zhang Z, Mortier E, Melchior A, Degeest G, Geeraerts A, Ivarsson Y, Depoortere F, Coomans C, Vermeiren E, *et al* (2012) Syndecan-syntenin-ALIX regulates the biogenesis of exosomes. *Nat Cell Biol* 14: 677–685

Bang I, Kim HR, Beaven AH, Kim J, Ko S-B, Lee GR, Kan W, Lee H, Im W, Seok C, *et al* (2018) Biophysical and functional characterization of Norrin signaling through Frizzled4. *Proc Natl Acad Sci* 115: 8787–8792

Baran J, Baj-Krzyworzeka M, Weglarczyk K, Szatanek R, Zembala M, Barbasz J, Czupryna A, Szczepanik A & Zembala M (2010) Circulating tumour-derived microvesicles in plasma of gastric cancer patients. *Cancer Immunol Immunother CII* 59: 841–850

Barker N, Hurlstone A, Musisi H, Miles A, Bienz M & Clevers H (2001) The chromatin remodelling factor Brg-1 interacts with β-catenin to promote target gene activation. *EMBO J* 20: 4935–4943

Bayerlová M, Menck K, Klemm F, Wolff A, Pukrop T, Binder C, Beißbarth T & Bleckmann A (2017) Ror2 Signaling and Its Relevance in Breast Cancer Progression. *Front Oncol* 0

Bazhin AV, Tambor V, Dikov B, Philippov PP, Schadendorf D & Eichmüller SB (2010) cGMP-phosphodiesterase 6, transducin and Wnt5a/Frizzled-2-signaling control cGMP and Ca(2+) homeostasis in melanoma cells. *Cell Mol Life Sci CMLS* 67: 817–828

Bell J (1989) The polymerase chain reaction. *Immunol Today* 10: 351–355

Bienz M & Clevers H (2000) Linking colorectal cancer to Wnt signaling. *Cell* 103: 311–320

Bilic J, Huang Y-L, Davidson G, Zimmermann T, Cruciat C-M, Bienz M & Niehrs C (2007) Wnt induces LRP6 signalosomes and promotes dishevelled-dependent LRP6 phosphorylation. *Science* 316: 1619–1622

Binda E, Visioli A, Giani F, Trivieri N, Palumbo O, Restelli S, Dezi F, Mazza T, Fusilli C, Legnani F, *et al* (2017) Wnt5a Drives an Invasive Phenotype in Human Glioblastoma Stem-like Cells. *Cancer Res* 77: 996–1007

Bisson JA, Mills B, Paul Helt J-C, Zwaka TP & Cohen ED (2015) Wnt5a and Wnt11 inhibit the canonical Wnt pathway and promote cardiac progenitor development via the Caspase-dependent degradation of AKT. *Dev Biol* 398: 80–96

Bleckmann A, Conradi L-C, Menck K, Schmick NA, Schubert A, Rietkötter E, Arackal J, Middel P, Schambony A, Liersch T, *et al* (2016) β-catenin-independent WNT signaling and Ki67 in contrast to the estrogen receptor status are prognostic and associated with poor prognosis in breast cancer liver metastases. *Clin Exp Metastasis* 33: 309–323

Bond J, Sedmera D, Jourdan J, Zhang Y, Eisenberg CA, Eisenberg LM & Gourdie RG (2003) Wnt11 and Wnt7a are up-regulated in association with differentiation of cardiac conduction cells in vitro and in vivo. *Dev Dyn Off Publ Am Assoc Anat* 227: 536–543

Borcherding N, Kusner D, Liu G-H & Zhang W (2014) ROR1, an embryonic protein with an emerging role in cancer biology. *Protein Cell* 5: 496–502

Brauker JH, Trautman MS & Bernfield M (1991) Syndecan, a cell surface proteoglycan, exhibits a molecular polymorphism during lung development. *Dev Biol* 147: 285–292

Brooks SC, Locke ER & Soule HD (1973) Estrogen receptor in a human cell line (MCF-7) from breast carcinoma. *J Biol Chem* 248: 6251–6253

Bryja V, Andersson ER, Schambony A, Esner M, Bryjová L, Biris KK, Hall AC, Kraft B, Cajanek L, Yamaguchi TP, *et al* (2009) The Extracellular Domain of Lrp5/6 Inhibits Noncanonical Wnt Signaling In Vivo. *Mol Biol Cell* 20: 924–936

Burstein HJ, Keshaviah A, Baron AD, Hart RD, Lambert-Falls R, Marcom PK, Gelman R & Winer EP (2007) Trastuzumab plus vinorelbine or taxane chemotherapy for HER2-overexpressing metastatic breast cancer: the trastuzumab and vinorelbine or taxane study. *Cancer* 110: 965–972

Cailleau R, Young R, Olivé M & Reeves WJ (1974) Breast tumor cell lines from pleural effusions. *J Natl Cancer Inst* 53: 661–674

Cavodeassi F, Carreira-Barbosa F, Young RM, Concha ML, Allende ML, Houart C, Tada M & Wilson SW (2005) Early stages of zebrafish eye formation require the coordinated activity of Wnt11, Fz5, and the Wnt/beta-catenin pathway. *Neuron* 47: 43–56

Charras GT (2008) A short history of blebbing. *J Microsc* 231: 466–478

Chen L, Cao R, Wang G, Yuan L, Qian G, Guo Z, Wu C-L, Wang X & Xiao Y (2017a) Downregulation of TRPM7 suppressed migration and invasion by regulating epithelial-mesenchymal transition in prostate cancer cells. *Med Oncol Northwood Lond Engl* 34: 127

Chen Y, Chen Z, Tang Y & Xiao Q (2021) The involvement of noncanonical Wnt signaling in cancers. *Biomed Pharmacother* 133: 110946

Chen Y, Zeng C, Zhan Y, Wang H, Jiang X & Li W (2017b) Aberrant low expression of p85α in stromal fibroblasts promotes breast cancer cell metastasis through exosome-mediated paracrine Wnt10b. *Oncogene* 36: 4692–4705

Cheng W-C, Liao T-T, Lin C-C, Yuan L-TE, Lan H-Y, Lin H-H, Teng H-W, Chang H-C, Lin C-H, Yang C-Y, *et al* (2019) RAB27B-activated secretion of stem-like tumor exosomes delivers the biomarker microRNA-146a-5p, which promotes tumorigenesis and associates with an immunosuppressive tumor microenvironment in colorectal cancer. *Int J Cancer* 145: 2209–2224

Chien H-P, Ueng S-H, Chen S-C, Chang Y-S, Lin Y-C, Lo Y-F, Chang H-K, Chuang W-Y, Huang Y-T, Cheung Y-C, *et al* (2016) Expression of ROR1 has prognostic significance in triple negative breast cancer. *Virchows Arch Int J Pathol* 468: 589–595

Christianson HC, Svensson KJ, Kuppevelt TH van, Li J-P & Belting M (2013) Cancer cell exosomes depend on cell-surface heparan sulfate proteoglycans for their internalization and functional activity. *Proc Natl Acad Sci* 110: 17380–17385

Ciardiello C, Cavallini L, Spinelli C, Yang J, Reis-Sobreiro M, de Candia P, Minciacchi VR & Di Vizio D (2016) Focus on Extracellular Vesicles: New Frontiers of Cell-to-Cell Communication in Cancer. *Int J Mol Sci* 17: 175

Ciardiello C, Leone A, Lanuti P, Roca MS, Moccia T, Minciacchi VR, Minopoli M, Gigantino V, De Cecio R, Rippa M, *et al* (2019) Large oncosomes overexpressing integrin alpha-V promote prostate cancer adhesion and invasion via AKT activation. *J Exp Clin Cancer Res CR* 38: 317

Ciardiello C, Migliorino R, Leone A & Budillon A (2020) Large extracellular vesicles: Size matters in tumor progression. *Cytokine Growth Factor Rev* 51: 69–74

Cong F, Schweizer L & Varmus H (2004) Wnt signals across the plasma membrane to activate the beta-catenin pathway by forming oligomers containing its receptors, Frizzled and LRP. *Dev Camb Engl* 131: 5103–5115

Corcoran RB, Ebi H, Turke AB, Coffee EM, Nishino M, Cogdill AP, Brown RD, Della Pelle P, Dias-Santagata D, Hung KE, *et al* (2012) EGFR-mediated re-activation of MAPK signaling contributes to insensitivity of BRAF mutant colorectal cancers to RAF inhibition with vemurafenib. *Cancer Discov* 2: 227–235

Corda G & Sala A (2017) Non-canonical WNT/PCP signalling in cancer: Fzd6 takes centre stage. *Oncogenesis* 6: e364–e364

Corda G, Sala G, Lattanzio R, Iezzi M, Sallese M, Fragassi G, Lamolinara A, Mirza H, Barcaroli D, Ermler S, *et al* (2017) Functional and prognostic significance of the genomic amplification of frizzled 6 (FZD6) in breast cancer. *J Pathol* 241: 350–361

Corrigan PM, Dobbin E, Freeburn RW & Wheadon H (2009) Patterns of Wnt/Fzd/LRP gene expression during embryonic hematopoiesis. *Stem Cells Dev* 18: 759–772

Costa Verdera H, Gitz-Francois JJ, Schiffelers RM & Vader P (2017) Cellular uptake of extracellular vesicles is mediated by clathrin-independent endocytosis and macropinocytosis. *J Control Release Off J Control Release Soc* 266: 100–108

Crawford S, Diamond D, Brustolon L & Penarreta R (2010) Effect of Increased Extracellular Ca++ on Microvesicle Production and Tumor Spheroid Formation. *Cancer Microenviron* 4: 93–103

Dai B, Yan T & Zhang A (2017) ROR2 receptor promotes the migration of osteosarcoma cells in response to Wnt5a. *Cancer Cell Int* 17: 112

Daikuzono H, Yamazaki M, Sato Y, Takahashi T & Yamagata K (2021) Development of a DELFIA method to detect oncofetal antigen ROR1-positive exosomes. *Biochem Biophys Res Commun* 578: 170–176

Davidson G, Wu W, Shen J, Bilic J, Fenger U, Stannek P, Glinka A & Niehrs C (2005) Casein kinase 1 γ couples Wnt receptor activation to cytoplasmic signal transduction. *Nature* 438: 867–872

De P, Carlson JH, Wu H, Marcus A, Leyland-Jones B & Dey N (2016) Wnt-beta-catenin pathway signals metastasis-associated tumor cell phenotypes in triple negative breast cancers. *Oncotarget* 7: 43124–43149

Debebe Z & Rathmell WK (2015) Ror2 as a Therapeutic Target in Cancer. *Pharmacol Ther* 150: 143–148

Del Conde I, Shrimpton CN, Thiagarajan P & López JA (2005) Tissue-factor-bearing microvesicles arise from lipid rafts and fuse with activated platelets to initiate coagulation. *Blood* 106: 1604–1611

Deng F & Miller J (2019) A review on protein markers of exosome from different bio-resources and the antibodies used for characterization. *J Histotechnol* 42: 226–239

Di Vizio D, Kim J, Hager MH, Morello M, Yang W, Lafargue CJ, True LD, Rubin MA, Adam RM, Beroukhim R, *et al* (2009) Oncosome formation in prostate cancer: association with a region of frequent chromosomal deletion in metastatic disease. *Cancer Res* 69: 5601–5609

Di Vizio D, Morello M, Dudley AC, Schow PW, Adam RM, Morley S, Mulholland D, Rotinen M, Hager MH, Insabato L, *et al* (2012) Large oncosomes in human prostate cancer tissues and in the circulation of mice with metastatic disease. *Am J Pathol* 181: 1573–1584

Dijksterhuis JP, Baljinnyam B, Stanger K, Sercan HO, Ji Y, Andres O, Rubin JS, Hannoush RN & Schulte G (2015) Systematic Mapping of WNT-FZD Protein Interactions Reveals Functional Selectivity by Distinct WNT-FZD Pairs. *J Biol Chem* 290: 6789–6798

Dillekås H, Rogers MS & Straume O (2019) Are 90% of deaths from cancer caused by metastases? *Cancer Med* 8: 5574–5576

Djiane A, Riou J, Umbhauer M, Boucaut J & Shi D (2000) Role of frizzled 7 in the regulation of convergent extension movements during gastrulation in Xenopus laevis. *Dev Camb Engl* 127: 3091–3100

Dozio V & Sanchez J-C (2017) Characterisation of extracellular vesicle-subsets derived from brain endothelial cells and analysis of their protein cargo modulation after TNF exposure. *J Extracell Vesicles* 6: 1302705

Drescher DG, Ramakrishnan NA & Drescher MJ (2009) Surface Plasmon Resonance (SPR) Analysis of Binding Interactions of Proteins in Inner-Ear Sensory Epithelia. *Methods Mol Biol Clifton NJ* 493: 323–343

Dunnwald LK, Rossing MA & Li CI (2007) Hormone receptor status, tumor characteristics, and prognosis: a prospective cohort of breast cancer patients. *Breast Cancer Res BCR* 9: R6

Dwyer MA, Joseph JD, Wade HE, Eaton ML, Kunder RS, Kazmin D, Chang C & McDonnell DP (2010) WNT11 expression is induced by estrogen-related receptor alpha and beta-catenin and acts in an autocrine manner to increase cancer cell migration. *Cancer Res* 70: 9298–9308

Elia I, Doglioni G & Fendt S-M (2018) Metabolic Hallmarks of Metastasis Formation. *Trends Cell Biol* 28: 673–684

Elsherbini A & Bieberich E (2018) Ceramide and Exosomes: A Novel Target in Cancer Biology and Therapy. *Adv Cancer Res* 140: 121–154

Ender F, Bubnoff NV & Gieseler F (2019) Extracellular Vesicles: Subcellular Organelles With the Potential to Spread Cancer Resistance. *Anticancer Res* 39: 3395–3404

Endo M, Nishita M & Minami Y (2012) Analysis of Wnt/planar cell polarity pathway in cultured cells. *Methods Mol Biol Clifton NJ* 839: 201–214

Endo Y, Wolf V, Muraiso K, Kamijo K, Soon L, Uren A, Barshishat-Küpper M & Rubin JS (2005) Wnt-3a-dependent cell motility involves RhoA activation and is specifically regulated by dishevelled-2. *J Biol Chem* 280: 777–786

Enomoto M, Hayakawa S, Itsukushima S, Ren DY, Matsuo M, Tamada K, Oneyama C, Okada M, Takumi T, Nishita M, *et al* (2009) Autonomous regulation of osteosarcoma cell invasiveness by Wnt5a/Ror2 signaling. *Oncogene* 28: 3197–3208

Exman P & Tolaney SM (2021) HER2-positive metastatic breast cancer: a comprehensive review. *Clin Adv Hematol Oncol HO* 19: 40–50

Flaherty MP, Abdel-Latif A, Li Q, Hunt G, Ranjan S, Ou Q, Tang X-L, Johnson RK, Bolli R & Dawn B (2008) Noncanonical Wnt11 signaling is sufficient to induce cardiomyogenic differentiation in unfractionated bone marrow mononuclear cells. *Circulation* 117: 2241–2252

FLORESCU-ŢENEA R, KAMAL A, MITRUŢ P, MITRUŢ R, ILIE D, NICOLAESCU A & MOGOANTĂ L (2019) Colorectal Cancer: An Update on Treatment Options and Future Perspectives. *Curr Health Sci J* 45: 134–141

Flores-Hernández E, Velázquez DM, Castañeda-Patlán MC, Fuentes-García G, Fonseca-Camarillo G, Yamamoto-Furusho JK, Romero-Avila MT, García-Sáinz JA & Robles-Flores M (2020) Canonical and non-canonical Wnt signaling are simultaneously activated by Wnts in colon cancer cells. *Cell Signal* 72: 109636

Freake HC, Marcocci C, Iwasaki J & MacIntyre I (1981) 1,25-dihydroxyvitamin D3 specifically binds to a human breast cancer cell line (T47D) and stimulates growth. *Biochem Biophys Res Commun* 101: 1131–1138

Fu Y, Chen Y, Huang J, Cai Z & Wang Y (2020) RYK, a receptor of noncanonical Wnt ligand Wnt5a, is positively correlated with gastric cancer tumorigenesis and potential of liver metastasis. *Am J Physiol-Gastrointest Liver Physiol* 318: G352–G360

Fuerer C, Habib SJ & Nusse R (2010) A study on the interactions between heparan sulfate proteoglycans and Wnt proteins. *Dev Dyn Off Publ Am Assoc Anat* 239: 184–190

Fukuda T, Chen L, Endo T, Tang L, Lu D, Castro JE, Widhopf GF, Rassenti LZ, Cantwell MJ, Prussak CE, *et al* (2008) Antisera induced by infusions of autologous Ad-CD154-leukemia B cells identify ROR1 as an oncofetal antigen and receptor for Wnt5a. *Proc Natl Acad Sci U S A* 105: 3047–3052

Fultang N, Illendula A, Lin J, Pandey MK, Klase Z & Peethambaran B (2020) ROR1 regulates chemoresistance in Breast Cancer via modulation of drug efflux pump ABCB1. *Sci Rep* 10: 1821

Gajria D & Chandarlapaty S (2011) HER2-amplified breast cancer: mechanisms of trastuzumab resistance and novel targeted therapies. *Expert Rev Anticancer Ther* 11: 263–275

Galindo-Hernandez O, Villegas-Comonfort S, Candanedo F, González-Vázquez M-C, Chavez-Ocaña S, Jimenez-Villanueva X, Sierra-Martinez M & Salazar EP (2013) Elevated concentration of microvesicles isolated from peripheral blood in breast cancer patients. *Arch Med Res* 44: 208–214

Gao S-L, Kong C-Z, Zhang Z, Li Z-L, Bi J-B & Liu X-K (2017) TRPM7 is overexpressed in bladder cancer and promotes proliferation, migration, invasion and tumor growth. *Oncol Rep* 38: 1967–1976

Gao Z-H, Seeling JM, Hill V, Yochum A & Virshup DM (2002) Casein kinase I phosphorylates and destabilizes the beta-catenin degradation complex. *Proc Natl Acad Sci U S A* 99: 1182–1187

Geetha-Loganathan P, Nimmagadda S, Fu K & Richman JM (2014) Avian facial morphogenesis is regulated by c-Jun N-terminal kinase/planar cell polarity (JNK/PCP) wingless-related (WNT) signaling. *J Biol Chem* 289: 24153–24167

George JN, Thoi LL, McManus LM & Reimann TA (1982) Isolation of human platelet membrane microparticles from plasma and serum. *Blood* 60: 834–840

Ginestra A, Miceli D, Dolo V, Romano FM & Vittorelli ML (1999) Membrane vesicles in ovarian cancer fluids: a new potential marker. *Anticancer Res* 19: 3439–3445

Gorroño-Etxebarria I, Aguirre U, Sanchez S, González N, Escobar A, Zabalza I, Quintana JM, Vivanco M dM, Waxman J & Kypta RM (2019) Wnt-11 as a Potential Prognostic Biomarker and Therapeutic Target in Colorectal Cancer. *Cancers* 11: 908

Gross JC, Chaudhary V, Bartscherer K & Boutros M (2012) Active Wnt proteins are secreted on exosomes. *Nat Cell Biol* 14: 1036–1045

Gujral TS, Chan M, Peshkin L, Sorger PK, Kirschner MW & MacBeath G (2014) A noncanonical Frizzled2 pathway regulates epithelial-mesenchymal transition and metastasis. *Cell* 159: 844–856

Guo M, Ma G, Zhang X, Tang W, Shi J, Wang Q, Cheng Y, Zhang B & Xu J (2020) ROR2 knockdown suppresses breast cancer growth through PI3K/ATK signaling. *Aging* 12: 13115–13127

Gurney A, Axelrod F, Bond CJ, Cain J, Chartier C, Donigan L, Fischer M, Chaudhari A, Ji M, Kapoun AM, *et al* (2012) Wnt pathway inhibition via the targeting of Frizzled receptors results in decreased growth and tumorigenicity of human tumors. *Proc Natl Acad Sci U S A* 109: 11717–11722

Győrffy B (2021) Survival analysis across the entire transcriptome identifies biomarkers with the highest prognostic power in breast cancer. *Comput Struct Biotechnol J* 19: 4101–4109

György B, Módos K, Pállinger E, Pálóczi K, Pásztói M, Misják P, Deli MA, Sipos A, Szalai A, Voszka I, *et al* (2011) Detection and isolation of cell-derived microparticles are

compromised by protein complexes resulting from shared biophysical parameters. *Blood* 117: e39-48

Ha N-C, Tonozuka T, Stamos JL, Choi H-J & Weis WI (2004) Mechanism of phosphorylation-dependent binding of APC to beta-catenin and its role in beta-catenin degradation. *Mol Cell* 15: 511–521

Hagemann T, Robinson SC, Schulz M, Trümper L, Balkwill FR & Binder C (2004) Enhanced invasiveness of breast cancer cell lines upon co-cultivation with macrophages is due to TNF-alpha dependent up-regulation of matrix metalloproteases. *Carcinogenesis* 25: 1543–1549

Han K, Lang T, Zhang Z, Zhang Y, Sun Y, Shen Z, Beuerman RW, Zhou L & Min D (2018) Luteolin attenuates Wnt signaling via upregulation of FZD6 to suppress prostate cancer stemness revealed by comparative proteomics. *Sci Rep* 8: 8537

Hanahan D, Jessee J & Bloom FR (1991) Plasmid transformation of Escherichia coli and other bacteria. *Methods Enzymol* 204: 63–113

Harada T, Yamamoto H, Kishida S, Kishida M, Awada C, Takao T & Kikuchi A (2017) Wnt5b-associated exosomes promote cancer cell migration and proliferation. *Cancer Sci* 108: 42–52

Hasan MK, Yu J, Chen L, Cui B, Widhopf II GF, Rassenti L, Shen Z, Briggs SP & Kipps TJ (2017) Wnt5a induces ROR1 to complex with HS1 to enhance migration of chronic lymphocytic leukemia cells. *Leukemia* 31: 2615–2622

Hayes M, Naito M, Daulat A, Angers S & Ciruna B (2013) Ptk7 promotes non-canonical Wnt/PCP-mediated morphogenesis and inhibits Wnt/β-catenin-dependent cell fate decisions during vertebrate development. *Dev Camb Engl* 140: 1807–1818

He W, Wong SC, Ma B, Ng SS, Lam MY, Chan CM, Au TC, Chan JK & Chan AT (2011) The expression of frizzled-3 receptor in colorectal cancer and colorectal adenoma. *J Clin Oncol* 29: 444–444

Henry C, Llamosas E, Knipprath-Meszaros A, Schoetzau A, Obermann E, Fuenfschilling M, Caduff R, Fink D, Hacker N, Ward R, *et al* (2015a) Targeting the ROR1 and ROR2 receptors in epithelial ovarian cancer inhibits cell migration and invasion. *Oncotarget* 6: 40310–40326

Henry C, Quadir A, Hawkins NJ, Jary E, Llamosas E, Kumar D, Daniels B, Ward RL & Ford CE (2015b) Expression of the novel Wnt receptor ROR2 is increased in breast cancer and may regulate both β-catenin dependent and independent Wnt signalling. *J Cancer Res Clin Oncol* 141: 243–254

Hermsen M, Postma C, Baak J, Weiss M, Rapallo A, Sciutto A, Roemen G, Arends J-W, Williams R, Giaretti W, *et al* (2002) Colorectal adenoma to carcinoma progression follows multiple pathways of chromosomal instability. *Gastroenterology* 123: 1109–1119

Heusermann W, Hean J, Trojer D, Steib E, von Bueren S, Graff-Meyer A, Genoud C, Martin K, Pizzato N, Voshol J, *et al* (2016) Exosomes surf on filopodia to enter cells at

endocytic hot spots, traffic within endosomes, and are targeted to the ER. *J Cell Biol* 213: 173–184

Hikasa H, Shibata M, Hiratani I & Taira M (2002) The Xenopus receptor tyrosine kinase Xror2 modulates morphogenetic movements of the axial mesoderm and neuroectoderm via Wnt signaling. *Dev Camb Engl* 129: 5227–5239

Hirano H, Yonezawa H, Yunoue S, Habu M, Uchida H, Yoshioka T, Kishida S, Kishida M, Oyoshi T, Fujio S, *et al* (2014) Immunoreactivity of Wnt5a, Fzd2, Fzd6, and Ryk in glioblastoma: evaluative methodology for DAB chromogenic immunostaining. *Brain Tumor Pathol* 31: 85–93

Ho H-YH, Susman MW, Bikoff JB, Ryu YK, Jonas AM, Hu L, Kuruvilla R & Greenberg ME (2012) Wnt5a-Ror-Dishevelled signaling constitutes a core developmental pathway that controls tissue morphogenesis. *Proc Natl Acad Sci U S A* 109: 4044–4051

Holme PA, Orvim U, Hamers MJ, Solum NO, Brosstad FR, Barstad RM & Sakariassen KS (1997) Shear-induced platelet activation and platelet microparticle formation at blood flow conditions as in arteries with a severe stenosis. *Arterioscler Thromb Vasc Biol* 17: 646–653

Höög JL & Lötvall J (2015) Diversity of extracellular vesicles in human ejaculates revealed by cryo-electron microscopy. *J Extracell Vesicles* 4: 28680

Hoshino A, Costa-Silva B, Shen T-L, Rodrigues G, Hashimoto A, Tesic Mark M, Molina H, Kohsaka S, Di Giannatale A, Ceder S, *et al* (2015) Tumour exosome integrins determine organotropic metastasis. *Nature* 527: 329–335

Hovens CM, Stacker SA, Andres AC, Harpur AG, Ziemiecki A & Wilks AF (1992) RYK, a receptor tyrosine kinase-related molecule with unusual kinase domain motifs. *Proc Natl Acad Sci U S A* 89: 11818–11822

Hu S-Q, Zhang Q-C, Meng Q-B, Hu A-N, Zou J-P & Li X-L (2020) Autophagy regulates exosome secretion in rat nucleus pulposus cells via the RhoC/ROCK2 pathway. *Exp Cell Res* 395: 112239

Huang Y-L, Anvarian Z, Döderlein G, Acebron SP & Niehrs C (2015) Maternal Wnt/STOP signaling promotes cell division during early Xenopus embryogenesis. *Proc Natl Acad Sci U S A* 112: 5732–5737

Imjeti NS, Menck K, Egea-Jimenez AL, Lecointre C, Lembo F, Bouguenina H, Badache A, Ghossoub R, David G, Roche S, *et al* (2017) Syntenin mediates SRC function in exosomal cell-to-cell communication. *Proc Natl Acad Sci U S A* 114: 12495–12500

Inic Z, Zegarac M, Inic M, Markovic I, Kozomara Z, Djurisic I, Inic I, Pupic G & Jancic S (2014) Difference between Luminal A and Luminal B Subtypes According to Ki-67, Tumor Size, and Progesterone Receptor Negativity Providing Prognostic Information. *Clin Med Insights Oncol* 8: 107–111

Ishii K, Morii N & Yamashiro H (2019) Pertuzumab in the treatment of HER2-positive breast cancer: an evidence-based review of its safety, efficacy, and place in therapy. *Core Evid* 14: 51–70

Janovska P, Poppova L, Plevova K, Plesingerova H, Behal M, Kaucka M, Ovesna P, Hlozkova M, Borsky M, Stehlikova O, *et al* (2016) Autocrine Signaling by Wnt-5a Deregulates Chemotaxis of Leukemic Cells and Predicts Clinical Outcome in Chronic Lymphocytic Leukemia. *Clin Cancer Res Off J Am Assoc Cancer Res* 22: 459–469

Jitariu A-A, Cîmpean AM, Ribatti D & Raica M (2017) Triple negative breast cancer: the kiss of death. *Oncotarget* 8: 46652–46662

Kamino M, Kishida M, Kibe T, Ikoma K, Iijima M, Hirano H, Tokudome M, Chen L, Koriyama C, Yamada K, *et al* (2011) Wnt-5a signaling is correlated with infiltrative activity in human glioma by inducing cellular migration and MMP-2. *Cancer Sci* 102: 540–548

Kang M, Kim S & Ko J (2019) Roles of CD133 in microvesicle formation and oncoprotein trafficking in colon cancer. *FASEB J Off Publ Fed Am Soc Exp Biol* 33: 4248–4260

Karvonen H, Perttilä R, Niininen W, Hautanen V, Barker H, Murumägi A, Heckman CA & Ungureanu D (2019) Wnt5a and ROR1 activate non-canonical Wnt signaling via RhoA in TCF3-PBX1 acute lymphoblastic leukemia and highlight new treatment strategies via Bcl-2 co-targeting. *Oncogene* 38: 3288–3300

Khramtsov AI, Khramtsova GF, Tretiakova M, Huo D, Olopade OI & Goss KH (2010) Wnt/β-Catenin Pathway Activation Is Enriched in Basal-Like Breast Cancers and Predicts Poor Outcome. *Am J Pathol* 176: 2911–2920

Kilander MBC, Dahlström J & Schulte G (2014) Assessment of Frizzled 6 membrane mobility by FRAP supports G protein coupling and reveals WNT-Frizzled selectivity. *Cell Signal* 26: 1943–1949

Kim G-H, Her J-H & Han J-K (2008) Ryk cooperates with Frizzled 7 to promote Wnt11-mediated endocytosis and is essential for Xenopus laevis convergent extension movements. *J Cell Biol* 182: 1073–1082

Kim J, Jung E, Ahn SS, Yeo H, Lee JY, Seo JK, Lee YH & Shin SY (2020) WNT11 is a direct target of early growth response protein 1. *BMB Rep* 53: 628–633

Kirikoshi H, Sekihara H & Katoh M (2001) Molecular cloning and characterization of human WNT11. *Int J Mol Med* 8: 651–656

Klemm F, Bleckmann A, Siam L, Chuang HN, Rietkötter E, Behme D, Schulz M, Schaffrinski M, Schindler S, Trümper L, *et al* (2011) β-catenin-independent WNT signaling in basal-like breast cancer and brain metastasis. *Carcinogenesis* 32: 434–442

Koch R, Demant M, Aung T, Diering N, Cicholas A, Chapuy B, Wenzel D, Lahmann M, Güntsch A, Kiecke C, *et al* (2014) Populational equilibrium through exosome-mediated Wnt signaling in tumor progression of diffuse large B-cell lymphoma. *Blood* 123: 2189–2198

König L, Kasimir-Bauer S, Bittner A-K, Hoffmann O, Wagner B, Santos Manvailer LF, Kimmig R, Horn PA & Rebmann V (2017) Elevated levels of extracellular vesicles are associated with therapy failure and disease progression in breast cancer patients undergoing neoadjuvant chemotherapy. *Oncoimmunology* 7: e1376153

Koval A & Katanaev VL (2018) Dramatic dysbalancing of the Wnt pathway in breast cancers. *Sci Rep* 8: 7329

Koveitypour Z, Panahi F, Vakilian M, Peymani M, Seyed Forootan F, Nasr Esfahani MH & Ghaedi K (2019) Signaling pathways involved in colorectal cancer progression. *Cell Biosci* 9: 97

Kowal J, Arras G, Colombo M, Jouve M, Morath JP, Primdal-Bengtson B, Dingli F, Loew D, Tkach M & Théry C (2016) Proteomic comparison defines novel markers to characterize heterogeneous populations of extracellular vesicle subtypes. *Proc Natl Acad Sci* 113: E968–E977

Kozielewicz P, Turku A, Bowin C-F, Petersen J, Valnohova J, Cañizal MCA, Ono Y, Inoue A, Hoffmann C & Schulte G (2020) Structural insight into small molecule action on Frizzleds. *Nat Commun* 11: 414

Kramer N, Schmöllerl J, Unger C, Nivarthi H, Rudisch A, Unterleuthner D, Scherzer M, Riedl A, Artaker M, Crncec I, *et al* (2017) Autocrine WNT2 signaling in fibroblasts promotes colorectal cancer progression. *Oncogene* 36: 5460–5472

Kunzelmann-Marche C, Freyssinet JM & Martínez MC (2001) Regulation of phosphatidylserine transbilayer redistribution by store-operated Ca2+ entry: role of actin cytoskeleton. *J Biol Chem* 276: 5134–5139

Kurayoshi M, Yamamoto H, Izumi S & Kikuchi A (2007) Post-translational palmitoylation and glycosylation of Wnt-5a are necessary for its signalling. *Biochem J* 402: 515–523

Lako M, Strachan T, Bullen P, Wilson DI, Robson SC & Lindsay S (1998) Isolation, characterisation and embryonic expression of WNT11, a gene which maps to 11q13.5 and has possible roles in the development of skeleton, kidney and lung. *Gene* 219: 101–110

Lamb R, Ablett MP, Spence K, Landberg G, Sims AH & Clarke RB (2013) Wnt Pathway Activity in Breast Cancer Sub-Types and Stem-Like Cells. *PLOS ONE* 8: e67811

Lander R & Petersen CP (2016) Wnt, Ptk7, and FGFRL expression gradients control trunk positional identity in planarian regeneration. *eLife* 5: e12850

Lee Y-TN (Margaret) (1983) Breast carcinoma: Pattern of metastasis at autopsy. *J Surg Oncol* 23: 175–180

Leibovitz A, Stinson JC, McCombs WB, McCoy CE, Mazur KC & Mabry ND (1976) Classification of human colorectal adenocarcinoma cell lines. *Cancer Res* 36: 4562–4569

Lhoumeau A-C, Martinez S, Boher J-M, Monges G, Castellano R, Goubard A, Doremus M, Poizat F, Lelong B, Chaisemartin C de, *et al* (2015) Overexpression of the Promigratory and Prometastatic PTK7 Receptor Is Associated with an Adverse Clinical Outcome in Colorectal Cancer. *PLOS ONE* 10: e0123768

Li B, Antonyak MA, Zhang J & Cerione RA (2012a) RhoA triggers a specific signaling pathway that generates transforming microvesicles in cancer cells. *Oncogene* 31: 4740–4749

Li C, Chen H, Hu L, Xing Y, Sasaki T, Villosis MF, Li J, Nishita M, Minami Y & Minoo P (2008) Ror2 modulates the canonical Wnt signaling in lung epithelial cells through cooperation with Fzd2. *BMC Mol Biol* 9: 11

Li F, Zhao X, Sun R, Ou J, Huang J, Yang N, Xu T, Li J, He X, Li C, *et al* (2020) EGFR-rich extracellular vesicles derived from highly metastatic nasopharyngeal carcinoma cells accelerate tumour metastasis through PI3K/AKT pathway-suppressed ROS. *J Extracell Vesicles* 10: e12003

Li VSW, Ng SS, Boersema PJ, Low TY, Karthaus WR, Gerlach JP, Mohammed S, Heck AJR, Maurice MM, Mahmoudi T, *et al* (2012b) Wnt signaling through inhibition of β-catenin degradation in an intact Axin1 complex. *Cell* 149: 1245–1256

Li Y, Wu Y & Hu Y (2021) Metabolites in the Tumor Microenvironment Reprogram Functions of Immune Effector Cells Through Epigenetic Modifications. *Front Immunol* 12: 1017

Lim E, Metzger-Filho O & Winer EP (2012) The natural history of hormone receptor-positive breast cancer. *Oncol Williston Park N* 26: 688–694, 696

Lin S, Baye LM, Westfall TA & Slusarski DC (2010) Wnt5b-Ryk pathway provides directional signals to regulate gastrulation movement. *J Cell Biol* 190: 263–278

Liu C, Li Y, Semenov M, Han C, Baeg GH, Tan Y, Zhang Z, Lin X & He X (2002) Control of beta-catenin phosphorylation/degradation by a dual-kinase mechanism. *Cell* 108: 837–847

Liu D, Gunther K, Enriquez LA, Daniels B, O'Mara TA, Tang K, Spurdle AB & Ford CE (2020) ROR1 is upregulated in endometrial cancer and represents a novel therapeutic target. *Sci Rep* 10: 13906

Liu W, Sato A, Khadka D, Bharti R, Diaz H, Runnels LW & Habas R (2008) Mechanism of activation of the Formin protein Daam1. *Proc Natl Acad Sci U S A* 105: 210–215

Lowry OH, Rosebrough NJ, Farr AL & Randall RJ (1951) Protein measurement with the Folin phenol reagent. *J Biol Chem* 193: 265–275

Lu X, Borchers AGM, Jolicoeur C, Rayburn H, Baker JC & Tessier-Lavigne M (2004) PTK7/CCK-4 is a novel regulator of planar cell polarity in vertebrates. *Nature* 430: 93–98

Luga V, Zhang L, Viloria-Petit AM, Ogunjimi AA, Inanlou MR, Chiu E, Buchanan M, Hosein AN, Basik M & Wrana JL (2012) Exosomes Mediate Stromal Mobilization of Autocrine Wnt-PCP Signaling in Breast Cancer Cell Migration. *Cell* 151: 1542–1556

Lyberg T, Nakstad B, Hetland O & Boye NP (1990) Procoagulant (thromboplastin) activity in human bronchoalveolar lavage fluids is derived from alveolar macrophages. *Eur Respir J* 3: 61–67

Lyons JP, Mueller UW, Ji H, Everett C, Fang X, Hsieh J-C, Barth AM & McCrea PD (2004) Wnt-4 activates the canonical beta-catenin-mediated Wnt pathway and binds Frizzled-6 CRD: functional implications of Wnt/beta-catenin activity in kidney epithelial cells. *Exp Cell Res* 298: 369–387

Macheda ML, Sun WW, Kugathasan K, Hogan BM, Bower NI, Halford MM, Zhang YF, Jacques BE, Lieschke GJ, Dabdoub A, *et al* (2012) The Wnt Receptor Ryk Plays a Role in Mammalian Planar Cell Polarity Signaling *. *J Biol Chem* 287: 29312–29323

Maji S, Chaudhary P, Akopova I, Nguyen PM, Hare RJ, Gryczynski I & Vishwanatha JK (2017) Exosomal Annexin II Promotes Angiogenesis and Breast Cancer Metastasis. *Mol Cancer Res MCR* 15: 93–105

Mali P, Esvelt KM & Church GM (2013) Cas9 as a versatile tool for engineering biology. *Nat Methods* 10: 957–963

Malinowsky K, Nitsche U, Janssen K-P, Bader FG, Späth C, Drecoll E, Keller G, Höfler H, Slotta-Huspenina J & Becker K-F (2014) Activation of the PI3K/AKT pathway correlates with prognosis in stage II colon cancer. *Br J Cancer* 110: 2081–2089

Mao J, Wang J, Liu B, Pan W, Farr GH, Flynn C, Yuan H, Takada S, Kimelman D, Li L, *et al* (2001) Low-Density Lipoprotein Receptor-Related Protein-5 Binds to Axin and Regulates the Canonical Wnt Signaling Pathway. *Mol Cell* 7: 801–809

Marinissen MJ, Chiariello M, Tanos T, Bernard O, Narumiya S & Gutkind JS (2004) The small GTP-binding protein RhoA regulates c-jun by a ROCK-JNK signaling axis. *Mol Cell* 14: 29–41

Mármol I, Sánchez-de-Diego C, Pradilla Dieste A, Cerrada E & Rodriguez Yoldi MJ (2017) Colorectal Carcinoma: A General Overview and Future Perspectives in Colorectal Cancer. *Int J Mol Sci* 18: E197

Martinez S, Scerbo P, Giordano M, Daulat AM, Lhoumeau A-C, Thomé V, Kodjabachian L & Borg J-P (2015) The PTK7 and ROR2 Protein Receptors Interact in the Vertebrate WNT/Planar Cell Polarity (PCP) Pathway. *J Biol Chem* 290: 30562–30572

Masiakowski P & Carroll RD (1992) A novel family of cell surface receptors with tyrosine kinase-like domain. *J Biol Chem* 267: 26181–26190

McQuate A, Latorre-Esteves E & Barria A (2017) A Wnt/Calcium Signaling Cascade Regulates Neuronal Excitability and Trafficking of NMDARs. *Cell Rep* 21: 60–69

Menck K, Heinrichs S, Baden C & Bleckmann A (2021) The WNT/ROR Pathway in Cancer: From Signaling to Therapeutic Intervention. *Cells* 10: 142

Menck K, Heinrichs S, Wlochowitz D, Sitte M, Noeding H, Janshoff A, Treiber H, Ruhwedel T, Schatlo B, von der Brelie C, Bleckmann A, et al WNT11 is a Novel Ligand for ROR2 in Human Breast cancer. bioRxiv, 2020

Menck K, Klemm F, Gross JC, Pukrop T, Wenzel D & Binder C (2013) Induction and transport of Wnt 5a during macrophage-induced malignant invasion is mediated by two types of extracellular vesicles. *Oncotarget* 4: 2057–2066

Menck K, Scharf C, Bleckmann A, Dyck L, Rost U, Wenzel D, Dhople VM, Siam L, Pukrop T, Binder C, *et al* (2015) Tumor-derived microvesicles mediate human breast cancer invasion through differentially glycosylated EMMPRIN. *J Mol Cell Biol* 7: 143–153

Menck K, Sivaloganathan S, Bleckmann A & Binder C (2020) Microvesicles in Cancer: Small Size, Large Potential. *Int J Mol Sci* 21: 5373

Menck K, Sönmezer C, Worst TS, Schulz M, Dihazi GH, Streit F, Erdmann G, Kling S, Boutros M, Binder C, *et al* (2017) Neutral sphingomyelinases control extracellular vesicles budding from the plasma membrane. *J Extracell Vesicles* 6: 1378056

Mikels A, Minami Y & Nusse R (2009) Ror2 Receptor Requires Tyrosine Kinase Activity to Mediate Wnt5A Signaling. *J Biol Chem* 284: 30167–30176

Mikels AJ & Nusse R (2006) Purified Wnt5a protein activates or inhibits beta-catenin-TCF signaling depending on receptor context. *PLoS Biol* 4: e115

Minciacchi VR, You S, Spinelli C, Morley S, Zandian M, Aspuria P-J, Cavallini L, Ciardiello C, Reis Sobreiro M, Morello M, *et al* (2015) Large oncosomes contain distinct protein cargo and represent a separate functional class of tumor-derived extracellular vesicles. *Oncotarget* 6: 11327–11341

Minn AJ, Kang Y, Serganova I, Gupta GP, Giri DD, Doubrovin M, Ponomarev V, Gerald WL, Blasberg R & Massagué J (2005) Distinct organ-specific metastatic potential of individual breast cancer cells and primary tumors. *J Clin Invest* 115: 44–55

Miyoshi H, Umeshita K, Sakon M, Imajoh-Ohmi S, Fujitani K, Gotoh M, Oiki E, Kambayashi J & Monden M (1996) Calpain activation in plasma membrane bleb formation during tert-butyl hydroperoxide-induced rat hepatocyte injury. *Gastroenterology* 110: 1897–1904

Moo T-A, Sanford R, Dang C & Morrow M (2018) Overview of Breast Cancer Therapy. *PET Clin* 13: 339–354

Morin PJ, Sparks AB, Korinek V, Barker N, Clevers H, Vogelstein B & Kinzler KW (1997) Activation of beta-catenin-Tcf signaling in colon cancer by mutations in beta-catenin or APC. *Science* 275: 1787–1790

Morioka K, Tanikawa C, Ochi K, Daigo Y, Katagiri T, Kawano H, Kawaguchi H, Myoui A, Yoshikawa H, Naka N, *et al* (2009) Orphan receptor tyrosine kinase ROR2 as a potential therapeutic target for osteosarcoma. *Cancer Sci* 100: 1227–1233

Mossie K, Jallal B, Alves F, Sures I, Plowman GD & Ullrich A (1995) Colon carcinoma kinase-4 defines a new subclass of the receptor tyrosine kinase family. *Oncogene* 11: 2179–2184

Mullis K, Faloona F, Scharf S, Saiki R, Horn G & Erlich H (1986) Specific enzymatic amplification of DNA in vitro: the polymerase chain reaction. *Cold Spring Harb Symp Quant Biol* 51 Pt 1: 263–273

Muralidharan-Chari V, Clancy J, Plou C, Romao M, Chavrier P, Raposo G & D'Souza-Schorey C (2009) ARF6-regulated shedding of tumor cell-derived plasma membrane microvesicles. *Curr Biol CB* 19: 1875–1885

Murillo-Garzón V, Gorroño-Etxebarria I, Åkerfelt M, Puustinen MC, Sistonen L, Nees M, Carton J, Waxman J & Kypta RM (2018) Frizzled-8 integrates Wnt-11 and transforming growth factor-β signaling in prostate cancer. *Nat Commun* 9: 1747

Nakamura N (2010) Emerging new roles of GM130, a cis-Golgi matrix protein, in higher order cell functions. *J Pharmacol Sci* 112: 255–264

Nanou A, Miller MC, Zeune LL, de Wit S, Punt CJA, Groen HJM, Hayes DF, de Bono JS & Terstappen LWMM (2020) Tumour-derived extracellular vesicles in blood of metastatic cancer patients associate with overall survival. *Br J Cancer* 122: 801–811

Neophytou CM, Panagi M, Stylianopoulos T & Papageorgis P (2021) The Role of Tumor Microenvironment in Cancer Metastasis: Molecular Mechanisms and Therapeutic Opportunities. *Cancers* 13: 2053

Nie X, Liu H, Liu L, Wang Y-D & Chen W-D (2020) Emerging Roles of Wnt Ligands in Human Colorectal Cancer. *Front Oncol* 10: 1341

Nikolai BC, Lanz RB, York B, Dasgupta S, Mitsiades N, Creighton CJ, Tsimelzon A, Hilsenbeck SG, Lonard DM, Smith CL, *et al* (2016) HER2 Signaling Drives DNA Anabolism and Proliferation through SRC-3 Phosphorylation and E2F1-Regulated Genes. *Cancer Res* 76: 1463–1475

Nishioka M, Ueno K, Hazama S, Okada T, Sakai K, Suehiro Y, Okayama N, Hirata H, Oka M, Imai K, *et al* (2013) Possible involvement of Wnt11 in colorectal cancer progression. *Mol Carcinog* 52: 207–217

van Noort M, Meeldijk J, van der Zee R, Destree O & Clevers H (2002) Wnt signaling controls the phosphorylation status of beta-catenin. *J Biol Chem* 277: 17901–17905

Nusse R & Varmus HE (1982) Many tumors induced by the mouse mammary tumor virus contain a provirus integrated in the same region of the host genome. *Cell* 31: 99–109

Nüsslein-Volhard C & Wieschaus E (1980) Mutations affecting segment number and polarity in Drosophila. *Nature* 287: 795–801

Nüsslein-Volhard C, Wieschaus E & Kluding H (1984) Mutations affecting the pattern of the larval cuticle inDrosophila melanogaster : I. Zygotic loci on the second chromosome. *Wilhelm Rouxs Arch Dev Biol* 193: 267–282

Nygren MK, Døsen G, Hystad ME, Stubberud H, Funderud S & Rian E (2007) Wnt3A activates canonical Wnt signalling in acute lymphoblastic leukaemia (ALL) cells and inhibits the proliferation of B-ALL cell lines. *Br J Haematol* 136: 400–413

Oishi I, Suzuki H, Onishi N, Takada R, Kani S, Ohkawara B, Koshida I, Suzuki K, Yamada G, Schwabe GC, *et al* (2003) The receptor tyrosine kinase Ror2 is involved in non-canonical Wnt5a/JNK signalling pathway. *Genes Cells* 8: 645–654

Okamoto M, Udagawa N, Uehara S, Maeda K, Yamashita T, Nakamichi Y, Kato H, Saito N, Minami Y, Takahashi N, *et al* (2014) Noncanonical Wnt5a enhances Wnt/β-catenin signaling during osteoblastogenesis. *Sci Rep* 4: 4493

Ortega FG, Piguillem SV, Messina GA, Tortella GR, Rubilar O, Jiménez Castillo MI, Lorente JA, Serrano MJ, Raba J & Fernández Baldo MA (2019) EGFR detection in extracellular vesicles of breast cancer patients through immunosensor based on silica-chitosan nanoplatform. *Talanta* 194: 243–252

Ouko L, Ziegler TR, Gu LH, Eisenberg LM & Yang VW (2004) Wnt11 Signaling Promotes Proliferation, Transformation, and Migration of IEC6 Intestinal Epithelial Cells. *J Biol Chem* 279: 26707–26715

Pandey G, Borcherding N, Kolb R, Kluz P, Li W, Sugg S, Zhang J, Lai DA & Zhang W (2019) ROR1 Potentiates FGFR Signaling in Basal-Like Breast Cancer. *Cancers* 11: 718

Pandur P, Läsche M, Eisenberg LM & Kühl M (2002) Wnt-11 activation of a non-canonical Wnt signalling pathway is required for cardiogenesis. *Nature* 418: 636–641

Park J-Y, Kang S-E, Ahn KS, Um J-Y, Yang WM, Yun M & Lee S-G (2020) Inhibition of the PI3K-AKT-mTOR pathway suppresses the adipocyte-mediated proliferation and migration of breast cancer cells. *J Cancer* 11: 2552–2559

Park S-K, Lee H-S & Lee S-T (1996) Characterization of the Human Full-Length *PTK7* cDNA Encoding a Receptor Protein Tyrosine Kinase-Like Molecule Closely Related to Chick KLG. *J Biochem (Tokyo)* 119: 235–239

Parsons MJ, Tammela T & Dow LE (2021) WNT as a Driver and Dependency in Cancer. *Cancer Discov* 11: 2413–2429

Peart O (2017) Metastatic Breast Cancer. *Radiol Technol* 88: 519M-539M

Penna C & Nordlinger B (2002) Colorectal metastasis (liver and lung). *Surg Clin North Am* 82: 1075–1090, x–xi

Piccin A, Murphy WG & Smith OP (2007) Circulating microparticles: pathophysiology and clinical implications. *Blood Rev* 21: 157–171

Planutis K, Planutiene M & Holcombe RF (2014) A novel signaling pathway regulates colon cancer angiogenesis through Norrin. *Sci Rep* 4: 5630

Ran FA, Hsu PD, Wright J, Agarwala V, Scott DA & Zhang F (2013) Genome engineering using the CRISPR-Cas9 system. *Nat Protoc* 8: 2281–2308

Raposo G & Stoorvogel W (2013) Extracellular vesicles: Exosomes, microvesicles, and friends. *J Cell Biol* 200: 373–383

Rasmussen NR, Wright TM, Brooks SA, Hacker KE, Debebe Z, Sendor AB, Walker MP, Major MB, Green J, Wahl GM, *et al* (2013) Receptor Tyrosine Kinase-like Orphan Receptor 2 (Ror2) Expression Creates a Poised State of Wnt Signaling in Renal Cancer. *J Biol Chem* 288: 26301–26310

Recio-Boiles A & Cagir B (2021) Colon Cancer. In *StatPearls* Treasure Island (FL): StatPearls Publishing

Ren D, Chen J, Li Z, Yan H, Yin Y, Wo D, Zhang J, Ao L, Chen B, Ito TK, *et al* (2015) LRP5/6 directly bind to Frizzled and prevent Frizzled-regulated tumour metastasis. *Nat Commun* 6: 6906

Roarty K, Pfefferle AD, Creighton CJ, Perou CM & Rosen JM (2017) Ror2-mediated alternative Wnt signaling regulates cell fate and adhesion during mammary tumor progression. *Oncogene* 36: 5958–5968

Rodriguez-Hernandez I, Maiques O, Kohlhammer L, Cantelli G, Perdrix-Rosell A, Monger J, Fanshawe B, Bridgeman VL, Karagiannis SN, Penin RM, *et al* (2020) WNT11-FZD7-DAAM1 signalling supports tumour initiating abilities and melanoma amoeboid invasion. *Nat Commun* 11: 5315

Rodriguez-Salas N, Dominguez G, Barderas R, Mendiola M, García-Albéniz X, Maurel J & Batlle JF (2017) Clinical relevance of colorectal cancer molecular subtypes. *Crit Rev Oncol Hematol* 109: 9–19

Roucourt B, Meeussen S, Bao J, Zimmermann P & David G (2015) Heparanase activates the syndecan-syntenin-ALIX exosome pathway. *Cell Res* 25: 412–428

Rowan AJ, Lamlum H, Ilyas M, Wheeler J, Straub J, Papadopoulou A, Bicknell D, Bodmer WF & Tomlinson IP (2000) APC mutations in sporadic colorectal tumors: A mutational 'hotspot' and interdependence of the 'two hits'. *Proc Natl Acad Sci U S A* 97: 3352–3357

Roy HK & Bianchi LK (2009) Differences in Colon Adenomas and Carcinomas Among Women and Men Potential Clinical Implications. *JAMA J Am Med Assoc* 302: 1696–1697

Rybarczyk P, Gautier M, Hague F, Dhennin-Duthille I, Chatelain D, Kerr-Conte J, Pattou F, Regimbeau J-M, Sevestre H & Ouadid-Ahidouch H (2012) Transient receptor potential melastatin-related 7 channel is overexpressed in human pancreatic ductal adenocarcinomas and regulates human pancreatic cancer cell migration. *Int J Cancer* 131: E851-861

Sándor GO, Soós AÁ, Lörincz P, Rojkó L, Harkó T, Bogyó L, Tölgyes T, Bursics A, Buzás EI, Moldvay J, *et al* (2021) Wnt Activity and Cell Proliferation Are Coupled to Extracellular Vesicle Release in Multiple Organoid Models. *Front Cell Dev Biol* 9: 1597

Sanger F, Nicklen S & Coulson AR (1977) DNA sequencing with chain-terminating inhibitors. *Proc Natl Acad Sci U S A* 74: 5463–5467

Santos MF, Rappa G, Karbanová J, Kurth T, Corbeil D & Lorico A (2018) VAMP-associated protein-A and oxysterol-binding protein–related protein 3 promote the entry of late endosomes into the nucleoplasmic reticulum. *J Biol Chem* 293: 13834–13848

Scavo MP, Cigliano A, Depalo N, Fanizza E, Bianco MG, Denora N, Laquintana V, Curri ML, Lorusso D, Lotesoriere C, *et al* (2019a) Frizzled-10 Extracellular Vesicles Plasma Concentration Is Associated with Tumoral Progression in Patients with Colorectal and Gastric Cancer. *J Oncol* 2019: 2715968

Scavo MP, Depalo N, Rizzi F, Ingrosso C, Fanizza E, Chieti A, Messa C, Denora N, Laquintana V, Striccoli M, *et al* (2019b) FZD10 Carried by Exosomes Sustains Cancer Cell Proliferation. *Cells* 8: E777

Schell MJ, Yang M, Teer JK, Lo FY, Madan A, Coppola D, Monteiro ANA, Nebozhyn MV, Yue B, Loboda A, *et al* (2016) A multigene mutation classification of 468 colorectal cancers reveals a prognostic role for APC. *Nat Commun* 7: 11743

Schindelin J, Arganda-Carreras I, Frise E, Kaynig V, Longair M, Pietzsch T, Preibisch S, Rueden C, Saalfeld S, Schmid B, *et al* (2012) Fiji: an open-source platform for biological-image analysis. *Nat Methods* 9: 676–682

Schubert M & Holland LZ (2013) The Wnt Gene Family and the Evolutionary Conservation of Wnt Expression Landes Bioscience

Sebastian A, Hum NR, Murugesh DK, Hatsell S, Economides AN & Loots GG (2017) Wnt co-receptors Lrp5 and Lrp6 differentially mediate Wnt3a signaling in osteoblasts. *PLOS ONE* 12: e0188264

Sharp PA, Sugden B & Sambrook J (1973) Detection of two restriction endonuclease activities in Haemophilus parainfluenzae using analytical agarose--ethidium bromide electrophoresis. *Biochemistry* 12: 3055–3063

Sheldahl LC, Park M, Malbon CC & Moon RT (1999) Protein kinase C is differentially stimulated by Wnt and Frizzled homologs in a G-protein-dependent manner. *Curr Biol CB* 9: 695–698

Sheldahl LC, Slusarski DC, Pandur P, Miller JR, Kühl M & Moon RT (2003) Dishevelled activates Ca2+ flux, PKC, and CamKII in vertebrate embryos. *J Cell Biol* 161: 769–777

Shen T, Nitta H, Wei L, Parwani AV & Li Z (2020) HER2 intratumoral heterogeneity is independently associated with distal metastasis and overall survival in HER2-positive breast carcinomas. *Breast Cancer Res Treat* 181: 519–527

Shin W-S, Gim J, Won S & Lee S-T (2018) Biphasic regulation of tumorigenesis by PTK7 expression level in esophageal squamous cell carcinoma. *Sci Rep* 8: 8519

Siegel RL, Miller KD & Jemal A (2020) Cancer statistics, 2020. *CA Cancer J Clin* 70: 7–30

Slamon DJ, Clark GM, Wong SG, Levin WJ, Ullrich A & McGuire WL (1987) Human breast cancer: correlation of relapse and survival with amplification of the HER-2/neu oncogene. *Science* 235: 177–182

Soule HD, Vazquez J, Long A, Albert S & Brennan M (1973) A Human Cell Line From a Pleural Effusion Derived From a Breast Carcinoma2. *JNCI J Natl Cancer Inst* 51: 1409–1416

Sullivan R, Maresh G, Zhang X, Salomon C, Hooper J, Margolin D & Li L (2017) The Emerging Roles of Extracellular Vesicles As Communication Vehicles within the Tumor Microenvironment and Beyond. *Front Endocrinol* 8: 194

Sung H, Ferlay J, Siegel RL, Laversanne M, Soerjomataram I, Jemal A & Bray F (2021) Global Cancer Statistics 2020: GLOBOCAN Estimates of Incidence and Mortality Worldwide for 36 Cancers in 185 Countries. *CA Cancer J Clin* 71: 209–249

Sur D, Havasi A, Cainap C, Samasca G, Burz C, Balacescu O, Lupan I, Deleanu D & AlexandruIrimie null (2020) Chimeric Antigen Receptor T-Cell Therapy for Colorectal Cancer. *J Clin Med* 9: E182

Surman M, Hoja-Łukowicz D, Szwed S, Drożdż A, Stępień E & Przybyło M (2018) Human melanoma-derived ectosomes are enriched with specific glycan epitopes. *Life Sci* 207: 395–411

Svensson KJ, Christianson HC, Wittrup A, Bourseau-Guilmain E, Lindqvist E, Svensson LM, Mörgelin M & Belting M (2013) Exosome uptake depends on ERK1/2-heat shock protein 27 signaling and lipid Raft-mediated endocytosis negatively regulated by caveolin-1. *J Biol Chem* 288: 17713–17724

Takemaru KI & Moon RT (2000) The transcriptional coactivator CBP interacts with beta-catenin to activate gene expression. *J Cell Biol* 149: 249–254

Tamai K, Semenov M, Kato Y, Spokony R, Liu C, Katsuyama Y, Hess F, Saint-Jeannet J-P & He X (2000) LDL-receptor-related proteins in Wnt signal transduction. *Nature* 407: 530–535

Tamai K, Zeng X, Liu C, Zhang X, Harada Y, Chang Z & He X (2004) A mechanism for Wnt coreceptor activation. *Mol Cell* 13: 149–156

Tao Q, Yokota C, Puck H, Kofron M, Birsoy B, Yan D, Asashima M, Wylie CC, Lin X & Heasman J (2005) Maternal wnt11 activates the canonical wnt signaling pathway required for axis formation in Xenopus embryos. *Cell* 120: 857–871

Taylor J & Bebawy M (2019) Proteins Regulating Microvesicle Biogenesis and Multidrug Resistance in Cancer. *Proteomics* 19: e1800165

Tesselaar MET, Romijn FPHTM, Van Der Linden IK, Prins FA, Bertina RM & Osanto S (2007) Microparticle-associated tissue factor activity: a link between cancer and thrombosis? *J Thromb Haemost* 5: 520–527

Thanki K, Nicholls ME, Gajjar A, Senagore AJ, Qiu S, Szabo C, Hellmich MR & Chao C (2017) Consensus Molecular Subtypes of Colorectal Cancer and their Clinical Implications. *Int Biol Biomed J* 3: 105–111

Théry C, Amigorena S, Raposo G & Clayton A (2006) Isolation and Characterization of Exosomes from Cell Culture Supernatants and Biological Fluids. *Curr Protoc Cell Biol* 30: 3.22.1-3.22.29

Théry C, Witwer KW, Aikawa E, Alcaraz MJ, Anderson JD, Andriantsitohaina R, Antoniou A, Arab T, Archer F, Atkin-Smith GK, *et al* (2018) Minimal information for studies of extracellular vesicles 2018 (MISEV2018): a position statement of the International Society for Extracellular Vesicles and update of the MISEV2014 guidelines. *J Extracell Vesicles* 7: 1535750

Thiele S, Zimmer A, Göbel A, Rachner TD, Rother S, Fuessel S, Froehner M, Wirth MP, Muders MH, Baretton GB, *et al* (2018) Role of WNT5A receptors FZD5 and RYK in prostate cancer cells. *Oncotarget* 9: 27293–27304

Tian T, Zhu Y-L, Zhou Y-Y, Liang G-F, Wang Y-Y, Hu F-H & Xiao Z-D (2014) Exosome Uptake through Clathrin-mediated Endocytosis and Macropinocytosis and Mediating miR-21 Delivery. *J Biol Chem* 289: 22258–22267

Tian X, Yan L, Zhang D, Guan X, Dong B, Zhao M & Hao C (2016) PTK7 overexpression in colorectal tumors: Clinicopathological correlation and prognosis relevance. *Oncol Rep* 36: 1829–1836

Topol L, Jiang X, Choi H, Garrett-Beal L, Carolan PJ & Yang Y (2003) Wnt-5a inhibits the canonical Wnt pathway by promoting GSK-3–independent β-catenin degradation. *J Cell Biol* 162: 899–908

Toulouie S, Johanning G & Shi Y (2021) Chimeric antigen receptor T-cell immunotherapy in breast cancer: development and challenges. *J Cancer* 12: 1212–1219

Trajkovic K, Hsu C, Chiantia S, Rajendran L, Wenzel D, Wieland F, Schwille P, Brügger B & Simons M (2008) Ceramide triggers budding of exosome vesicles into multivesicular endosomes. *Science* 319: 1244–1247

Trempe GL (1976) Human breast cancer in culture. *Recent Results Cancer Res Fortschritte Krebsforsch Progres Dans Rech Sur Cancer*: 33–41

Tseng J-C, Huang S-H, Lin C-Y, Wang B-J, Huang S-F, Shen Y-Y & Chuu C-P (2020) ROR2 suppresses metastasis of prostate cancer via regulation of miR-199a-5p-PIAS3-AKT2 signaling axis. *Cell Death Dis* 11: 376

Ueno K, Hiura M, Suehiro Y, Hazama S, Hirata H, Oka M, Imai K, Dahiya R & Hinoda Y (2008) Frizzled-7 as a potential therapeutic target in colorectal cancer. *Neoplasia N Y N* 10: 697–705

Valadi H, Ekström K, Bossios A, Sjöstrand M, Lee JJ & Lötvall JO (2007) Exosome-mediated transfer of mRNAs and microRNAs is a novel mechanism of genetic exchange between cells. *Nat Cell Biol* 9: 654–659

VanderVorst K, Dreyer CA, Konopelski SE, Lee H, Ho H-YH & Carraway KL (2019) Wnt/PCP Signaling Contribution to Carcinoma Collective Cell Migration and Metastasis. *Cancer Res* 79: 1719–1729

VanderVorst K, Hatakeyama J, Berg A, Lee H & Carraway KL (2018) Cellular and molecular mechanisms underlying planar cell polarity pathway contributions to cancer malignancy. *Semin Cell Dev Biol* 81: 78–87

Varricchio L, Falchi M, Dall'Ora M, De Benedittis C, Ruggeri A, Uversky VN & Migliaccio AR (2017) Calreticulin: Challenges Posed by the Intrinsically Disordered Nature of Calreticulin to the Study of Its Function. *Front Cell Dev Biol* 5: 96

Vinson CR, Conover S & Adler PN (1989) A Drosophila tissue polarity locus encodes a protein containing seven potential transmembrane domains. *Nature* 338: 263–264

Viñuela-Berni V, Doníz-Padilla L, Figueroa-Vega N, Portillo-Salazar H, Abud-Mendoza C, Baranda L & González-Amaro R (2015) Proportions of several types of plasma and urine microparticles are increased in patients with rheumatoid arthritis with active disease. *Clin Exp Immunol* 180: 442–451

Vogel CL, Cobleigh MA, Tripathy D, Gutheil JC, Harris LN, Fehrenbacher L, Slamon DJ, Murphy M, Novotny WF, Burchmore M, *et al* (2002) Efficacy and safety of trastuzumab as a single agent in first-line treatment of HER2-overexpressing metastatic breast cancer. *J Clin Oncol Off J Am Soc Clin Oncol* 20: 719–726

Voloshanenko O, Gmach P, Winter J, Kranz D & Boutros M (2017) Mapping of Wnt-Frizzled interactions by multiplex CRISPR targeting of receptor gene families. *FASEB J Off Publ Fed Am Soc Exp Biol* 31: 4832–4844

Wang H, Jin H & Rapraeger AC (2015) Syndecan-1 and Syndecan-4 Capture Epidermal Growth Factor Receptor Family Members and the α3β1 Integrin Via Binding Sites in Their Ectodomains: NOVEL SYNSTATINS PREVENT KINASE CAPTURE AND INHIBIT α6β4-INTEGRIN-DEPENDENT EPITHELIAL CELL MOTILITY. *J Biol Chem* 290: 26103–26113

Wang X, Wang Q, Hu W & Evers BM (2004) Regulation of phorbol ester-mediated TRAF1 induction in human colon cancer cells through a PKC/RAF/ERK/NF-kappaB-dependent pathway. *Oncogene* 23: 1885–1895

Wang Z, Shu W, Lu MM & Morrisey EE (2005) Wnt7b Activates Canonical Signaling in Epithelial and Vascular Smooth Muscle Cells through Interactions with Fzd1, Fzd10, and LRP5. *Mol Cell Biol* 25: 5022–5030

Wei H, Wang N, Zhang Y, Wang S, Pang X & Zhang S (2016) Wnt-11 overexpression promoting the invasion of cervical cancer cells. *Tumour Biol J Int Soc Oncodevelopmental Biol Med* 37: 11789–11798

White TJ, Arnheim N & Erlich HA (1989) The polymerase chain reaction. *Trends Genet TIG* 5: 185–189

WNT11 is a novel ligand for ROR2 in human breast cancer | bioRxiv

Wolf P (1967) The nature and significance of platelet products in human plasma. *Br J Haematol* 13: 269–288

Wong H-C, Bourdelas A, Krauss A, Lee H-J, Shao Y, Wu D, Mlodzik M, Shi D-L & Zheng J (2003) Direct Binding of the PDZ Domain of Dishevelled to a Conserved Internal Sequence in the C-Terminal Region of Frizzled. *Mol Cell* 12: 1251–1260

Wright PK, Jones SB, Ardern N, Ward R, Clarke RB, Sotgia F, Lisanti MP, Landberg G & Lamb R (2014) 17β-estradiol regulates giant vesicle formation via estrogen receptor-alpha in human breast cancer cells. *Oncotarget* 5: 3055–3065

Wright TM, Brannon AR, Gordan JD, Mikels AJ, Mitchell C, Chen S, Espinosa I, van de Rijn M, Pruthi R, Wallen E, *et al* (2009) Ror2, a developmentally regulated kinase, promotes tumor growth potential in renal cell carcinoma. *Oncogene* 28: 2513–2523

Wu Q-L, Zierold C & Ranheim EA (2009) Dysregulation of Frizzled 6 is a critical component of B-cell leukemogenesis in a mouse model of chronic lymphocytic leukemia. *Blood* 113: 3031–3039

Xu YK & Nusse R (1998) The Frizzled CRD domain is conserved in diverse proteins including several receptor tyrosine kinases. *Curr Biol CB* 8: R405-406

Yamada M, Udagawa J, Matsumoto A, Hashimoto R, Hatta T, Nishita M, Minami Y & Otani H (2010) Ror2 is required for midgut elongation during mouse development. *Dev Dyn* 239: 941–953

Yamaguchi T, Yamamoto M, Yamazaki M, Tani N, Sakamoto M, Daikuzono H, Li H, Oneyama C, Fujimoto T & Takahashi T (2020) ROR1 sustains multivesicular endosomes by interacting with HRS and STAM1 In Review

Yamanaka H & Nishida E (2007) Wnt11 stimulation induces polarized accumulation of Dishevelled at apical adherens junctions through Frizzled7. *Genes Cells Devoted Mol Cell Mech* 12: 961–967

Yan J, Liu T, Zhou X, Dang Y, Yin C & Zhang G (2016a) FZD6, targeted by miR-21, represses gastric cancer cell proliferation and migration via activating non-canonical wnt pathway. *Am J Transl Res* 8: 2354–2364

Yan L, Du Q, Yao J & Liu R (2016b) ROR2 inhibits the proliferation of gastric carcinoma cells via activation of non-canonical Wnt signaling. *Exp Ther Med* 12: 4128–4134

Yáñez-Mó M, Siljander PR-M, Andreu Z, Zavec AB, Borràs FE, Buzas EI, Buzas K, Casal E, Cappello F, Carvalho J, *et al* (2015) Biological properties of extracellular vesicles and their physiological functions. *J Extracell Vesicles* 4: 27066

Yang C-M, Ji S, Li Y, Fu L-Y, Jiang T & Meng F-D (2017) Ror2, a Developmentally Regulated Kinase, Is Associated With Tumor Growth, Apoptosis, Migration, and Invasion in Renal Cell Carcinoma. *Oncol Res* 25: 195–205

Yang S, Wu Y, Xu T-H, de Waal PW, He Y, Pu M, Chen Y, DeBruine ZJ, Zhang B, Zaidi SA, *et al* (2018) Crystal structure of the Frizzled 4 receptor in a ligand-free state. *Nature* 560: 666–670

Ye X, Wang Y, Rattner A & Nathans J (2011) Genetic mosaic analysis reveals a major role for frizzled 4 and frizzled 8 in controlling ureteric growth in the developing kidney. *Dev Camb Engl* 138: 1161–1172

Yekula A, Minciacchi VR, Morello M, Shao H, Park Y, Zhang X, Muralidharan K, Freeman MR, Weissleder R, Lee H, *et al* (2020) Large and small extracellular vesicles released by glioma cells in vitro and in vivo. *J Extracell Vesicles* 9: 1689784

Yiu GK, Kaunisto A, Chin YR & Toker A (2011) NFAT promotes carcinoma invasive migration through glypican-6. *Biochem J* 440: 157–166

Yoshida N, Kinugasa T, Ohshima K, Yuge K, Ohchi T, Fujino S, Shiraiwa S, Katagiri M & Akagi Y (2015) Analysis of Wnt and β-catenin Expression in Advanced Colorectal Cancer. *Anticancer Res* 35: 4403–4410

Young CS, Kitamura M, Hardy S & Kitajewski J (1998) Wnt-1 induces growth, cytosolic beta-catenin, and Tcf/Lef transcriptional activation in Rat-1 fibroblasts. *Mol Cell Biol* 18: 2474–2485

Yu J, Chen L, Chen Y, Hasan MK, Ghia EM, Zhang L, Wu R, Rassenti LZ, Widhopf GF, Shen Z, *et al* (2017) Wnt5a induces ROR1 to associate with 14-3-3ζ for enhanced

chemotaxis and proliferation of chronic lymphocytic leukemia cells. *Leukemia* 31: 2608–2614

Yu J, Chen L, Cui B, Widhopf GF, Shen Z, Wu R, Zhang L, Zhang S, Briggs SP & Kipps TJ (2016) Wnt5a induces ROR1/ROR2 heterooligomerization to enhance leukemia chemotaxis and proliferation. *J Clin Invest* 126: 585–598

Yu X, Harris SL & Levine AJ (2006) The regulation of exosome secretion: a novel function of the p53 protein. *Cancer Res* 66: 4795–4801

Yuan Y, Niu CC, Deng G, Li ZQ, Pan J, Zhao C, Yang ZL & Si WK (2011) The Wnt5a/Ror2 noncanonical signaling pathway inhibits canonical Wnt signaling in K562 cells. *Int J Mol Med* 27: 63–69

Zhan T, Rindtorff N & Boutros M (2017) Wnt signaling in cancer. *Oncogene* 36: 1461–1473

Zhang J, Wang J-L, Zhang C-Y, Ma Y-F, Zhao R & Wang Y-Y (2020) The prognostic role of FZD6 in esophageal squamous cell carcinoma patients. *Clin Transl Oncol Off Publ Fed Span Oncol Soc Natl Cancer Inst Mex* 22: 1172–1179

Zhang S, Chen L, Cui B, Chuang H-Y, Yu J, Wang-Rodriguez J, Tang L, Chen G, Basak GW & Kipps TJ (2012) ROR1 is expressed in human breast cancer and associated with enhanced tumor-cell growth. *PloS One* 7: e31127

Zhang S, Chen L, Wang-Rodriguez J, Zhang L, Cui B, Frankel W, Wu R & Kipps TJ (2012c) The Onco-Embryonic Antigen ROR1 Is Expressed by a Variety of Human Cancers. *Am J Pathol* 181: 1903–1910

Zhao L, Bi Y, Kou J, Shi J & Piao D (2016) Phosphatidylserine exposing-platelets and microparticles promote procoagulant activity in colon cancer patients. *J Exp Clin Cancer Res* 35: 54

Zhao S, Ma W, Zhang M, Tang D, Shi Q, Xu S, Zhang X, Liu Y, Song Y, Liu L, *et al* (2013) High expression of CD147 and MMP-9 is correlated with poor prognosis of triple-negative breast cancer (TNBC) patients. *Med Oncol Northwood Lond Engl* 30: 335

Zhou Q, Zhou S, Wang H, Li Y, Xiao X & Yang J (2020) Stable silencing of ROR1 regulates cell cycle, apoptosis, and autophagy in a lung adenocarcinoma cell line. *Int J Clin Exp Pathol* 13: 1108–1120

Zhou W, Lin L, Majumdar A, Li X, Zhang X, Liu W, Etheridge L, Shi Y, Martin J, Van de Ven W, *et al* (2007) Modulation of morphogenesis by noncanonical Wnt signaling requires ATF/CREB family-mediated transcriptional activation of TGFbeta2. *Nat Genet* 39: 1225–1234

Zonneveld MI, Brisson AR, van Herwijnen MJC, Tan S, van de Lest CHA, Redegeld FA, Garssen J, Wauben MHM & Nolte-'t Hoen ENM (2014) Recovery of extracellular vesicles from human breast milk is influenced by sample collection and vesicle isolation procedures. *J Extracell Vesicles* 3

# Acknowledgments

First of all, I would like to thank Univ.-Prof. Dr. med. Annalen Bleckmann for giving me this great opportunity to not only work in an ambitious team on such an interesting and important topic, but also enabling me to write my thesis about that project. Thanks for the circumspect willingness and instructive way of lending a hand in scientific issues, which she proved in countless discussions. Thank you for great support from start to finish, including several occasions to present my results at scientific congresses and seminars.

For the scientific support in all bioinformatic matters and beyond I would like to thank Prof. Dr. Tim Beisbarth. In this regard also special thanks to Maren Sitte and Darius Wlochowitz. Also a thank you to all members of the MyPathSem consortium and all further examination board members.

I further would like to thank Prof. Dr. med. Claudia Binder for her advice and patient support during the whole time.

I would especially like to thank Dr. Kerstin Menck for the always prudent supervision of my work in the laboratory and beyond, particularly for her advices and help with problems and many stimulating scientific discussions throughout the work.

Thanks to Sophia Papaiannou, Cedric Weich, Janes Efing, Nadja Kamper, and especially Suganja Sivaloganathan and Barnabas Irmer for the pleasant working atmosphere, the motivated discussions on private and scientific topics and the nice time in- and outside the lab.

Furthermore, I thank Claudia Bieber-Tuschen for the administrative and sometimes tough to handle bureaucratic support and Matthias Schulz, Lena Ries, Meike Schaffrinski, Buket Celik and Annette Westermann for the technical support, the enormous relief and enrichment of the daily laboratory routine; for the many great conversations, for not rejecting a single question and for lending a helping hand or an open ear whenever it got necessary. Thanks for great hours in- and outside of work.

Many thanks to all my friends, who I can rely on and are there when it counts; for all the funny,inspiring moments and consistent support. A special thanks to Rabea Jesser, who helped me with words and deeds, offering eloquent solutions when I ran short on words, particularly during the writing process of this thesis.

Last but not least, I would like to thank my whole family for all the love, support, helpfulness and backing. I thank my parents for encouraging my scientific curiosity, sharpen my critical thinking and keeping track of my work-life-balance, in a word: for always being there for me. I thank my brothers Stefan and Christian for being my best friends and always being there for me when I need them and helping me with advice and support. Thanks also for the fun times besides my studies. Last but not least, I would like to thank my grandma Anna, who always kept her fingers crossed for me when I needed it and gave me great advice.